UNIVERSITÀ
DEGLI STUDI
DI PADOVA

Sede amministrativa: Università degli Studi di Padova

Dipartimento di Principi e Impianti di Ingegneria Chimica "I. Sorgato"

SCUOLA DI DOTTORATO DI RICERCA IN INGEGNERIA INDUSTRIALE
INDIRIZZO INGEGNERIA CHIMICA
CICLO XXIII

HIGH SHEAR WET GRANULATION: PROCESS UNDERSTANDING AND SCALE UP

Direttore della Scuola: Ch.mo Prof. Paolo Bariani
Coordinatore dell'Indirizzo: Ch.mo Prof. Alberto Bertucco
Supervisore: Dr. Andrea Santomaso

Dottorando: Mauro Cavinato

Aknowledgements / Ringraziamenti

At end of this three years PhD program, I can definitely say that this PhD gave me indeed the opportunity to grow up professionally and work with very smart people. But what is most important is that I had the opportunity to meet special friends and live unforgettable moments.
For this reason I would like to thank my supervisors, Dr. Andrea Santomaso e Prof. Paolo Canu for their support and for giving me the opportunity to travel during my PhD. I am grateful to both of you for your advice and encouragement. Thank you also to my colleagues Dr. Erica Franceschinis and Dr. Riccardo Artoni, who has been a great friend. It was definitely great to work with you guys.
From the time I spent in GlaxoSmithKline, Verona, I would like to thank all the former Pharmaceutical Development Dpt. for making my internship a very informative experience. Thank you especially to Massimo Bresciani, Dionigio Franchi, Guido Bellazzi, Marianna Machin, Roberto Bartolini, Gianluigi Faiella, Isabella Pignatone and everyone who helped me with my research and my experiments. Thank you to GlaxoSmithKline for partially funding this PhD project.
From Purdue University, I would like to thank Prof. Jim Litster and Dr. Defne Kayrak-Talay for sharing their knowledge and for giving me the opportunity of being a member of their group. Special thanks must go to all Prof. Jim Litster's group, in particular Heather Emady, Nyah Zarate, Jiangfeng Li, Ben Freireich and Shaunok Vora.
I truly enjoyed the time I spent with you guys.
From my time at Nestlé Research Centre, Lausanne, I would like to thank Prof. Stefan Palzer, Dr. Gerhard Niederreiter and all the Solid Product Group. I am grateful to all of you for sharing your time and experience.

~ ~ ~

In conclusione, vorrei dedicare questo lavoro alle persone a me più care.
Vorrei ringraziare i miei genitori, Ivo e Lucilla, e mia sorella Cristina per il supporto durante tutti questi anni di studio e lavoro. Vorrei ringraziarvi semplicemente per essere sempre stati presenti, poiché la vostra presenza mi ha permesso di affrontare tanti momenti difficili.
Un ringraziamento speciale va a Laura per la comprensione, la pazienza e per essermi sempre stata vicina durante questi tre anni anche a chilometri di distanza.
Non avrei raggiunto questo traguardo senza il vostro sostegno. Grazie.

Summary

Among all the powder agglomeration processes, high shear wet granulation is one of the most commonly used techniques. It consists of the agglomeration of different powders through the addition of a granulating fluid and a vigorous mixing. Industries often turn to high shear granulation mainly to avoid segregation of critical components in a powder mixture, improve flowability and compactibility. Despite the great importance of this technique in many industrial activities, it is not totally clear how changes in the initial powder mixture or in process variables can affect the final product properties. Moreover, scale-up of high shear granulators is still difficult to perform.

The present research mainly focuses on the high shear wet granulation of pharmaceutical powders. Particularly, this research aims at closing the gap in understanding the role of primary particle properties (e.g. composition, primary particle size distribution) and process parameters (e.g. mixing speed, liquid flow rate and amount) on the final granule characteristics. Scale-up effects on the powder flow patterns were investigated as well.
The research activities were mainly carried out in:

- Dipartimento di Principi e Impianti per l'Ingegneria Chimica, Università degli Studi di Padova, Padova (Italy);
- former Pharmaceutical Development Dpt., GlaxoSmithKline R&D, Verona (Italy);
- Chemical Engineering Dpt., Purdue University, West Lafayette, Indiana (U.S.A.);
- Solid Products Group, Nestle Research Centre, Lausanne (Switzerland).

Results of research activities are here summarized in five chapters:

- Chapter 1 gives a brief overview on the main powder agglomeration techniques and mainly focuses on high shear wet granulation;
- In Chapter 2 a new formulation map for the prediction of granulation onset as a function of formulation properties is presented;
- Description of the granule growth behaviour during the granulation of three common active ingredients is provided by Chapter 3;
- Effects of operative variables on the granule growth kinetics are analyzed in Chapter 4;
- Chapter 5 is about the application of emulsions as alternative liquid binders;
- Chapter 6 presents important considerations about the effect of scale-up on powder flow patterns;
- Conclusions and proposals for future work can be found in Chapter 7.

Riassunto

Tra tutti i processi di agglomerazione di polveri, la granulazione ad elevato shear risulta essere una delle tecniche più usate. Questa tecnica consiste nell'agglomerazione di diverse polveri dovuta all'aggiunta di un liquido legante e a un mescolamento energico. La granulazione ad elevato shear è utilizzata principalmente per evitare la segregazione di componenti critici in una miscela di polveri, per migliorare la scorrevolezza e comprimibilità. Nonostante l'importanza di questa tecnica in numerosi settori industriali, l'effetto delle proprietà delle polveri e dei parametri di processo sul prodotto finale è ancora poco chiaro. Lo scale up dei granulatori ad elevato shear risulta inoltre ancora difficile da portare a termine.

La presente ricerca riguarda la granulazione high shear di polveri farmaceutiche. Lo scopo della ricerca è approfondire la conoscenza sul ruolo delle proprietà delle particelle nella miscela iniziale (p.e. composizione e distribuzione granulometrica) e parametri di processo (p.e. velocità di agitazione, portata e quantità di liquido) nel determinare le caratteristiche del prodotto finale. È stato inoltre analizzato l'effetto dello scale up sul regime di mescolamento.
L'attività di ricerca è stata svolta prevalentemente presso:

- il Dipartimento di Principi e Impianti per l'Ingegneria Chimica, Università degli Studi di Padova, Padova (Italia);
- ex Dipartimento di Sviluppo Farmaceutico., GlaxoSmithKline R&D, Verona (Italia);
- Chemical Engineering Dpt., Purdue University, West Lafayette, Indiana (Stati Uniti);
- Solid Products Group, Nestle Research Centre, Lausanne (Svizzera).I risultati dell'attività di ricerca sono qui riassunti in sette capitoli:

- capitolo 1 riassume brevemente i metodi principali di agglomerazione di polveri e in particolare si focalizza sulla granulazione ad elevato shear;
- nel capitolo 2 viene presentata una nuova mappa di formulazione per la previsione dell'inizio della crescita del granulo in funzione delle proprietà della miscela iniziale;
- la descrizione del meccanismo di crescita del granulo durante la granulazione di tre comuni principi attivi viene presentata nel capitolo 3;
- gli effetti delle variabili operative sulla crescita del granulo sono analizzati nel capitolo 4
- il capitolo 5 riguarda l'applicazione di emulsioni come liquidi leganti alternativi;
- il capitolo 6 contiene considerazioni importanti riguardo all'effetto dello scale up sul regime di mescolamento;
- le conclusioni e le prospettive di lavoro futuro sono presentate nel capitolo 7.

Contents

Chapter 1

Introduction

Granular materials are widely used by several types of industry. As an instance, they can be present as raw materials, intermediates and final products in the of pharmaceuticals, food, detergents, agrochemicals, coal and mining powders. The reasons for this widespread use are various: powders are often easy to handle, they can be dissolved in liquids, compressed to form tablets and swallowed in order to transfer nourishment or medicines in the human body.

Granulation (or agglomeration) is one of the most important operations involving granular materials. During this process the primary powder particles are forced to adhere and form granules (or agglomerates).
Granulation is performed for many reasons. For example, it is often required to prevent the segregation of critical components in a powder mixture by reducing the difference in size and density between different powders. A good granulation process can therefore create agglomerates having similar size and composition, thus reducing the segregation phenomena.
Moreover, powder flowability and wettability can be considerably improved by using granulation (Litster and Ennis, 1999; Ennis, 2006).

1.1 Granulation technologies

The variety of equipment for powder granulation is huge: production processes largely vary in capacity and can be operated in batch-wise or continuously. The choice of a specific process often depends on the desired final product characteristics (e.g. granule density, dissolution time, final particle size distribution and shape) or can be strongly affected by handling aspects (e.g. inert conditions, caking problems) or economical constraints (Flore et al., 2009).
However, two main equipment categories can be identified: wet granulation and dry granulation processes.

Wet granulation is performed by adding a granulating liquid into the powder mixture. This liquid promotes the formation of bonds between primary particles. Mixing is usually involved by using mechanical mixers or by introducing air in order to promote the collision between particles.

In the frame of mechanical mixers, powder is usually fluidized by using stirrers or paddles. In this case two types of granulators can be identified according to the mixer tip speed: low shear (< 5 m/s) and high shear (5-10 m/s) granulators (Knight et al., 2001). Powder can be also kept in movement by the rotation of the container (pan, disk or drum granulation).
On the other hand, fluid bed agglomeration is usually performed by fluidizing powders with upward-directed air stream (Palzer, 2010).
Whether in the case of mechanical mixer and fluid bed, granulating fluid is added into the system by spraying or dripping the liquid on the powder surface. Granulating fluid can be a pure liquid (e.g. water) or a solution, depending on the product final application.

In dry granulation, agglomerates are formed by using high pressure: stress exerted on powders in confined volumes deforms the particles and leads to an increase of Van der Waals forces. Sintering at the contact points can also occur and determine the formation of stronger bonds.
For instance, dry granulation can be performed by compression of powders within a cavity to form tablets (i.e. tabletting). Dry agglomerates can be also formed by forcing a continuous powder stream into the gap between two counter-rotating rollers (i.e. roller compaction).
Some granulation techniques can be classified as a combination between dry and wet granulation. As an example, extruders can be used to knead and compress wet powders. The resulting strand is then cut or broken in order to form several agglomerates (Palzer, 2010).

1.2 Introduction to high shear wet granulation

High shear wet granulation is a batch process and one of the most commonly used techniques, especially for the production of solid oral dosage forms in pharmaceutical industry and the production of detergents. Granules produced with high shear mixer usually present lower friability and more spherical shape (Ennis, 2006).
Most of the high shear granulators consist of a mixing bowl, a three bladed impeller and a secondary mixer or chopper (see Fig.1.1). Vertical high shear granulators can be either top driven or bottom driven. The tip speed of the impeller in these mixers is usually of the order of 10 m/s).

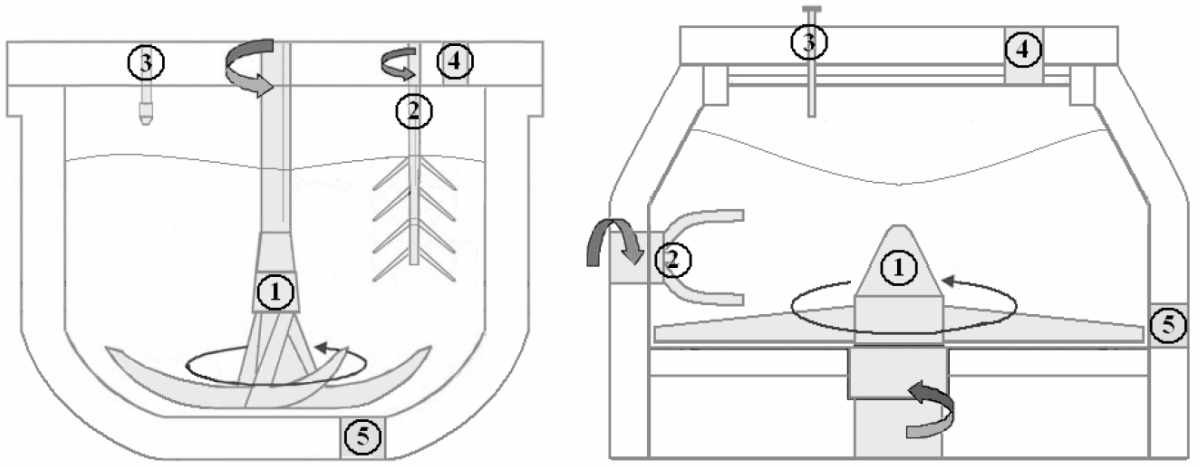

Fig.1.1. Schematic of a top-driven (left) and bottom-driven (right) high shear granulator: (1) impeller, (2) secondary mixer or chopper, (3) liquid addition system, (4) product filter and (5) discharge valve.

The composition of a pharmaceutical powder mixture in high shear wet granulation generally consists of an active ingredient and some excipients.

Excipients have different roles and can be roughly divided in three main categories: filler, disintegrant and solid binder. The solid binder is usually an amorphous polymer, which is added to the initial mixture or as a solution in order to promote the formation of inter-particle bonds. Disintegrants expand and dissolve when wet causing the tablet to break apart, releasing the active ingredients for absorption. Some ingredients can be often considered as both dry binder and disintegrant.

The high shear wet granulation process usually includes the following steps (Ennis, 2006):

1. loading the powder mixture into the mixer bowl;
2. mixing of dry powders at high impeller and chopper speed for a short period of time (a few minutes);
3. addition of granulating liquid on the powder mixture surface, while both the impeller and the chopper are running;
4. wet massing, with the liquid addition system turned off and both the impeller and the chopper running;
5. discharge of granules from the mixer and drying in a fluid bed dryer or oven;
6. sieving of dry granules.

Granule growth is generally very fast during a high shear granulation process: this is often an advantage since resulting processing time is short, but the process needs to be thoroughly controlled in order to avoid over-granulation.

For this reason several monitoring techniques have been developed in order to control the process and determine the time to end the granulation point (i.e. granulation end point). Some of the most commonly used monitoring techniques are: power consumption, impeller torque

or impeller current monitoring, acoustic emission monitoring, particle size distribution measurements (off-line and on-line techniques), powder surface velocity measurements.
Nevertheless the attention has been primarily devoted to end-point determination whereas less effort has been put on the understating of the early stage of the granulation. In addition, particles have been often considered inert materials from the engineering point of view, i.e. interactions between solid particles and liquid have been rarely contemplated.
This research was therefore aimed at developing more systematic and quantitative criteria for high-shear wet granulation design on the basis of the single components physical properties. The overall granule growth has been considered (from the early stage to the end point) and a method for the prediction of the granule growth onset as a function of formulation composition has been proposed. The effects of active ingredient properties (i.e. primary particle size and shape, water-solid interactions) as well as some important process variables (i.e. impeller speed, liquid flow rate and amount) on the granule growth behaviour have been analyzed and quantified. Alternative liquid binders (e.g. emulsions containing a lipophilic active ingredient) were furthermore used and resulting granules compared with those obtained from conventional water granulation.
Scale up from bench scale (2 l) to pilot plant (65 l) was also performed. Effects of changes in mass fill and impeller speed at different scales were thoroughly analyzed.

1.3 References

B.J. Ennis, Theory of Granulation: an Engineering Perspective, Handbook of Pharmaceutical Granulation Technology (2nd Ed.), Taylor and Francis Group, 2006.

K. Flore, M. Schoenherr, H. Feise. Aspects of granulation in the chemical industry. Powder Technology 189 (2009) 327-331.

P.C. Knight, J.P.K. Seville, A.B. Wellm, T. Instone. Prediction of impeller torque in high shear powder mixers. Chemical Engineering Science 56 (2001) 4457-4471.

J.D. Litster, B. J. Ennis, Size reduction and size enlargement, Perry's Chemical Engineers' Handbook. McGraw-Hill Companies, 1999.

S. Palzer, Agglomeration of pharmaceutical, detergent, chemical and food powders — Similarities and differences of materials and processes. Powder Technology (2010) doi: 10.1016/j.powtec.2010.05.006.

Chapter 2

The development of a novel formulation map for the optimization of high shear wet granulation

2.1 Summary

With a view to describing the powder agglomeration process, particles have often been considered as inert material and the solid-liquid interactions have rarely been contemplated.
The present research aims to fill the gap in understanding how the nucleation and the early stage of the granule growth depend on some important formulation properties.
The glass transition concept coupled with on-line impeller torque monitoring and measurements of the time evolution of the particle size distribution was used to give a description of the early stage of the agglomeration process in high-shear wet granulation. A mixture of commonly-used pharmaceutical powders, which are amorphous and crystalline in nature, was processed.
Accordingly, a new formulation map is presented which describes the onset of significant granule growth as a function of the key formulation components (i.e. diluent, dry and liquid binder).
From this map, the minimum amount of liquid binder required to induce appreciable granule growth is determined as a function of the type, quantity, hygroscopicity and particle size distribution of the diluent and the solid binder. This map can be obtained from a priori glass transition measurement using a static humidity conditioning system and by fitting the experimentally obtained data using a modified Gordon-Taylor equation.

2.2 Introduction

The pharmaceutical industry frequently applies high shear wet granulation to a powder mixture in order to improve the particle characteristics, the homogeneity and the flowability properties (Litster and Ennis, 1999; Ennis, 2006). High shear wet granulation is therefore an

Published in:
M. Cavinato, M. Bresciani, M. Machin, G. Bellazzi, P. Canu, A. Santomaso. International Journal of Pharmaceutics 387 (2010) 48-55.
M. Cavinato, M. Bresciani, M. Machin, G. Bellazzi, P. Canu, A. Santomaso. Chemical Engineering Journal 164 (2010) 350-358.

example of particle design, since an initial powder mixture composed of a drug and some excipients can be transformed in design structured agglomerates through liquid addition and vigorous mixing (Knight, 2001).

In spite of the importance and the widespread use of this industrial operation, currently it is not completely clear how a change in the process conditions and formulation variables can affect the evolution of the granule properties. Many efforts have been made with a view to engineering the process, splitting up the agglomeration process into different stages, such as the initial granule formation phase or nucleation (Wildeboer et al., 2005), the granule growth and finally breakage (Iveson and Litster, 2005). However, wet granulation has remained in practice more an art than a science, as pointed out by Iveson et al. (2001).

Therefore our ability to control the high shear granulation process in order to establish a key factor such as the end-point conditions, for instance, is still an unsolved problem.

Several and varied methods have been explored for this purpose. Briens et al. (2007) and Daniher et al. (2008) proposed an end-point monitoring technique based on the acoustic emission survey. However, at present, the granulator power consumption and impeller torque monitoring are the most widespread methods to monitor the agglomeration process since they are a direct measurement of the resistance of the wet mass to mixing (Landin et al.,1995; Landin et al., 1996; Betz et al., 2004). The power consumption or impeller torque profiles have been traditionally subdivided into different phases, as described by Leuenberger et al. (2009): (1) a first slight increase in the profile, usually related to nuclei formation and moisture sorption, (2) a rapid increase in the profile slope, due to the attainment of the pendular state (formation of liquid bridges), (3) a plateau phase in the profile which indicates the transition from the pendular to the funicular state. Some authors consider this plateau region as an equilibrium stage between granule growth and breakage, corresponding to optimal granule characteristics (Leuenberger, 1982).

Modern and scientific approaches to granulation understanding aim to split and analyze every single agglomeration phase. In this work we focus on the early stage of the growth phase and on the potential of on-line impeller torque measurements to monitor the granule growth. Whereas most research has been primarily devoted to end-point determination, less effort has been dedicated to the understanding of the granulation on-set.

In addition, particles have often been considered inert materials, i.e. interactions between solid particles and liquid have seldom been considered. Notable exceptions are those of a few authors which explained the agglomeration of different powder mixtures as a consequence of increased powder stickiness (Fitzpatrick, 2007) or a change in the deformability and viscosity of the wet mass (Palzer, 2005) when the powder temperature is below the material glass transition temperature.

The aim of this work is to close the gap in understanding how the main formulation properties affect the early stage in the agglomeration of a powder mixture, which is not composed by

inert glass beads but by amorphous and crystalline particles. In order to achieve this result, the impeller torque profile analysis has been coupled with the binder glass transition concept. It has been demonstrated that the granulation onset can be identified as an abrupt increase in the impeller torque value when the amount of the added liquid exceeds a critical threshold indicated here as minimum liquid volume (MLV).
The experimental results have been, thus, gathered in a new formulation map which combines the key elements of the powder mixture and gives the minimum liquid volume necessary to start the agglomeration process. It has been also demonstrated how to construct the formulation map using independent measurement of the dry binder glass transition temperature.

2.3 Materials and methods

Variations of a common, active-free pharmaceutical formulation were considered. The resultant formulations were mixtures of amorphous and crystalline powders.
Lactose monohydrate 150 mesh (Lactochem® Regular Powder 150 M, Friesland Foods, Zwolte, The Netherlands) and microcrystalline cellulose (MCC) (Pharmacel® 101, DMV International, Veghel, The Netherlands) were used as main diluents. Croscarmellose sodium (Ac-Di-Sol®, FMC Biopolymer, Philadelphia, USA) was used as disintegrant while the solid binders were Hydroxypropylmethylcellulose HPMC (Pharmacoat® 603/Methocel® E5, Shin-Etsu Chemicals, Niigata, Japan) or Polyvinylpyrrolidone PVP (Kollidon® K30, BASF, Ludwigshafen, Germany). Excipients were granulated using deionized water at 20°C.
Experiments were performed in a small scale, top driven granulator (MiPro 1900 ml, ProCepT, Zelzate, Belgium) with a stainless steel vessel, a chopper and a three bladed impeller. Granulator was equipped with a measuring/registering system for impeller torque and powder temperature values during granulation.
The volumetric fill level of the vessel was 40%, for a weight of about 400 g. A premixing stage at 1000 rpm and for 5 min was performed prior each of the granulation experiments. Granulating liquid was added through a tube with a 1 mm diameter by a computer controlled dosimeter.

Two experimental sets were performed. In the first set three granulation experiments were carried out to determine the influence of impeller speed on impeller torque profiles and on particle size distribution of the final granules. At this stage powder mixture composition was held constant and was (on weight basis): lactose monohydrate 150M (73.5%), microcrystalline cellulose (20%), HPMC (5%) and croscarmellose sodium (1.5%). All the experiments were stopped immediately after liquid addition so that the massing phase was not carried out.

Variable conditions were: the impeller speeds at 500, 850 and 1200 rpm, whereas the total amount of liquid and liquid addition flow rate were always fixed at 100 ml and 10 ml/min respectively.

A second set of granulation experiments was performed with different formulation compositions under the same process conditions (i.e. impeller speed of 850 rpm, chopper speed of 3000 rpm, total amount of water added of 100 ml and water addition rate of 10 ml/min).
This experimentation was designed to determine the role of the dry binder on the granule growth phase. The changes in the formulation composition involved the binder type (HPMC and PVP) and amount (in the range 2.5-10% w/w) as shown in Table 2.1.

Table 2.1 Formulation composition for the second experimental set

Experiment	Lactose Monohydrate 150 M amount (% w/w)	Microcrystalline Cellulose MCC amount (% w/w)	Binder type and amount (% w/w)	Croscarmellose sodium amount (% w/w)
1	76.0%	20% constant	HPMC, 2.5%	1.5% constant
2	73.5%		HPMC, 5.0%	
3	71.0%		HPMC, 7.5%	
4	68.5%		HPMC, 10.0%	
5	76.0%	20% constant	PVP, 2.5%	1.5% constant
6	73.5%		PVP, 5.0%	
7	71.0%		PVP, 7.5%	
8	68.5%		PVP, 10.0%	

Granule samples were taken immediately after the end of the wetting time and dried. Drying was given a special care to preserve as much as possible the granules' size. A first gentle drying was carried out at constant temperature and pressure (20°C and 1 bar) in a mildly ventilated drying room, and a second drying in an oven for 1 h with a temperature of 50°C and a pressure of 5 mbar. The wet material was arranged as a thin layer (thickness was about 5 mm). This procedure was followed for minimizing incidental alteration in particle size distribution (PSD) due to the drying method (e.g. attrition in fluid bed dryer, caking in oven at high temperature).

The PSD was characterized by sieve analysis and image analysis. The sieving method consisted on 5 mm of vibration amplitude for a 10 min analysis time. Sieves apertures were: 45, 90, 180, 250, 355, 500, 710, 850 and 1000 μm. Image analysis of granulates was performed using a camera with a 2/3 inch CCD (Jai, CV-300) and interfaced with a Image Tool PC program (ImageTool©, Copyright 2008, Evans Technology, Inc.).

A gravimetric analysis system (IGAsorp, Hiden Isochema, Warrington, UK) was used in order to determine the water sorption isotherm for each formulation component at 25°C.
Binder samples were kept at different relative humidity grades under nitrogen flow; the weight change of each binder sample during the time course analysis was measured by a hygrometer. The exposure time of each sample to the different humidity grade corresponded to the time at which binder sample weight did not change anymore or otherwise to a maximum time of 12 h.

Curves representing influence of water content on binder glass transition temperature were determined by DSC. HPMC and PVP duplicate samples (about 500mg) were preconditioned in a atmosphere at given RH%. Samples were weighted and spread as a thin layer (about 0.5mm) in a series of 4 hermetic vessels, where the humidity was maintained by saturated salt solutions covering a wide range of relative humidity (11-90% RH). Samples remained in the controlled atmosphere for 7 days. Water content in binder samples was verified using Karl-Fisher titration.
Glass transition temperature for each sample was then measured by temperature modulated differential scanning calorimetry (TMDSC, TA Instruments Q2000, with T_0 technology). TMDSC applied the flowing heating policy: first equilibration stage at 80°C, then at -50°C for 5 min (heating rate respectively 10°C/min and -10°C/min); then heating up to a maximum temperature of 120°C (5°C/min), using a modulation amplitude of ± 1°C every 60 s. Measures were performed using hermetic aluminium pans (T_0 pans), in which 5-10 mg samples were weighted.

2.4 Results and discussion

The first experimental set was performed to analyze the effect of impeller speed on the shape of torque profiles, at constant formulation.
Fig. 2.1(a) shows the numerically filtered torque profiles obtained from the first granulation experiments as a function of the added liquid. As can be seen, the shape of the profiles obtained using different impeller speeds is very similar. In accordance with the explanation proposed by Leuenberger et al. (2009), the impeller torque profile is a measure of the resistance of the wet mass to mixing and it can be divided into different phases, characterizing different stages during the agglomeration process. Firstly, the torque value increases almost linearly with the water addition, suggesting a progressive densification of the wet mass. A decrease in the slope is then observed, which can be explained by an increased lubrication of the mass which causes a decrease of the stresses on the impeller. A sudden increase in the slope can be noted when the added water volume is larger than a critical value. This abrupt

increase in the slope denotes the formation of the liquid bridges and the achievement of the pendular state.

In order to best identify the liquid volume required to obtain the pendular state, the first derivative was calculated and plotted as a function of the added liquid in Fig. 2.1(b). As can be noticed in Fig. 2.1(b), the minimum value in the first derivative profile does not strongly depend on the impeller speed, suggesting it may depend mainly on the formulation properties.

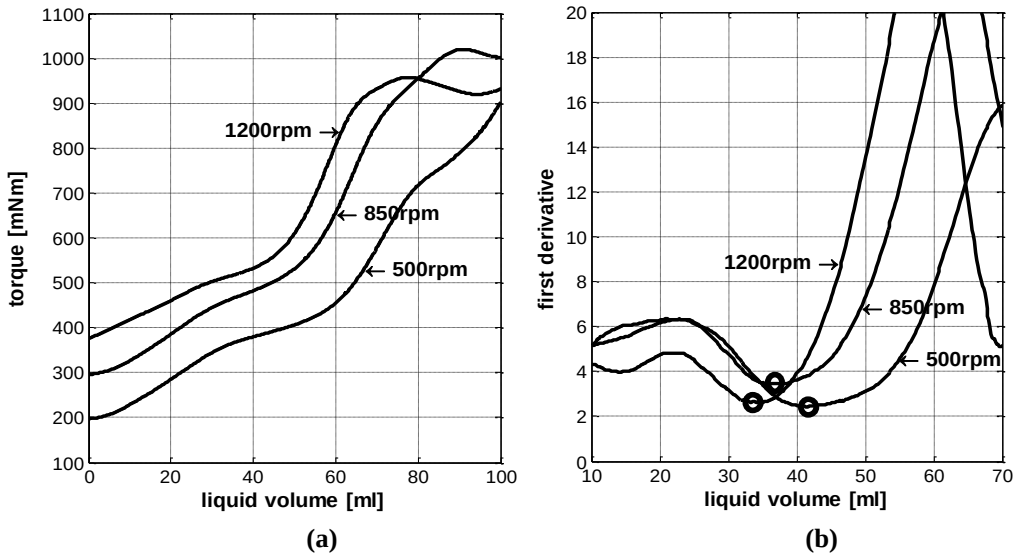

Fig.2.1. Results of the first experimental set: (a) impeller torque as a function of the liquid addition at different impeller speed and constant formulation and (b) determination of the points corresponding to the first derivative minimum value (circles)

In order to monitor the PSD evolution during the agglomeration, image analysis was used to obtain a more accurate description of the agglomeration phase. The operative conditions of the middle curve in Fig. 2.1(a) (that at 850 rpm) have been chosen as a reference and several samples have been collected during the granulation at different moisture contents (20, 40, 60, 80% of water addition). Since the dimension of collected samples were too small (1-2 g) to perform a sieve analysis, images of the samples were taken with a digital camcorder interfaced to an image analysis program. The binary images of the samples can be observed in Fig. 2.2 and compared with torque and torque first derivative profiles. The simple visual inspection of the images shows that a substantial increase of the size of the granules occurs after the addition of 40% out of 100ml of water which correspond to the minimum in the derivative profile.

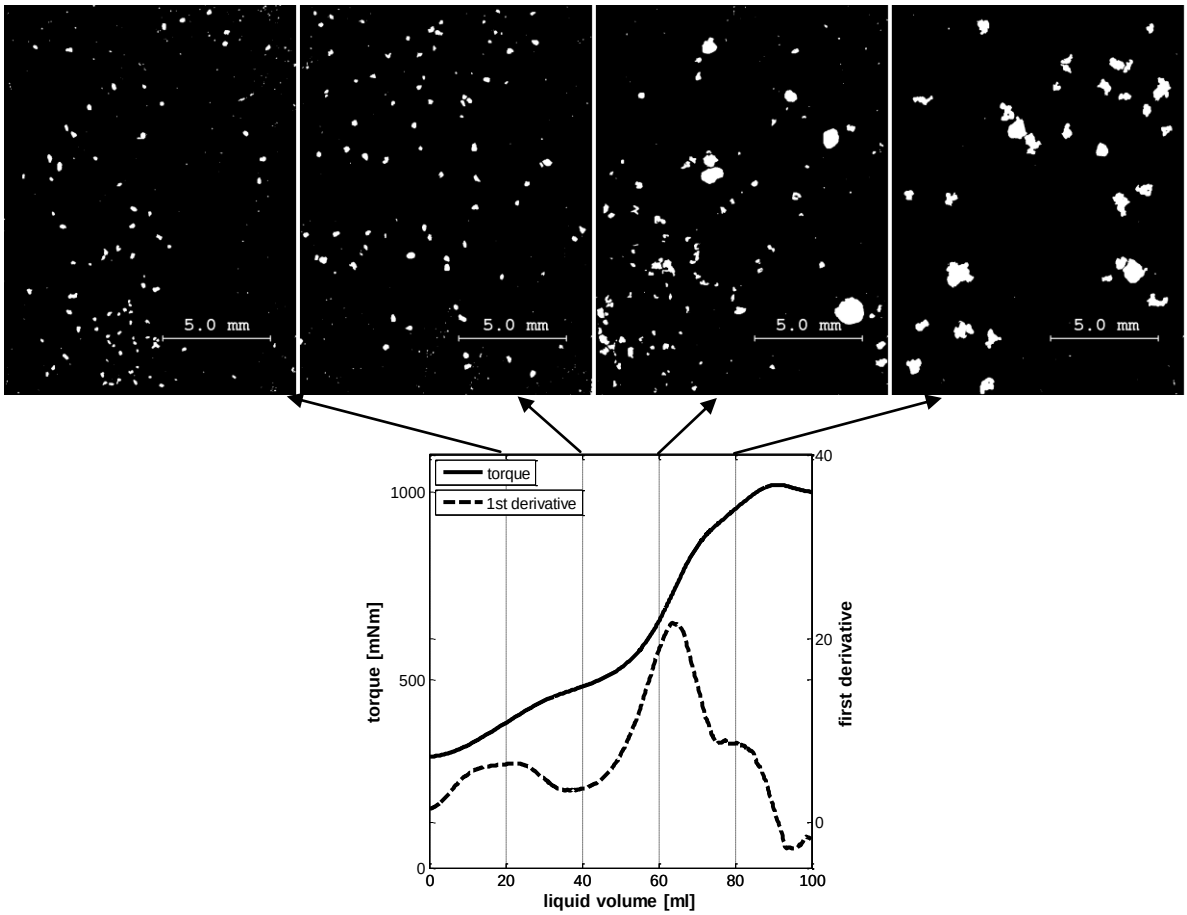

Fig.2.2. Effect of the moisture content on the granule size evolution during the granulation process: pictures of the granules show a negligible growth until the about 40 ml, whereas larger agglomerates can be counted after this point

In order to confirm this behaviour and to consider the particle size distribution of the whole batch (not just of a small sample), the experiment was repeated and stopped after the addition of two different quantities of liquid (40 and 100ml respectively). Sieve analysis was carried out in order to compare the PSDs. Point A in Fig. 2.3(a) was obtained interrupting the experiment at the condition of minimum value in the derivative profile. Whereas point B represents the condition immediately after all the liquid was added. Fig. 2.3(b) shows the corresponding PSDs (the PSD of the dry formulation has been also added). As can be noted in Fig. 2.3(b), there is a negligible difference between the PSD of the dry formulation and the PSD obtained at point A. A substantial difference between the point A and the point B can be instead appreciated, thus indicating that most of the granulation process occurs after the point A.

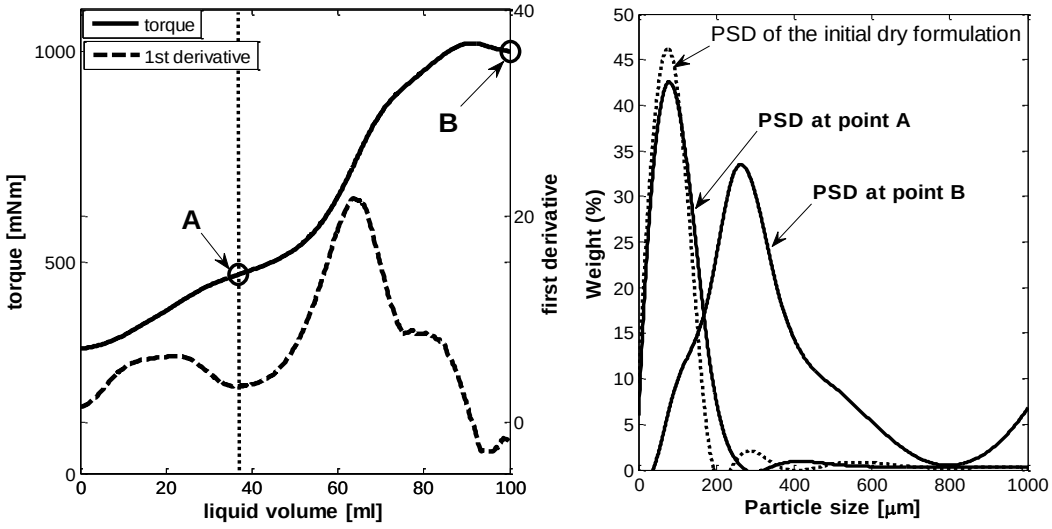

Fig.2.3. Results of the sieve analysis carried out in order to compare the PSD at point A (before the sudden increase in the slope) with the PSD at the end of the experiment

As can be inferred from Figs. 2.2 and 2.3, the point A corresponds to the liquid volume required to increase significantly torque value (i.e. minimum in the first derivative profile) and in this sense can be considered as the minimum liquid volume (MLV) required to start most granulation process.

Similar results were presented by some authors, for example by Ritala et al. (1988): dicalcium phosphate was granulated with different binder solutions observing an abrupt increase in mean granule diameter when the liquid saturation exceeded certain specific values.

It is also interesting to note the role of the dry binder on the torque profile shape and on the PSD obtained at the end of the experiment. As shown in Fig. 2.4(a), the impeller torque profile obtained without the dry binder does not show the sudden increase in the slope of the torque profile after about 40 ml. As a matter of fact, the PSD of the product without the dry binder is very similar to the PSD of the initial dry formulation thus indicating an unimportant and slower agglomeration process (compare PSDs in Fig. 2.4(b)).

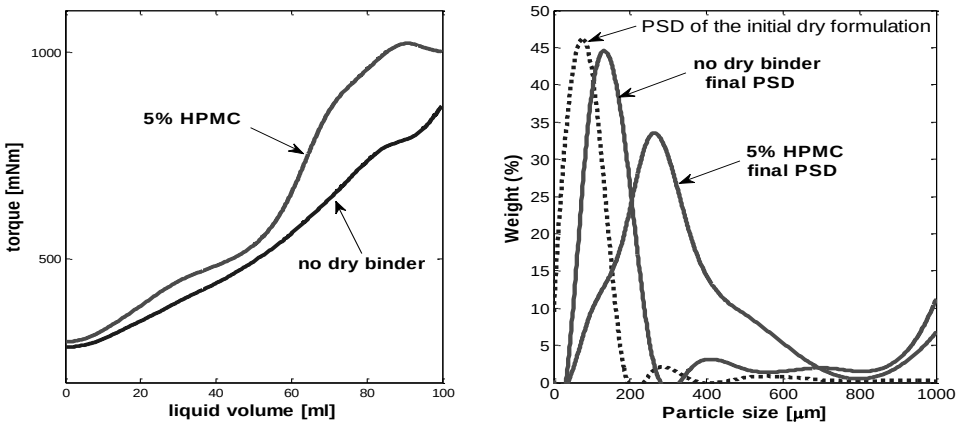

Fig.2.4. Comparison between the granulation experiments carried out with or without the dry binder: (a) comparison between the torque profiles and (b) the PSDs at the end of the granulation process

Having identified the MLV as a marker of the granulation onset, the second part of the experimentation has been designed to understand the impact of the formulation components on the MLV (as detailed in Table 2.1).

Particularly, two dry binder types (HPMC and PVP) at different amounts (i.e. from 2.5 to 10% w/w) were tested within the formulation of the first experimental set.

Figs. 2.5 and 2.6 summarize the results obtained in terms of first derivative of the torque profiles, with the two binders at various concentrations. MLVs were determined as local minimum of the first derivative. Figs 2.5 and 2.6 also report the PSD measured (sieve analysis) at the end of the granulation experiments. The relatively large weight fraction on the 1000 μm sieve was partially due to caking in the oven at high temperature.

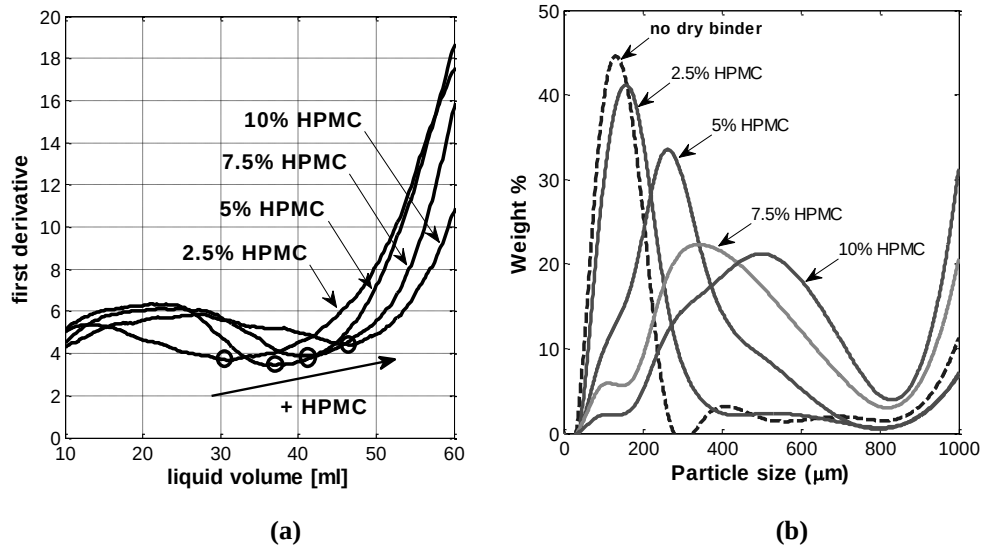

Fig.2.5. Effect of different concentration of (a) HPMC on MLV determination and (b) PSD at the end of the granulation experiments

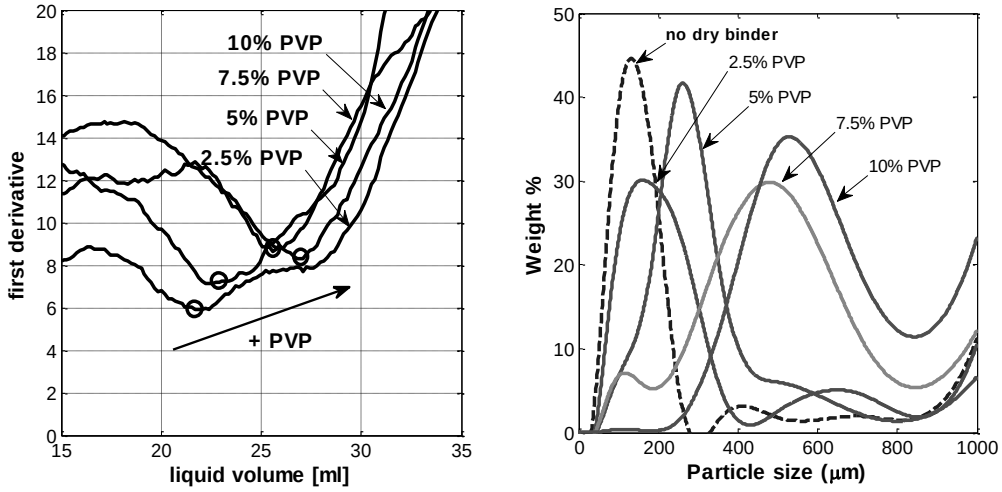

(a) **(b)**

Fig.2.6. Effect of different concentration of (a) PVP on MLV determination and (b) PSD at the end of the granulation experiments

As can be appreciated, the onset of granulation is delayed with increasing the binder amount (that means a higher amount of liquid is required), with both HPMC and PVP. MLV increase is larger for HPMC than PVP.

In addition, the rate of torque increase with PVP is higher than that with HPMC (Figs. 2.5(a) and 2.6(a)). It is suggested that this fact is due to a more relevant hygroscopicity of the PVP powder as compared with HPMC. The higher hygroscopicity determines a faster formation of a viscous solution.

The comparison between the PSDs of the final granules obtained using various dry binder concentrations highlights the essential role of the dry binder in the agglomeration process.

In order to explain the dissimilar growth behaviour due to a different dry binder concentration, the scheme in Fig. 2.7 can be considered. It represents the static yield strength of the wet granules as a function of the pore saturation (Ennis, 2006; Rumpf, 1962).

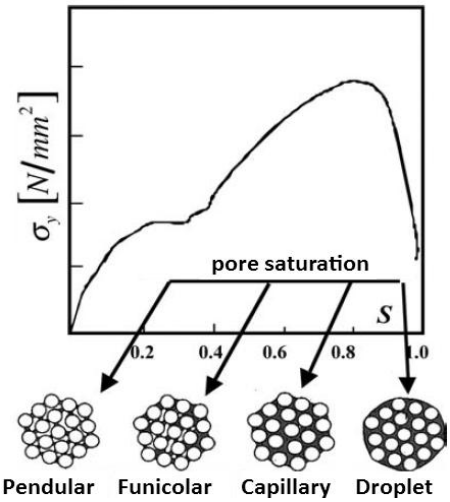

Fig.2.7. Static yield strength of the wet granule as a function of the pore saturation (Ennis, 2006; Rumpf, 1962)

As pointed out by Leuenberger et al. (2009), the point A (see Fig.2.3) indicates the achievement of the pendular state. This state of pore filling causes the formation of the first liquid bridges and the beginning of the granule growth.

However powder particles can be composed by crystalline or amorphous material or both. Adding water means decreasing the glass transition temperature of the amorphous material since water is a strong plasticizer. When the powder temperature is close to the glass transition temperature, the molecular mobility increases and leads to the migration of the amorphous material into the water on the particle surface. The increase in viscosity of the material on the particle surface causes a significant increase in stickiness which promotes the agglomeration process (Fitzpatrick, 2007; Palzer, 2005).

The penetration of the water into the capillaries leads to the achievement of the pendular state and, in presence of an amorphous material, the starting of stickiness (point A in Fig. 2.3).

Palzer (2009) described the strength of the adhesion forces as a sum of two contributes: the hygro-capacity (or hygroscopicity) and the hygro-sensitivity of the powder. The hygro-capacity is the ability to bind water by absorption in the molecular matrix or on the surface area, whereas the hygro-sensitivity is a marker of the increase in the viscosity due to the absorbed water.

Accordingly, amorphous water-soluble particles absorb important amounts of water (high hygro-capacity) and the variation of their visco-elastic properties is usually considerable (high hygro-sensitivity). On the other hand, the water amount in crystalline powders generally increases slightly with the relative humidity and their mechanical properties do not change (below the solubilization conditions). Moreover, the dissolution process of crystalline structures is much slower due to the lower permeability of the crystalline matrix and the endothermic dissolution process (Palzer, 2010).

The processed formulation presented:

- two main fillers: lactose monohydrate (mainly crystalline, water-soluble) and MCC (mainly crystalline, water-insoluble);
- dry binder: HPMC or PVP (both amorphous, water-soluble).

The hygro-capacity of the formulation components can be described by the water sorption isotherms in Fig. 2.8.

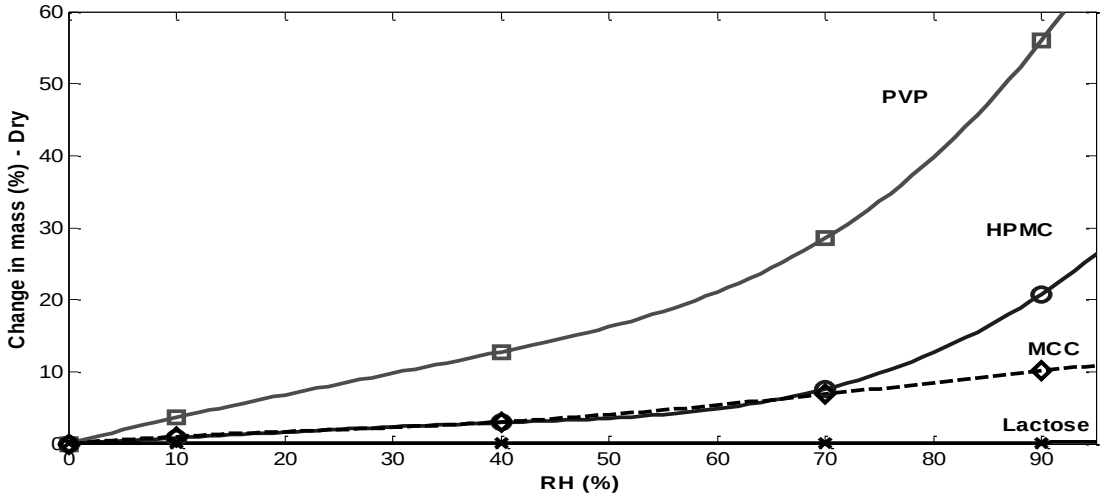

Fig.2.8. Sorption isotherms (25°C) of the formulation components: PVP (squares), HPMC (circles), MCC (diamonds) and lactose monohydrate (crosses)

The dry binder, amorphous and water-soluble in nature, presents a higher hygro-capacity and a much higher hygro-sensitivity in comparison to the fillers. For this reason the dry binder (HPMC or PVP) can be considered as the most important binding agent and the two fillers can be considered as a sole diluent, which absorbs water but has a weakly binding strength. As can be noticed in Fig. 2.8, PVP presents a higher hygro-capacity (or hygroscopicity) than HPMC. It is suggested that this fact leads to an advance formation of the viscous bridges (Figs. 2.5(a) and 2.6(a)).

In order to separate and quantify the effect of the key formulation components on the MLV, a triangular formulation map has been proposed (Fig. 2.9): the combinations of the main formulation components (diluent, dry binder and liquid binder) can be effectively represented in the ternary diagram where each component is pure in a vertex.

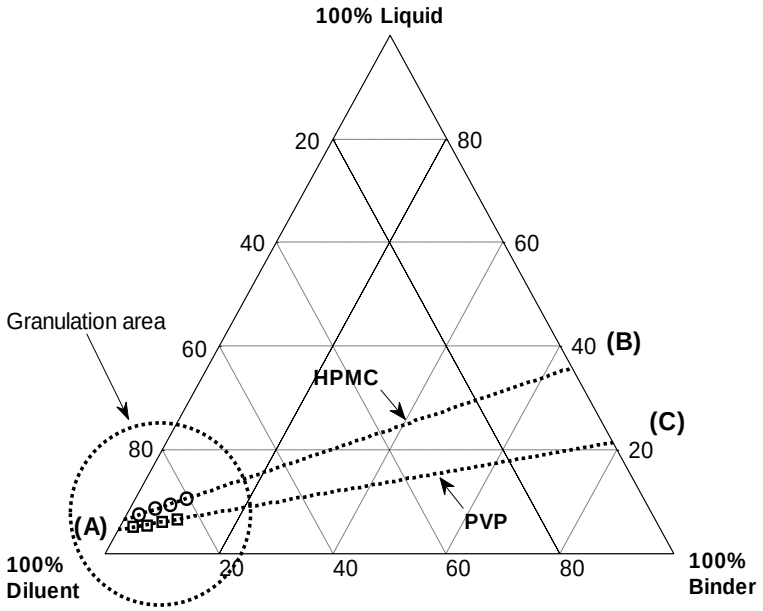

Fig.2.9. Formulation map: representation of the effect of the main formulation components on MLV through a ternary diagram. Each vertex represents a key component: the main diluent (lactose monohydrate and microcrystalline cellulose), dry binder (HPMC or PVP) and liquid (water). The MLV are experimentally determined in presence of HPMC or PVP and respectively marked with circles and squares

Dry formulation composition can be identified as a point on binder-diluent axis. With the addition of water, the point representing the actual composition of the granulation system moves from the binder-diluent axis towards the liquid vertex.

MLV experimentally measured from Table 2.1 experiments (Figs. 2.5 and 2.6) are represented in the ternary diagram by some markers (HPMC = circles; PVP = squares).

As can be observed in Fig. 2.9, the markers arrange in two straight lines. Each line represents a specific diluent-dry binder-liquid system and intersects the diluent-liquid and the binder-liquid axes.

Interestingly, the HPMC line and PVP line intersect the diluent-liquid axis very close to each other, outlining point A in Fig. 2.9. This point represents the water amount absorbed by the fillers and therefore not available for the dry binder. On the other hand, the intersection between the straight line and the binder-liquid axis appears to be strongly binder-specific. This difference clearly denotes a different dry binder-water interaction.

According to the previous explanation in the light of the glass transition concept, the agglomeration process of the powder mixture can be described as follows:

1) absorption of the granulating liquid and nucleation: the nuclei formation phase can be described by the nucleation regime map proposed by Litster et al. (2001);
2) water is split up among the formulation components on the basis of the hygro-capacity of each component;

3) water absorbed by the dry binder works as plasticizer and decrease the dry binder glass transition temperature T_g;
4) when the water addition decreases binder T_g to equal the powder temperature (i.e. ambient temperature), the binder becomes sticky, the impeller torque value rapidly increases and the growth accelerates. The bridges between the particles are mainly due to the stickiness, which causes stronger attractive interactions between the surfaces.

As pointed out by Iveson et al. (2001), the liquid may not have enough time to reach the equilibrium state therefore the maximum water amounts absorbed from diluent and binder (steps 2 and 3) are not equilibrium values: it is hypothesized that agreement between the theoretical equilibrium value and the actual absorbed water amount mainly depends on the different component hygro-capacity (Fig. 2.8) and on the water sorption kinetics, which is also affected by the mixing energy and efficiency.

In order to determine the effect of water content on HPMC and PVP glass transition temperatures, dry binder samples have been maintained in closed vessel at different relative humidity, as explained above. The curves representing glass transition temperature as a function of the equilibrium water content for HPMC and PVP are shown in Fig. 2.10.

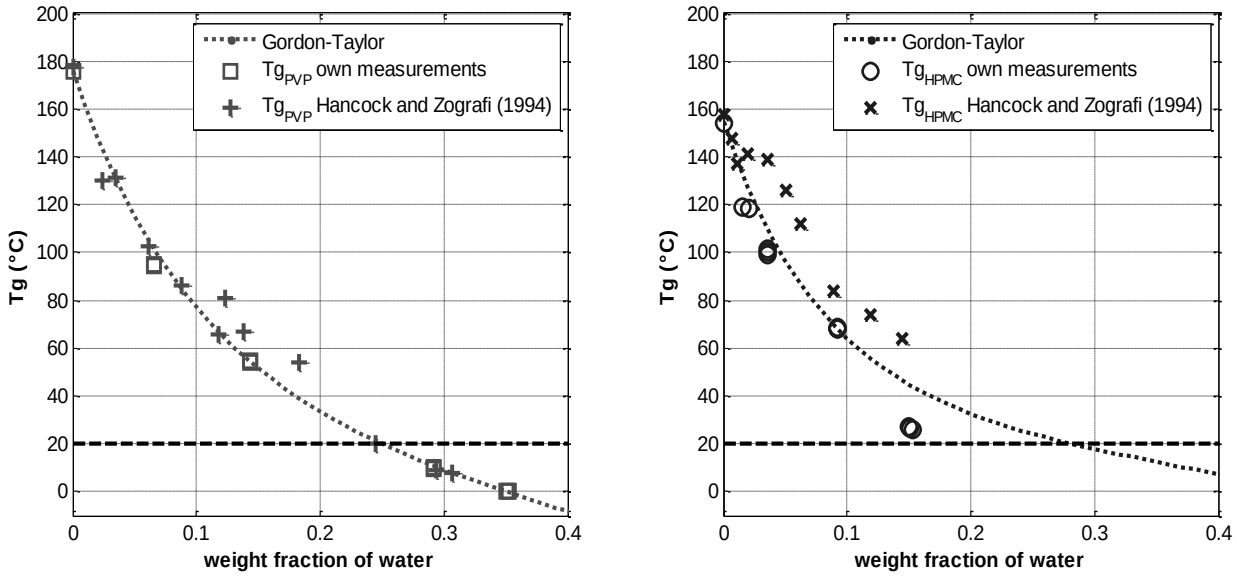

Fig.2.10. Glass transition temperature as a function of water content in samples of (a) PVP and (b) HPMC: comparison between the experimental data, literature (Hancock and Zografi, 1994) and the dotted line representing experimental data and literature fitted to modified Gordon-Taylor model (Hancock and Zografi, 1994)

Glass transition temperature of wet binder sample can be roughly estimated using Gordon-Taylor equation (Gordon and Taylor, 1952):

$$T_g = \frac{w_1 T_{g1} + k w_2 T_{g2}}{w_1 + k w_2} \qquad \text{Eq (2.1)}$$

where k is an empirical constant, T_{g1} is the dry binder glass transition temperature, T_{g2} is the water glass transition temperature (-138°C), w_1 and w_2 are respectively the binder and water weight fractions (with $w_1 = 1\text{-}w_2$).

k values for different binder types have been calculated for example by Hancock and Zografi (1952). In the same work, Hancock and Zografi (1952) proposed a modified Gordon-Taylor equation in order to best fit the experimental data: this equation introduces an additional quadratic parameter in Equation (2.1). The resulting T_g is:

$$T_g = \frac{w_1 T_{g1} + k w_2 T_{g2}}{w_1 + k w_2} + q w_1 w_2 \qquad \text{Eq (2.2)}$$

where q is an empirical constant reflecting the specific binder-water interaction.

Assuming the reference condition:

$$T_g = T_a \approx T_{powder}, \qquad \text{Eq (2.3)}$$

where T_a is the ambient temperature expected to be equal to the powder temperature T_{powder}, the corresponding water content w_2^* can be expressed as follows:

$$w_2^* = w_2(T_g \approx T_{powder}). \qquad \text{Eq (2.4)}$$

This water amount is the quantity needed for the dry binder glass transition and the formation of a highly viscous mixture.

Experimental and literature data (Hancock and Zografi, 1994) in Fig. 2.10 were fitted to the Equation (2.2). As can be seen in Fig. 2.10, the intersection between the glass transition curves and the ambient temperature gives the water amount required to obtain the dry binder glass transition.

It can be noted in Fig. 2.10 that the literature and the experimental data for the PVP are in agreement, thoroughly fitted to the modified Gordon-Taylor model. The moisture content required for the glass transition is furthermore in agreement with the water amount identified by point (C) in Fig.2.9 (respectively 0.24 in Fig.2.10 and 0.22 in Fig.2.9). The point (C) can thus be easily determined using static T_g measurements. As a first estimation, the water amount absorbed by the hygroscopic diluent components in point (A) can be measured from Fig.2.8: the RH% at which the PVP glass transition occurs (corresponding to the water content w_2^*) can be considered as a reference condition for the identification of the contribution of each hygroscopic component.

Regarding the HPMC glass transition temperatures, the agreement between experimental and literature data is fairly satisfactory except for the last experimental measurement (water weight fraction of about 0.15). Moreover, the maximum attainable moisture content for a HPMC sample in static conditions at 90% is about 0.20. This fact leads to a lower number of experimental points at high moisture contents compared to the PVP-water system. For this reason the data fitting for HPMC is not as suitable as for PVP. This fact could explain the discrepancy between the moisture content required for the glass transition and the point (B)

(respectively about 0.29 in Fig. 2.10 and 0.36 in Fig. 2.9). The delay in the actual moisture content - point (B) - compared to the equilibrium value obtained with static measurements could also be explained by considering the non-ideal water sorption kinetics in the granulator, which depends on many variables, e.g. the mixing energy, the nucleation conditions, the competition between the diluent and the binder in the water sorption mechanism and in the binding process. Since the mixing energy can be optimized in order to get a good liquid distribution (Litster et al., 2001), the competition between the diluent and the dry binder in the water sorption kinetics plays an important role. It follows that the competition is less critical when the dry binder is much more hygroscopic and hygro-sensitive than the diluent (e.g. PVP as dry binder). Whereas the diluent hygroscopicity is comparable to the dry binder hygroscopicity, the water sorption competition is more complex and needs further investigation to elucidate its role on the MLV determination.

2.5 Conclusions

The present research analyzes the role of some important formulation properties (e.g. glass transition temperature, hygroscopicity) on the early stage of the granule growth during a high-shear wet granulation process. A pharmaceutical powder mixture containing amorphous and crystalline particles was processed. The agglomeration process was monitored using on-line impeller torque measurements and systematic PSD analysis (sieve and image analysis).

The analysis of the torque profiles plotted as a function of the added water revealed the presence of a minimum liquid volume (MLV) required to strongly increase the torque value (i.e. the resistance of the wet mass to mixing) and to start most of the granule growth. The MLV was then chosen as a reference point and then a detailed study of the role of the powder properties in the granulation mechanism was carried out. As a result of this research, the initial powder mixture was ideally split into two main components (diluents and dry binder) according to their expected hygro-capacity and hygro-sensitivity (Palzer, 2005)

A new formulation map was therefore proposed in order to simplify the granulation system: a ternary diagram, through a graphical construction, identifies the moisture content required to make the dry binder sticky (i.e. required to yield the binder glass transition) and the water amount absorbed by the diluent. The initial dry formulation is represented by a point on the diluent-dry binder axis.

The interactions between the dry binders (HPMC and PVP) and water were analyzed performing independent measurements of the glass transition temperature at different moisture content and fitting the experimental data with a Gordon-Taylor based equation. The water sorption isotherm for each formulation component was measured as well. A method for obtaining the most important points on the edges of the formulation map using these independent measurements has therefore been proposed.

Results show that it is possible to carry out an early assessment of the minimum liquid volume required to start most of the granule growth through an application of a Gordon-Taylor model and performing some independent measurements of the initial formulation properties. It has been demonstrated that the procedure can easily be applied when the dry binder is clearly more hygroscopic and hygro-sensitive than the diluent. On the other hand, the competition dry binder/diluent in the water sorption might promote discrepancies between the actual and the predicted-equilibrium based values. In spite of these last considerations, the method proposed in this work can be considered a helpful tool for the formulation design and has a considerable potential to increase the predictability of the granule growth behaviour as a function of the formulation composition.

2.6. References

G. Betz, P. J. Bürgin, H. Leuenberger, Power consumption measurement and temperature recording during granulation, International Journal of Pharmaceutics 272 (2004) 137-149.

L. Briens, D. Daniher, A. Tallevi, Monitoring high-shear granulation using sound and vibration measurements, International Journal of Pharmaceutics, 331 (2007) 54-60.

D. Daniher, L. Briens, A. Tallevi, End-point detection in high-shear granulation using sound and vibration signal analysis, Powder Technology, 181 (2008) 130-136.

B.J. Ennis, Theory of Granulation: an Engineering Perspective, Handbook of Pharmaceutical Granulation Technology (2nd Ed.), Taylor and Francis Group, 2006.

J.J. Fitzpatrick, Particle properties and the design of solid food particle processing operations, Food and Bioproducts Processing 85 (2007) 308-314.

M. Gordon, J.S. Taylor, Ideal co-polymers and the second order transitions of synthetic rubbers. 1. Non-crystalline co-polymers, Journal of Applied Chemistry 2 (1952) 493-500.

B.C. Hancock, G. Zografi, The relationship between the glass transition temperature and the water content of amorphous pharmaceutical solids, Pharmaceutical Research 11 (1994) 471-477.

S.M. Iveson, J.D. Litster, Growth regime map for liquid-bound granules, AIChE Journal 44 (1998) 1510–1518.

S.M. Iveson, J.D. Litster, K.P. Hapgood, B.J. Ennis, Nucleation, growth and breakage phenomena in agitated wet granulation processes: a review, Powder Technology 117 (2001) 3–39.

P.C. Knight, Structuring agglomerated products for improved performance, Powder Technology 119 (2001) 14–25.

M. Landin, R. C. Rowe, P. York, Characterization of wet powder masses with a mixer torque rheometer. 3. Nonlinear effects of shaft speed and sample weight, Journal of Pharmaceutical Science 84/5 (1995) 557-560.

M. Landin, P. York, M. J. Cliff, R. C. Rowe, A. J. Wigmore, The effect of batch size on scale-up of pharmaceutical granulation in a fixed bowl mixer-granulator, International Journal of Pharmaceutics 134 (1996) 243-246.

H. Leuenberger, Granulation, new techniques, Pharma Acta Helvetica 57 (1982) 72–82.

H. Leuenberger, M. Puchkov, E. Krausbauer, G. Betz, Manufacturing pharmaceutical granules: Is the granulation end-point a myth?, Powder Technology 189 (2009) 141-148.

J.D. Litster, B. J. Ennis, Size reduction and size enlargement, Perry's Chemical Engineers' Handbook. McGraw-Hill Companies, 1999.

J.D. Litster, K.P. Hapgood, J.N. Michaels, A. Sims, M. Roberts, S.K. Kameneni, T. Hsu, Liquid distribution in wet granulation: dimensionless spray flux, Powder Technology 114 (2001) 29–32.

S. Palzer, The effect of glass transition on the desired and undesired agglomeration of amorphous food powders, Chemical Engineering Science 60 (2005) 3959-3968.

S. Palzer, Influence of material properties on the agglomeration of water-soluble amorphous particles, Powder Technology 189 (2009) 318-326.

S. Palzer, The relation between material properties and supra-molecular structure of water-soluble food solids, Trends in Food Science & Technology 21 (2010) 12-25.

M. Ritala, P. Holm, T. Schaefer, H. G. Kristensen, Influence of liquid bonding strength on power consumption during granulation in a high shear mixer, Drug Development and Industrial Pharmacy, 14:8 (1988) 1041 – 1060.

H. Rumpf, The strength of granules and agglomerates, Agglomeration, Interscience, 1962.

W.J. Wildeboer, J.D. Litster, I.T. Cameron, Modelling nucleation in wet granulation, Chemical Engineering Science 60 (2005) 3751 – 3761.

Chapter 3

Combining formulation and process aspects for optimizing the high-shear wet granulation of common drugs

3.1 Summary

The purpose of this research was to determine the effects of some important drug properties (such as the primary particle size distribution, hygroscopicity and solubility) and process variables on the granule growth behaviour and final drug distribution in high shear wet granulation. Results have been analyzed in the light of widely accepted theories and some recently developed approaches.

A mixture composed of drug, some excipients and a dry binder was processed using a lab-scale high-shear mixer. Three common active pharmaceutical ingredients (paracetamol, caffeine and acetylsalicylic acid) were used within the initial formulation. Drug load was 50% (on weight basis).

Influences of drug particle properties (e.g. primary particle size and shape, hygroscopicity) on the granule growth behaviour were analyzed. Particle size distribution (PSD) and granule morphology were monitored during the entire process through sieve analysis and scanning electron microscope (SEM) image analysis. Resistance of the wet mass to mixing was furthermore measured using the impeller torque monitoring technique.

Results showed that drug primary PSD clearly affects granule growth behaviour: the finest primary PSD leaded to slower and more gradual granule growth. On the other hand, as primary PSD increased, growth was more likely to occur via a crushing and layering mechanism.

Moreover, drug distribution in final product strongly depended on the process conditions: worse liquid distribution conditions determined poorer content uniformity, especially in the case of fine primary PSD.

To be submitted in:
M. Cavinato, E. Andreato, M. Bresciani, I. Pignatone, G. Bellazzi, E. Franceschinis, N. Realdon, P. Canu, A. Santomaso. International Journal of Pharmaceutics.

3.2 Introduction

Pharmaceutical industries frequently turn to high shear wet granulation in order to convert fine cohesive powders into dense and round granules. The granules are produced by vigorous mixing of a wet powdered mixture generally composed of drug, some excipients and binder [Litster and Ennis, 2004]. The overall purpose of this operation is to obtain a final product with improved characteristics, such as better flowability and compressibility. Other benefits can be obtained using high shear wet granulation: for example, the distribution of the drug in the final product as well as the dissolution properties of tablets can be improved [Gokhale et al., 2006].

Most of high shear mixers consist of a stainless steel vessel, a three-bladed impeller and a chopper. Typically, high shear wet granulation is performed as a batch operation. Firstly, dry powders are mixed together by the impeller blade which rotates through the powder bed. Secondly, liquid binder is added while the impeller ensures liquid spreading and the chopper breaks down wet, coarser agglomerates. Finally, densification of granules takes place during wet massing through impeller rotation and without liquid addition [Gokhale et al., 2006].

Besides the description of macroscopic phenomena, some researchers also tried to explain the agglomeration process in a high shear mixer at microscopic level. According to the saturation degree of pore spaces in the granule, Newitt and Conway-Jones (1958) firstly proposed the existence of three saturation states which represent a progressive increase in moisture content: pendular, funicular and capillary state. Firstly, surface tension at particle-liquid interface and the presence of liquid bridges cause the formation of first agglomerates, thus leading to the pendular state. With increasing the liquid content, a continuous network of liquid can be noted at the funicular state. The capillary state corresponds to the saturation degree at which pore spaces are completely filled. Barlow (1968) also introduced the droplet state, which occurs when liquid completely surrounds the granule.

Many attempts to follow the granule growth have been made by measuring either the power consumption or impeller torque. Leuenberger and co-workers [Leuenberger et al.,1979; Bier et al., 1979] compared both of these methods and realized that power consumption and torque noticeably depend on the cohesive force of the wet mass or the tensile strength of the agglomerates. Moreover, they found a reliable relationship between power or torque profiles and the saturation degree of the wet mass [Imanidis, 1986; Leuenberger et al., 1981; Leuenberger, 1982; Leuenberger and Imanidis, 1984]. Particularly, a sudden increase of the power/torque value was noted when the pendular state was reached. As more liquid binder was added, torque and power consumption resulted to be relatively constant.

According to these approaches, granule growth behaviour in high shear wet granulation has often been described considering primary particles as inert material held together by a simple Newtonian liquid added in the liquid phase. However, the reality is frequently more

complicated: pharmaceutical formulations are usually composed of powders with different characteristics, which interact with the wetting agent and change their properties. For example, the presence of an amorphous component within the initial powder mixture can have strong effects on the granule growth behaviour. Cavinato et al. (2010) showed that the sudden increase in torque profiles can be correlated with the liquid amount required to attain the dry binder glass transition. In these conditions, dry binder stickiness promotes a faster granule growth.

Palzer (2010) recently proposed a clear classification of pharmaceutical/food powders according to their molecular polarity and their supra-molecular structure, thus giving an effective explanation of the behaviour of the powder particles in different agglomeration processes.

Among all the formulation components, the active substance is usually the most critical ingredient. For example, differences in physical properties between drug and excipients or non-optimal process conditions often lead to selective agglomeration of certain components, causing content uniformity problems. Despite the essential importance of the active substance in pharmaceutical high shear wet granulation, relatively few works presented a detailed analysis on the role of drug characteristics (such as, for instance, drug type, primary particle size and shape, hygroscopicity) in the granule growth kinetics [Nguyen et al., 2010; Belohlav et al., 2007].

Thus, the present research is mainly focused on the role of the active ingredient in the agglomeration process. Particularly, the influence of some important drug particle characteristics on the granule growth behaviour has been analyzed: different drugs with different primary particle size and shape were used. Effects of changes in impeller speed or liquid flow rate have been studied as well.

3.3 Materials and methods

3.3.1 Materials

Granules containing a common active ingredient were prepared. The active ingredient was acetylsalicylic acid (Polichimica, Bologna, Italy), paracetamol (Suzhou Sintofarm Pharmaceutical, Jiangsu, China) or caffeine (Polichimica, Bologna, Italy).

Other ingredients included within the initial formulation were: lactose monohydrate 150 mesh (Lactochem® Regular Powder 150 M, Friesland Foods, Zwolte, The Netherlands), microcrystalline cellulose (MCC) (Pharmacel® 101, DMV International, Veghel, The Netherlands), polyvinylpyrrolidone (PVP) (Kollidon® K30, BASF, Ludwigshafen, Germany) and croscarmellose sodium (Ac-Di-Sol®, FMC Biopolymer, Philadelphia, USA).

Deionized water at 20°C was used as wetting agent.

3.3.2 Active ingredient characterization

A first qualitative analysis of drug particle size and shape was carried out using optic microscopy (Leica DM LM/P®, Leica Microsystem, Wetzlar, Germany). A small sample of each active ingredient was placed on a slide. Particles were dispersed using a small amount of silicone oil before analysis.
A more detailed analysis of drug PSD was performed using a laser light scattering (LLS) particle size analyzer (Sympatec Helos/KF®, Sympatec, Clausthal-Zellerfeld, Germany). Three different pressures of dispersing air (1, 2, 3 bar) were used in order to identify possible presence of primary agglomerates and break them. Each of the three active ingredients was analyzed in triplicate applying the highest pressure (3 bar). Measurement interval considered a minimum size of 0.5 µm to a maximum of 350, 875 or 1750 µm, according to drug particle dimension. Resulting PSDs will be represented by the normalized-sectional frequency distribution (volume-based) [Allen (1997), Litster and Ennis (2004)] in order to perform a more reliable and reproducible comparison between PSDs.

Water sorption isotherms at 25°C for active ingredients were determined using a gravimetric analysis system (IGAsorp, Hiden Isochema, Warrington, U.K.). Samples were kept at different relative humidity grades under nitrogen flow. Accordingly, the weight change of each drug sample during the analysis time was measured. The exposure time of each sample to the different humidity grade corresponded to the time at which sample weight did not change anymore or otherwise to a maximum of 4 h.

3.3.3 Granules preparation

An experimental plan was designed in order to analyze the effects of process parameters (impeller speed and liquid flow rate) and formulation variables (type of active ingredient and corresponding size/shape) on the granule growth behaviour and the final product characteristics.
A small scale high shear wet granulator was used (MiPro, 1900 ml vessel volume, ProCepT, Zelzate, Belgium) with a stainless steel vessel, a chopper and a three-bladed impeller. Both impeller torque and powder temperature were monitored during the experiments. Each experiment was stopped immediately at the end of the liquid addition phase, hence wet massing was not performed. Impeller speed during wetting was set at 500 or 1200 rpm, liquid flow rate at 8 or 12 ml/min. The other process variables were kept constant for each granulation experiment: batch size was 40% wt. compared to the vessel volume (i.e. about 400 g of powder, depending on the formulation bulk density) and the total amount of added

water was 25% wt. compared to the batch size. The formulation (on a weight basis) consisted of approximately: active ingredient (50%), lactose monohydrate 150 mesh (23.5%), micro-crystalline cellulose (20%), PVP (5%) and croscarmellose sodium (1.5%).
In total, 16 experiments were performed: values of process variables are reported in Table 3.1.

Table 3.1 Experimental plan: values of the process variables

Experiment number	Active ingredient type	Impeller speed (rpm)	Liquid flow rate (ml/min)
1	Paracetamol	500	8
2		500	12
3		1200	8
4		1200	12
5	Caffeine	500	8
6		500	12
7		1200	8
8		1200	12
9	Acetylsalicylic Acid	500	8
10		500	12
11		1200	8
12		1200	12
13	Without drug (Lactose 73.5% w/w)	500	8
14		500	12
15		1200	8
16		1200	12

3.3.4 Granules characterization

Granule samples were taken after the end of the wetting time and dried in oven at 40°C until constant weight was achieved. Granules were disposed as a thin layer on the oven plate. Drying procedure was designed in order to avoid noticeable alteration of particle size distribution due to caking and attrition phenomena.
Sieve analysis was then performed using a vibrating apparatus (Retsch AS200, Germany) at 5 mm vibration amplitude for 10 min in order to determine PSD of final product. Sieves apertures were: 45, 90, 125, 180, 250, 355, 500, 710, 850 and 1000 μm. Powder fractions were collected and then weighted. Resulting PSDs will be represented by the normalized-sectional frequency distribution (mass-based).

Content uniformity analysis was carried out in order to evaluate the distribution of the active ingredient in different sieve fractions of the final granules. Samples of size fractions corresponding to x_{10}, x_{50} and x_{90} (10^{th}, 50^{th} and 90^{th} percentile respectively) were chopped and dissolved in suitable solvents: deionized water for caffeine, ethanol for paracetamol and acetylsalicylic acid. Solutions were filtered after 3 min sonication and drug content measured

using UV/Vis spectrophotometry. Drug-free granules obtained under the same process conditions were chopped and dissolved in order to prepare the blank for the content uniformity analysis.

Several samples of 1 g each were collected during the granulation process at different moisture content (20, 40, 60, 80, 100% of the total added liquid amount). Magnified images of these samples were taken using a scanning electron microscope (SEM) (Quanta 200 FEG, FEI Company, Czech Republic). Accordingly, pictures were compared in order to study the growth mechanisms.

3.4 Results and discussion

A first analysis of drug particle size and shape was carried out using an optical microscope. This first investigation also permitted to make observations regarding the presence of secondary agglomerates caused by surface forces such as Van der Waals or electrostatic forces. Table 3.2 summarizes the observations derived from the optic microscopy analysis. Drug primary PSD was then accurately measured with a laser light scattering particle size analyzer. Pressure of dispersing air has been chosen in order to break secondary agglomerates and get reliable results. Fig.3.1 shows drug primary PSDs, represented by normalized-sectional frequency distributions (volume based).

Table 3.2 First investigation of active ingredients characteristics through optic microscopy

	Paracetamol	**Caffeine**	**Acetylsalicylic Acid**
Shape	irregular	irregular / columnar	columnar
Mean particle diameter d_{10} (µm)	62	113	328
Secondary agglomeration	weak	very weak	not present
Secondary agglomerate size (µm)	up to 400	n.a.	n.a.

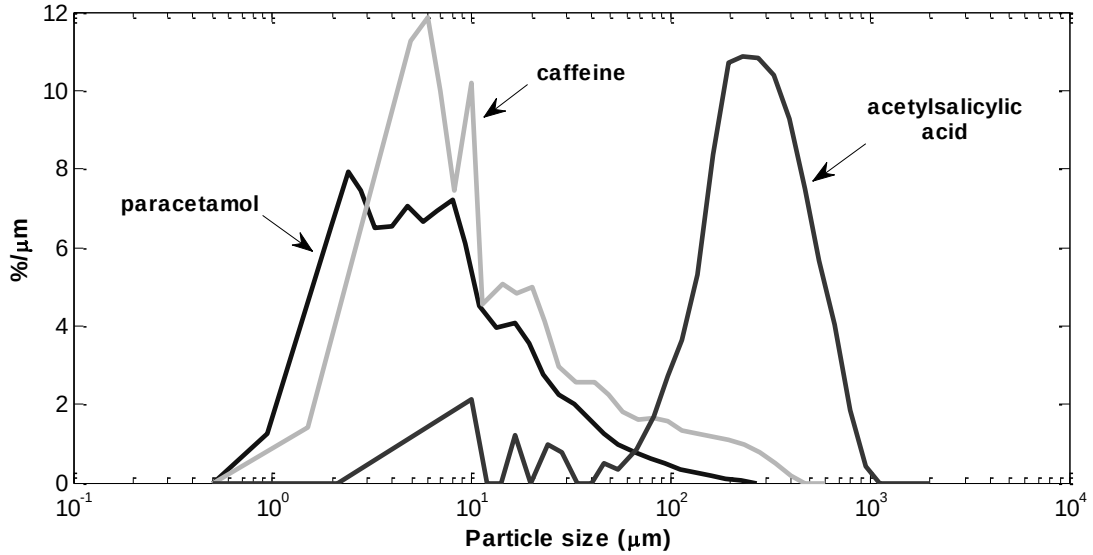

Fig.3.1 Primary particle size distributions of the active ingredients measured with laser light scattering particle size analyzer

As can be noted from the observations in Table 3.2, since paracetamol particle size is noticeably small, Van der Walls and electrostatic forces are relevant and cause the formation of secondary agglomerates. These agglomerates were visually detected by using an optic microscope. However, it has been noted that these secondary agglomerates are really weak: increase in pressure of dispersing air in the LLS particle size analyzer from 1 to 2 bar was sufficient to break them. Accordingly, paracetamol PSD in Fig.3.1 does not show the presence of secondary agglomerates.

On the other side, acetylsalicylic acid particles present the highest mean size. The crystalline habit of the drug particles is clearly columnar and it does not present secondary agglomerates. A low percentage of smaller acetylsalicylic acid particles (d_{10} < 100 µm) can be identified instead. Caffeine shows a higher mean size compared to paracetamol and a wider PSD.

10^{th}, 50^{th} and 90^{th} percentiles (x_{10}, x_{50} and x_{90}) for paracetamol, caffeine and acetylsalicylic acid are summarized in Table 3.3 and compared with percentiles of microcrystalline cellulose and lactose monohydrate.

Table 3.3 Percentiles (x_{10}, x_{50} and x_{90}) for the three active ingredients (paracetamol, caffeine and acetylsalicylic acid) and the two main excipients (microcrystalline cellulose and lactose monohydrate)

	x_{10} (µm)	x_{50} (µm)	x_{90} (µm)
Paracetamol	1.99	5.68	22.91
Caffeine	1.50	8.22	68.47
Acetylsalicylic acid	82.1600	194.42	468.29
Lactose monohydrate	6.77	22.91	78.69
Microcrystalline cellulose	1.99	7.98	78.69

As can be appreciated in Table 3.3, paracetamol particles result to be noticeably small compared to excipients particles as well. Mean size of caffeine particles is comparable with the mean size of the excipients particles, whereas acetylsalicylic acid particles are considerably bigger.

Solubility and hygroscopicity of the active ingredients and excipients can be compared in Table 3.4. Hygroscopicity is here represented by weight variation of powder samples under controlled humidity conditions. Three analysis cycles were performed: firstly, the relative humidity within the instrument chamber was raised from ambient humidity (i.e. about 50%) to 90%, secondly from 90% to dry conditions and finally from dry conditions to 90%. Accordingly, weight variations at the end of the cycles were recorded. The weight variation at the end of the last cycle is here considered as an indication of powder hygroscopicity.
As can be appreciated from the weight variation values recorded during water sorption analysis and reported in Table 3.4, caffeine results to be the most hygroscopic active ingredient, since it shows the highest weight variation at the end of the third cycle (i.e. 0 → 90 RH%). On the other hand, acetylsalicylic acid shows the lowest hygroscopicity. Regarding the solubility values reported in Table 3.4, active ingredients can be classified in the same order: caffeine is the most soluble active ingredient, paracetamol is less soluble and acetylsalicylic acid is almost water-insoluble.

Table 3.4 Solubility and hygroscopicity of the active ingredients: (a) solubility in water and (b) weight variations for the analysis cycles 50-90 RH%, 90-dry RH% and dry-90 RH%

	Solubility [a]	**Water sorption (weight variation %) [b]**		
	(g/100 ml H_2O)	**50 → 90 RH%**	**90 → 0 RH%**	**0 → 90 RH%**
Paracetamol	1.43	0.11	-0.01	0.12
Caffeine	1.67	0.17	-0.04	0.19
Acetylsalicylic acid	0.33	0.06	-0.03	0.05
Lactose monohydrate	15	0.21	0.01	0.25
Microcrystalline cellulose	-	11.2	-0.02	11.3

However, it can be noted that each active ingredient shows relatively low weight variations during water sorption analysis: these weight variations result to be negligible if compared with the most hygroscopic excipient (i.e. microcrystalline cellulose). Solubility values of the active ingredients result to be relatively low as well, especially if compared with lactose monohydrate solubility.

Formulations (50% w/w) of paracetamol, caffeine and acetylsalicylic acid were granulated by high shear wet granulation. Deionized water was added through a tube with 1 mm diameter. Impeller torque profiles were online monitored during the granulations and recorded.

Torque profiles recorded during the granulation experiments in Table 3.1 showed similar trends, see for example Fig.3.2. Similar results were also obtained in recent research works, with different excipients and dry binder types by Cavinato et al. (2010). An increase in impeller torque value at the beginning of the process has often been recognized, which is probably due to the progressive densification of the wet mass. A decrease in the profile slope is then observed, thus suggesting a lubrication of the wet mass and consequently the stress on the impeller decreases. After this initial phase, impeller torque profiles show a sudden increase. Betz et al. (2004) also reported similar results: they noted a sudden increase in the power consumption profile during the high shear wet granulation of a drug-free formulation composed of lactose monohydrate 200 mesh (86%), corn starch (10%) and PVP (4%). They explained this phenomenon by considering the initial formation of liquid bridges between particles after a first water uptake phase, thus leading to the achievement of the pendular state. As can be seen in Fig.3.2, the liquid amount required to cause the sudden increase in torque value can be easily identified as a minimum in first derivative profile. Such critical point can be used as a reference point in order to describe the first stage of the agglomeration process and the achievement of the pendular state.

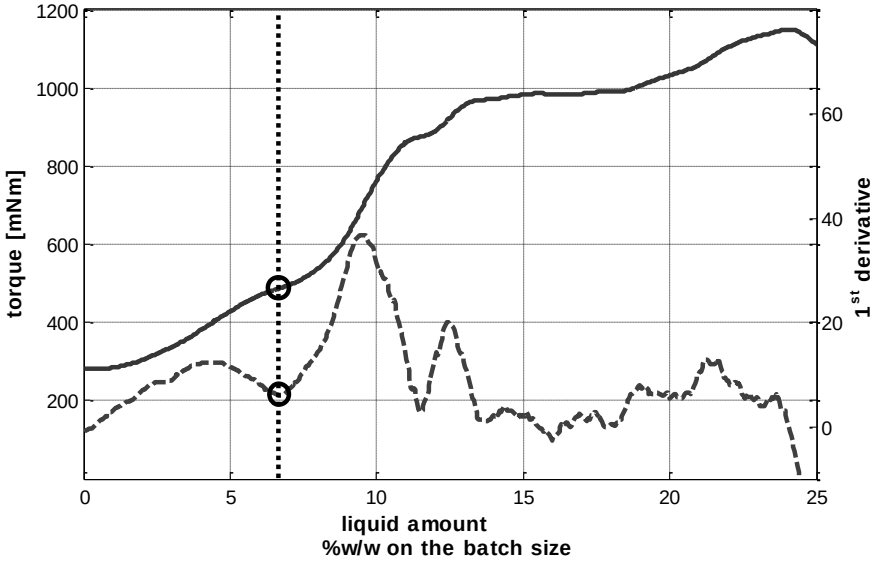

Fig.3.2. Impeller torque values (continuous line) and corresponding first derivative profile (dotted line) obtained during the high shear wet agglomeration of a drug-free formulation (dry binder PVP 5% w/w): determination of the minimum in the first derivative profile

The inflection point in impeller power profile has been considered as a reliable reference point also in a recent work presented by Campbell et al. (2010). Their results showed that granulation process can be scaled up using a linear relationship between the amount of liquid binder required to obtain the inflection point and Froude number.

Torque curves recorded during experiments in Table 3.1 have shown that the three different drugs present different liquid requirements corresponding to the sudden increase in torque profiles. Liquid amounts (%w/w on the initial batch size) corresponding to the inflection point in torque profiles (i.e. minimum in first derivative profiles) can be compared in Fig.3.3. Experiments with drug-free formulation were run in triplicate in order to test repeatability and reliability of the results: small error bars related to these points demonstrate the satisfactory reproducibility of the experimental method. As can be seen in Fig.3.3, the inflection point position clearly discriminates between the three different active ingredients.

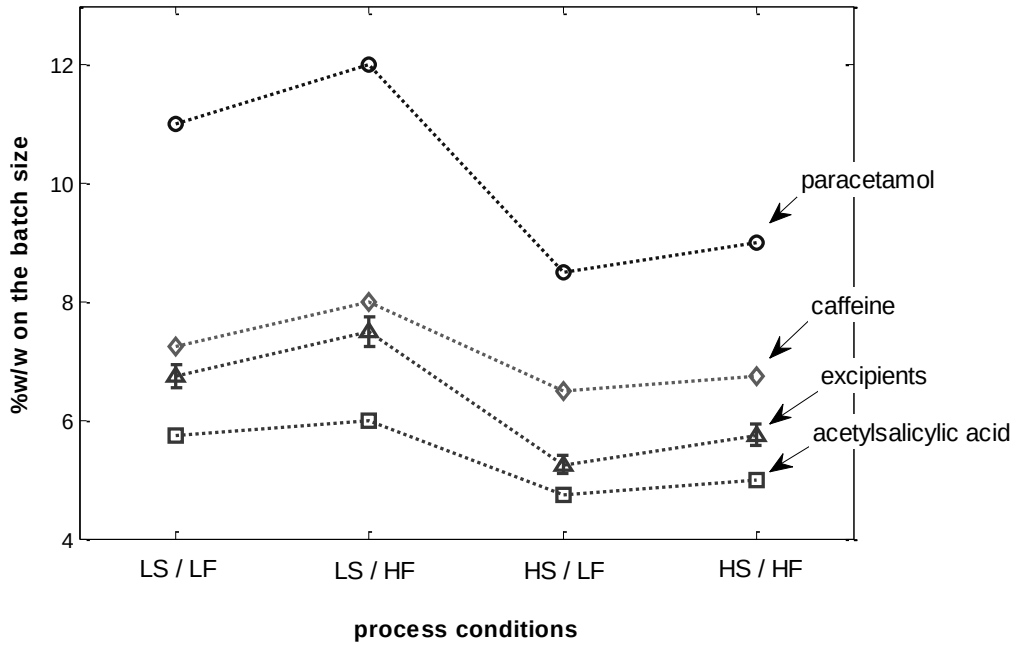

Fig.3.3. Liquid amount (%w/w on the batch size) required to determine sudden increase in the torque profiles during granulation experiments with different active ingredients and different process conditions: LS – lower impeller speed (500 rpm), HS – higher impeller speed (1200 rpm), LF – lower liquid flow rate (8 ml/min) and HF – higher liquid flow rate (12 ml/min).

Fig 3.3 clearly shows that the liquid amount required to strongly increase the impeller torque (i.e. inflection point in Fig.3.2) depends on the formulation composition. This means that different formulations, with or without active ingredient, markedly require different amounts of liquid to trigger the actual granule growth, in accordance with the interpretation proposed by Cavinato et al. (2010). Moreover, it is possible to state that drug primary PSD strongly affects the liquid amount required for the sudden increase in torque value. Particularly, the broader the primary PSD the lower is the liquid amount corresponding to the inflection point in torque profiles and required to start most of the granule growth. For example, inflection points for paracetamol occurred on average after 10 % water was added, whereas for acetylsalicylic acid about 5 % water was required.

Also process conditions make important differences in liquid amounts required to get torque profile inflection. As can be seen in Fig.3.3, the finer is the primary PSD the larger are the differences between inflection points obtained at low and high rotational speed. Especially for paracetamol, it can be noted that higher liquid amounts are necessary when impeller speed is lower. Moreover, the highest liquid flow rate gives higher liquid amount percentages.

Summarizing, finer primary PSD, lower impeller speed and higher liquid flow rate seem to cause a higher demand of liquid for the torque inflection point. According to the theory proposed by Leuenberger and co-workers (Leuenberger, 1982; Leuenberger and Bier, 1979; Leuenberger and Imanidis, 1984), a higher liquid amount required for the torque inflection point means that a higher liquid content is required to reach the pendular state and start the liquid bridges formation. According to Cavinato et al. (2010), also start of substantial granule growth might occur after the addition of higher liquid amount.

In order to validate these approaches, images of granulation samples collected during granulation experiments at different moisture contents were used for comparison with results of torque profile analysis. Hence, granule size evolution during the agglomeration of paracetamol, caffeine and acetylsalicylic acid are qualitatively described by Figs.3.4-3.6.

Images of granulation samples were taken with the same magnification (i.e. 122x) in order to facilitate the comparison between different moisture contents or active substances. Zooms of granules at 25% moisture content (i.e. at the end of the granulation process) are furthermore reported.

As can be seen in Fig.3.4, some big agglomerates with paracetamol can be noted at 20% moisture content (see Fig.3.4d), whereas pictures at 5, 10, 15% moisture content show non-granulated product.

On the other hand, first granules with caffeine can be located at 15% moisture content (see Fig.3.5c).

Granulations with acetylsalicylic acid in Fig.3.6 show some agglomerates at 10% moisture content (see Fig.3.5b) and at 15% moisture content only big granules are shown.

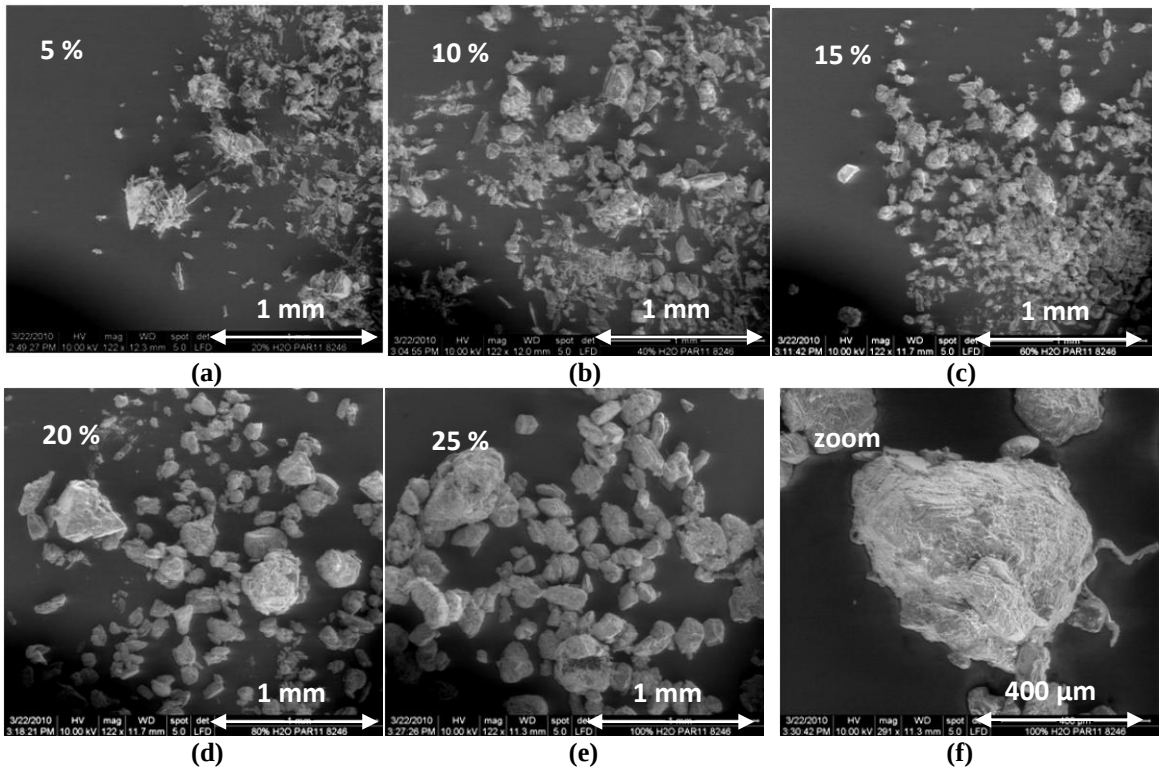

Fig.3.4. Granulation samples collected during high shear wet granulation of paracetamol - experiment 3 in Table 1 - at different moisture contents (%w/w on the batch size): (a) 5%, (b) 10%, (c) 15%, (d) 20%, (e) 25% at 122x magnification and (f) granule at 25% moisture content and 291x magnification

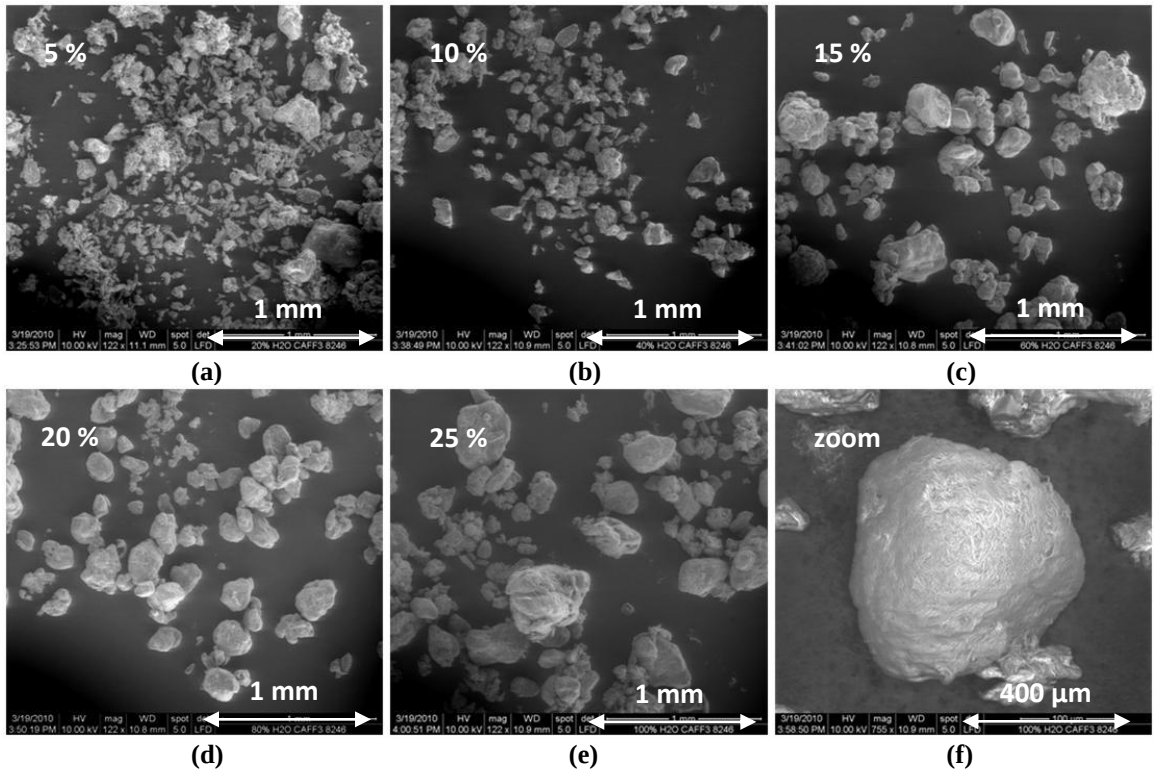

Fig.3.5. Granulation samples collected during high shear wet granulation of caffeine - experiment 7 in Table 1 - at different moisture contents (%w/w on the batch size): (a) 5%, (b) 10%, (c) 15%, (d) 20%, (e) 25% at 122x magnification and (f) granule at 25% moisture content and 755x magnification

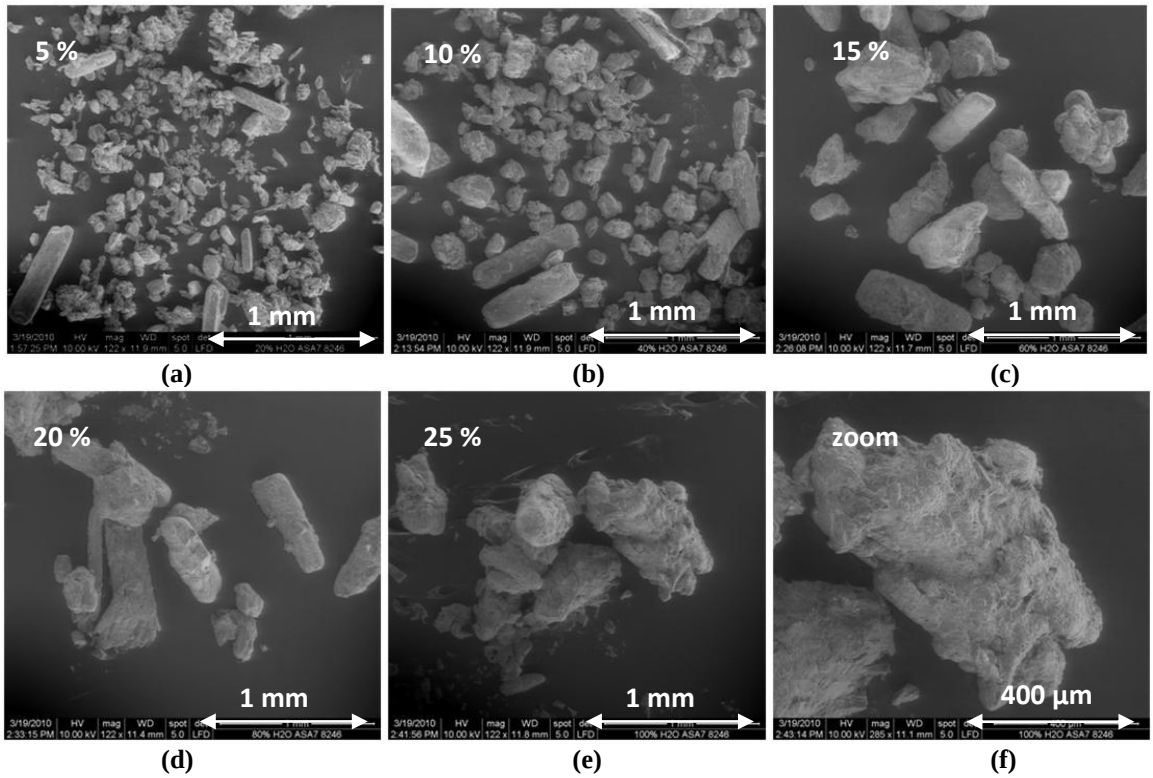

Fig.3.6. Granulation samples collected during high shear wet granulation of acetylsalicylic acid - experiment 11 in Table 1 - at different moisture contents (%w/w on the batch size): (a) 5%, (b) 10%, (c) 15%, (d) 20%, (e) 25% at 122x magnification and (f) granule at 25% moisture content and 285x magnification

Table 3.5 compares the results of torque profile analysis with those related to the analysis of the samples in Figs.3.4-3.6.

Table 3.5 Comparison between torque profile analysis (inflection point or granule growth onset) and results of image analysis (first visible agglomerates)

	Moisture content %	
	Torque inflection → growth start	**Image analysis → visible agglomerates**
Paracetamol	9 - 12%	20%
Caffeine	7 - 8%	15%
Acetylsalicylic acid	5 - 6%	10 – 15%

The comparison between the moisture contents corresponding to the torque inflection points (i.e. granule growth start) and those related to the images with the first clearly visible agglomerates (i.e. ongoing growth) suggests similar growth trend, since granule growth seems to occur at lower moisture contents for acetylsalicylic acid. Higher moisture contents are required when paracetamol or caffeine are used.

Regarding the effects of primary PSD on the initial nucleation and granule growth phase, similar results were obtained from Realpe and Velázquez (2008). As demonstrated by their results, formulations with rougher primary PSD showed a faster growth rate at the beginning

of the process and then a slower growth rate. On the other hand, the formulation with finer primary PSD showed a negligible growth at low moisture content and then a stage with faster growth rate after a certain amount of water was added. They explained this phenomenon by considering the higher cohesive force of small particles produced by larger contact surface, which leaded to stronger, poor deformable granules. Thus, poor deformability caused a lower growth rate at low moisture content and then a "ball growth" after a critical amount of water was added.
According to the approach proposed by Realpe and Velásquez (2008) and the results reported in the present research (see Table 3.5), it is therefore suggested that the higher contact surface of paracetamol particles compared to caffeine and acetylsalicylic acid particles can be considered as a predominant cause of the higher moisture content required to start the growth.

SEM images in Figs.3.4f, 3.5f, 3.6f also give some information about the growth mechanism types. It is interesting to see that granules with acetylsalicylic acid at 25% moisture content result to be less spherical than those composed of caffeine and paracetamol. This might be explained by considering the coarse primary PSD of acetylsalicylic acid. In particular, granules with acetylsalicylic acid tend to be composed of a bigger, columnar-shaped drug particle as a core and several smaller particles adhered on the core surface as a layer. The amorphous solid binder is supposed to play an important role in this case, promoting the layering mechanism (see for example results presented by Palzer, 2009). Other researchers (Capes and Danckwerts, 1965; Mackaplow et al., 2000) studied the effects of primary PSD on the growth mechanism and noted that as primary particle size increased, growth was more likely to occur via a crushing and layering mechanism.
On the other hand, spherical shape of paracetamol and caffeine-based granules can be explained by considering the lower granule deformability which leads to a slower action of shear forces on growing agglomerates.
Final granules size was furthermore measured by sieve analysis. Fig.3.7 shows final granules size represented by the normalized-sectional frequency distribution (mass based). The primary PSD of each active ingredient (volume based) is represented as well.

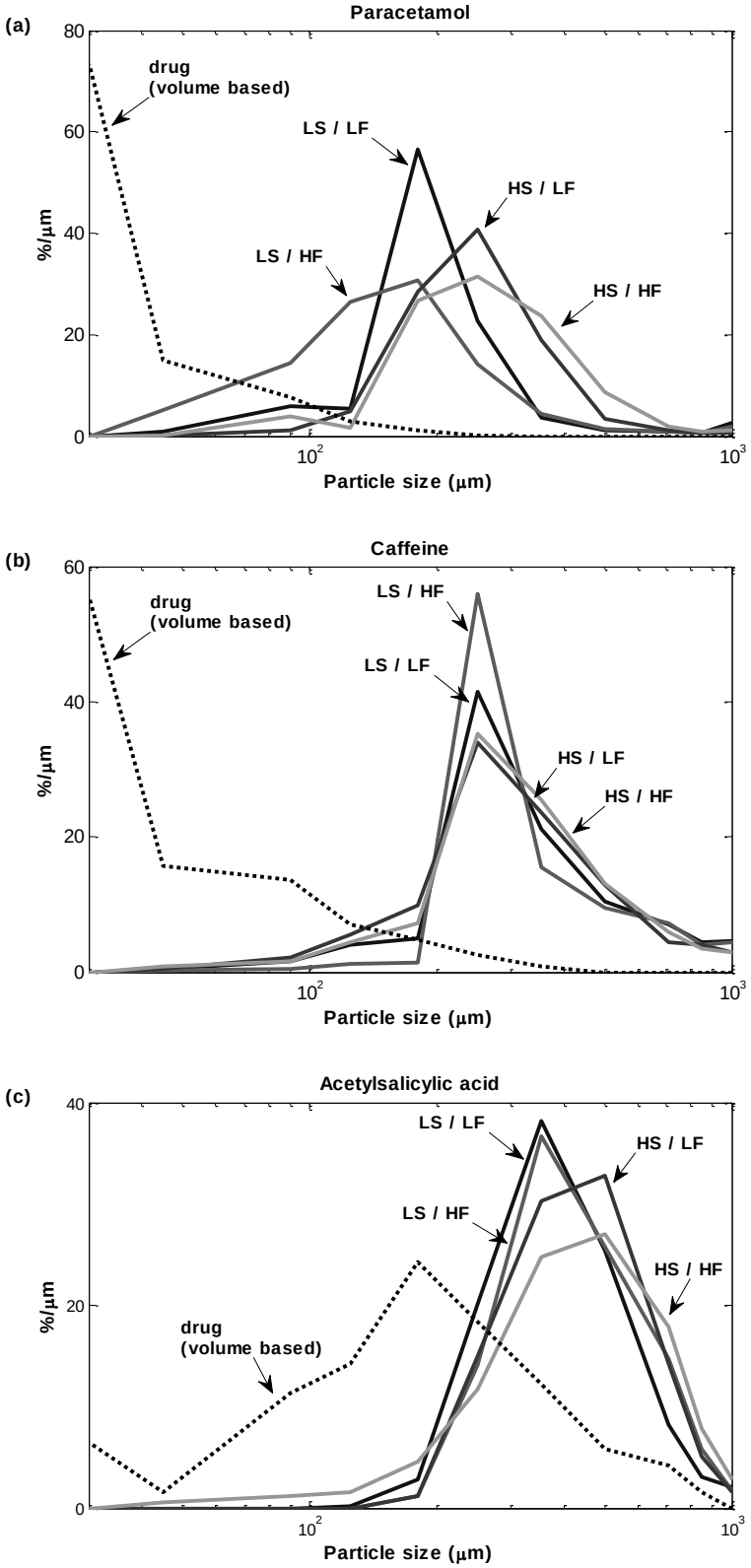

Fig.3.7. Particle size distribution measured by sieve analysis of the final granules (25% moisture content) for (a) paracetamol, (b) caffeine and (c) acetylsalicylic acid. Data are represented by the normalized-sectional frequency distributions (mass-based) and compared with the drug primary particle size (volume-based, see Fig.1). Process conditions are: LS – lower impeller speed (500 rpm), HS – higher impeller speed (1200 rpm), LF – lower liquid flow rate (8 ml/min) and HF – higher liquid flow rate (12 ml/min).

As can be seen in Fig.3.7, granules with paracetamol are smaller than those with caffeine and acetylsalicylic acid in order. This fact can be easily explained by considering the relatively smaller primary PSD of paracetamol compared to caffeine and acetylsalicylic acid.
It can be furthermore noted that difference between drug primary PSD and final PSDs of granules with acetylsalicylic acid is less marked than in presence of paracetamol and caffeine.
Interestingly, there are no noticeable differences between granules obtained at different process conditions in the case of granulation with caffeine or acetylsalicylic acid. Prominent differences between PSDs of paracetamol-based granules can be noted instead (see Fig.3.7a). In particular, granules obtained using the lowest impeller speed and highest liquid flow rate result to be much smaller than the others. In this case, non-granulated powder was found on the bottom sieve. This conclusion was partly anticipated by torque inflection point analysis, since discrepancies between points at different process conditions were more relevant for paracetamol (see Fig.3.3).
The last analysis involved the measurement of drug distribution in different size fractions of final granules. Size fractions corresponding to 10^{th}, 50^{th} and 90^{th} percentile for each granulation experiment were analyzed. Results of content uniformity measurements and corresponding error bars are shown in Fig.3.8. Broken line indicates the ideal condition of 50% w/w drug content in final granule, according to the initial active ingredient load.

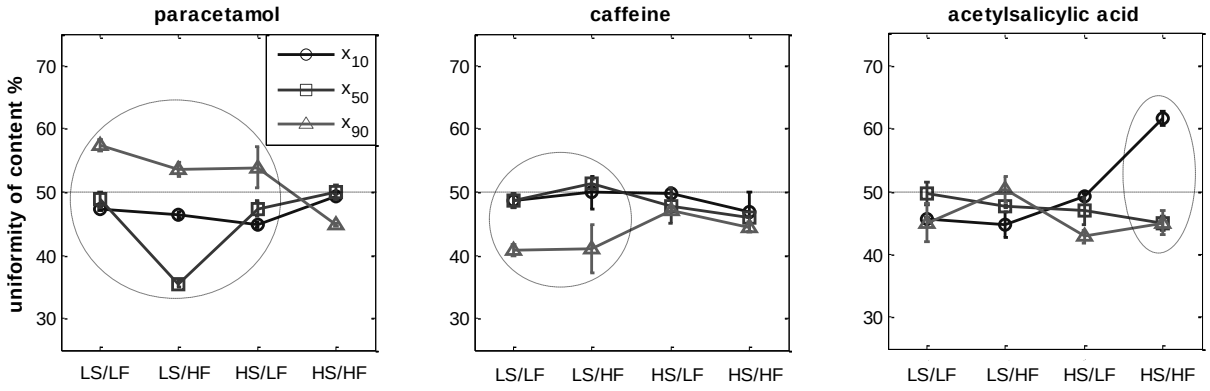

Fig.3.8. Content uniformity analysis results: distribution of (a) paracetamol, (b) caffeine and (c) acetylsalicylic acid in x_{10} (circles), x_{50} (squares) and x_{90} (triangles) size fraction. Process conditions: LS – lower impeller speed (500 rpm), HS – higher impeller speed (1200 rpm), LF – lower liquid flow rate (8 ml/min) and HF – higher liquid flow rate (12 ml/min).

Discrepancies between actual and ideal drug content might be due to selective agglomeration of certain components during the process. For example, in presence of hydrophobic and hydrophilic primary particles, granule growth of hydrophilic materials tends to take place selectively, as described by Belohlav et al. (2007). As a matter of fact, each active ingredient used in the present research showed poor hygroscopicity and poor solubility compared to the

two main excipients. These differences can be therefore considered as a potential cause of selective agglomeration.

It can be noted in Fig.3.8 that most of content uniformity problems occurred with paracetamol, especially at lower impeller speed. Paracetamol-based granules obtained using the lowest impeller speed and highest liquid flow rate showed the highest discrepancies: higher drug content in the biggest granules and very low drug content in the x_{50} size fraction. Caffeine-based granules obtained with the lowest impeller speed also showed content uniformity problems and lower drug concentration in the x_{90} size fraction. On the other hand, granules with acetylsalicylic acid showed the highest gap at high impeller speed and liquid flow rate. In this case, drug content was highest in fines and non granulated product.

The approach developed by Litster, Hapgood and co-workers (Hapgood et al., (2003); Litster et al., (2001)) can be considered in order to best explain the discrepancies between actual and ideal drug content. According to this approach, a finer primary PSD determines higher liquid penetration time, thus worsening the liquid distribution within the wet mass. Moreover, lower impeller speed and higher liquid flow rate determine higher dimensionless spray flux number and consequently worse liquid distribution. It is therefore suggested that poorer liquid distribution might lead to the presence of lumps and less wet areas, thus worsening drug distribution as well.

Whereas the cause of content uniformity issues for paracetamol and caffeine might be due to unsatisfactory liquid distribution conditions, the high concentration of acetylsalicylic acid in fines can be explained by considering breakage phenomena occurring when impeller speed is higher. These phenomena might be the cause of the layering mechanism detected with SEM image analysis (see Fig.3.6). The use of higher liquid flow rate probably leaded to less homogeneous wetting conditions, thus promoting the formation of less lubricated areas and leading to more intensive breakage phenomena.

3.5 Conclusions

The present research was carried out in order to evaluate the influences of some important drug properties (i.e. primary particle size, hygroscopicity and solubility) and process parameters on the granule growth behaviour in high shear wet granulation. Effects on drug distribution in final granules were evaluated as well. Formulations (50% w/w) of three common drugs (paracetamol, caffeine and acetylsalicylic acid) were granulated.

Results showed that drug primary particle size distribution (PSD) strongly affects trend of impeller torque profiles recorded during granulation experiments.

Inflection point in torque profile was therefore considered as reference point to best quantify the differences between different active ingredients, since this point can be correlated with the start of substantial granule growth.

Accordingly, it was noted that larger amounts of liquid were required to determine the torque inflection point and therefore the granule growth start during granulation of the drug with the finest primary PSD (i.e. paracetamol). Also process conditions resulted to affect the inflection point position in the case of granulation with paracetamol. In particular, using lower impeller speed and higher liquid flow rate resulted in a higher liquid amount needed for the inflection point. Since torque inflection point has often been correlated with the start of formation of liquid bridges between primary particles and, thus, the achievement of pendular state, images of granulation samples at different moisture content were taken with scanning electron microscope (SEM) and analyzed in order to describe granule growth kinetics. In accordance with torque profile analysis, SEM images showed that the smaller is the primary drug size, the slower tends to be the granule growth. In fact, smaller amount of liquid binder was necessary to form first agglomerates containing the drug with the highest mean size (i.e. acetylsalicylic acid).

It was therefore hypothesized that the presence of finer drug particles within the initial formulation leaded to stronger, poor deformable granules. Thus, poor deformability caused a lower growth rate at low moisture content and then a “ball growth” after a critical amount of water was added.

Granule growth mechanisms resulted to be dependant on the active ingredient type as well. Granules with paracetamol and caffeine resulted to be more spherical than those containing acetylsalicylic acid. Moreover, granules with acetylsalicylic acid were often composed of a bigger, columnar-shaped drug particle as a core and several smaller particles adhered on the core surface as a layer. In this case, granule growth was more likely to occur via a crushing and layering mechanism.

As resulted from sieve analysis, PSDs of paracetamol-based granules obtained under different process conditions were quite dissimilar as regards mean size and PSD width. In particular, PSD of granules obtained with the lowest impeller speed and highest liquid flow rate resulted to be wider than the others and presented a much lower mean size. On the other hand, granulations with caffeine or acetylsalicylic acid at different process conditions did not lead to noticeable differences between final PSDs.

Concluding, drug distribution in the final product was measured in order to best describe the growth behaviour of the three different formulations. Since each active ingredient showed negligible hygroscopicity and solubility compared to the two main excipients (i.e. lactose monohydrate and microcrystalline cellulose), the risk of selective agglomeration was considerable.

Paracetamol-based granules obtained with the lowest impeller speed and highest liquid flow rate showed more prominent content uniformity problems. Thus, granule growth of excipients particles and paracetamol particles seemed to occur separately. This situation was probably accentuated with worsening liquid distribution.

Analysis of granulations with acetylsalicylic acid showed a higher concentration of the drug in fines when the highest impeller speed and liquid flow rate were used. This fact might be due to a crushing and layering growth mechanism. It was suggested that the highest liquid flow rate value promoted breakage phenomena, probably because of inhomogeneous wetting conditions and thus the presence of less lubricated area.

3.6 References

C.G. Barlow. Granulation of powders. Chemical Engineering (London) 220 (1968) 196-201.

G. Betz, P.J. Bürgin, H. Leuenberger. Power consumption measurement and temperature recording during granulation. International Journal of Pharmaceutics 272 (2004) 137-149.

Z. Belohlav, L. Brenkova, J. Hanika, P. Durdil, P. Rapek, V. Tomasek. Effect of Drug Active Substance Particles on Wet Granulation Process. Chemical Engineering Research and Design 85 (2007) 974-980.

H.P. Bier, H. Leuenberger, H. Sucker. Determination of the uncritical quantity of granulating liquid by power measurements on planetary mixers. Pharmaceutical Industry 41 (1979) 375-380.

G.A. Campbell, D.J. Clancy, J.X. Zhang, M.K. Gupta, C.K. Oh. Closing the Gap in Series Scale Up of High Shear Wet Granulation Process Using Impeller Power and Blade Design, Powder Technology (2010), doi: 10.1016/j.powtec.2010.09.009.

C.E. Capes, G.C. Danckwerts. Granule formation by the agglomeration of damp powders: Part I. The mechanism of granule growth. Transactions of the Institution of Chemical Engineers 43 (1965) 116–123.

M. Cavinato, M. Bresciani, M. Machin, G. Bellazzi, P. Canu, A.C. Santomaso, Formulation design for optimal high-shear wet granulation using on-line torque measurements, International Journal of Pharmaceutics 387 (2010)a 48-55.

R. Gokhale, Y. Sun, A.J. Shukla. High-shear granulation. In: Parikh, D.M. (Ed.), Handbook of Pharmaceutical Granulation Technology (2^{nd} ed.). Taylor and Francis Group (2006) New York (U.S.A.).

K.P. Hapgood, J.D. Litster, R. Smith, Nucleation regime map for liquid bound granules, A.I.Ch.E. Journal 49 (2003) 350-361.

G. Imanidis. Untersuchungen über die Agglomerierkinetik und die elektrische Leistungsaufnahme beim Granulierprozess im Schnellmischer. Doctoral Thesis, University of Basel, 1986, Switzerland.

H. Leuenberger and H. P. Bier, Bestimmung der optimalen Menge Granulierflüssigkeit durch Messung der elektrischen Leistungsaufnahme eines Planetenmischers, Acta Pharmaceutical Technology, 41–44 (1979).

H. Leuenberger, H.P. Bier, H. Sucker. Determination of the liquid requirement for a conventional granulation process. German Chemical Engineering 4 (1981) 13-18.

H. Leuenberger, Granulation, new techniques, Pharm. Acta Helvetica 57 (3) (1982) 72–82.

H. Leuenberger and G. Imanidis, Steuerung der Granulatherstellung im Mischer durch Leistungsmessung, Chemical Industry XXXVI, 281–284 (1984).

J. Li, L. Tao, M. Dali, D. Buckley, J. Gao, M. Hubert, The effect of the physical states of binders on high-shear wet granulation and granule properties: A mechanistic approach toward understanding high-shear wet granulation process. Part II: granulation and granule properties, Journal of Pharmaceutical Sciences (2010) doi: 10.1002/jps.22261.

J.D. Litster, K.P. Hapgood, J.N. Michaels, A. Sims, M. Roberts, S.K. Kameneni, T. Hsu, Liquid distribution in wet granulation: dimensionless spray flux, Powder Technology 114 (2001) 32–39.

J.D. Litster, B. Ennis, The science and engineering of granulation processes, Kluwer Academic Publisher, 2004.

M.B. Mackaplow, L.A. Rosen, J.N. Michaels. Effect of primary particle size on granule growth and endpoint determination in high-shear wet granulation. Powder Technology 108 (2000) 32–45.

D.M. Newitt, J.M. Conway-Jones. A contribution to the theory and practice of granulation. Chemical Engineering Research and Design 36 (1958) 422-442.

T.H. Nguyen, W. Shen, K. Hapgood. Effect of formulation hydrophobicity on drug distribution in wet granulation. Chemical Engineering Journal (2010) in press.

S. Palzer. Influence of material properties on the agglomeration of water-soluble amorphous particles. Powder Technology 189 (2009) 318–326.

S. Palzer, The relation between material properties and supra-molecular structure of water-soluble food solids, Trends in Food Science & Technology 21 (2010), pp. 12–25.

S. Palzer, Agglomeration of pharmaceutical, detergent, chemical and food powders — Similarities and differences of materials and processes. Powder Technology (2010) doi: 10.1016/j.powtec.2010.05.006.

A. Realpe, C. Velázquez. Growth kinetics and mechanism of wet granulation in a laboratory-scale high shear mixer: Effect of initial polydispersity of particle size. Chemical Engineering Science 63 (2008) 1602 – 1611.

Chapter 4

Predicting the growth kinetics based on the formulation properties in high shear wet granulation

4.1 Summary

The granule growth behaviour in high shear wet granulation has often been described considering the particles as inert material held together by a simple Newtonian liquid added in the liquid phase. However, the reality is frequently more complicated: powder formulations are usually composed of crystalline and amorphous particles. They interact with the wetting agent, changing their properties.

The high shear wet granulation is therefore a very complex process and the final product is the result of the combination of process conditions and formulation properties. This research aims at coupling these two different aspects (process conditions vs. formulation properties) in order to give a more detailed description of the process, developing a more systematic and quantitative method for the prediction of the granule growth behaviour.

A mixture of some commonly-used pharmaceutical powders, composed of crystalline and amorphous materials, was processed. The dimensionless spray flux approach [Litster et al., Powder Technology 114 (2001) 29–32] was used in order to control the nucleation stage and obtain different liquid distributions. Thus, the effect of the liquid distribution on the growth onset and kinetics was deeply analysed.

The water amount required for the onset of significant granule growth was estimated according to a new procedure based on the glass transition concept [Cavinato et al., International Journal of Pharmaceutics 387 (2010) 48–55], which considers the presence of an amorphous material within the initial formulation. The influence of the main filler hygroscopicity was analysed as well.

In order to validate the theoretical predictions, a real time measurement of the particle size evolution was carried out using a Focus Bean Reflectance Measurement (FBRM) probe.

To be submitted in:
M. Cavinato, D. Kayrak-Talay, J.D. Litster. Powder Technology.

4.2 Introduction

The wet granulation is a well-known and widespread operation commonly used in many types of industries, such as the chemical and pharmaceutical industries. It consists of the agglomeration of different powders through liquid addition and it is usually performed in order to improve the powdered material properties, first of all: flowability, dustiness, structure, composition and resistance to segregation [Litster and Ennis, 2004]. Wet granulation is furthermore carried out in different types of equipments, which can be classified in accordance with the type of regime (e.g. batch or continuous) and type of mixing (e.g. fluidized beds, mixer granulators). Particularly, the high shear wet granulation is one of the most common operations, since wetting, agglomeration, consolidation and discharge are quickly performed in the same equipment [Ennis, 2006].

Moreover, fine chemicals or pharmaceuticals are widely batch processed, since the materials are usually expensive and the product amounts not so large to justify a continuous processing. For this reason, a good knowledge of how the equipments behave and the powdered materials respond is more and more necessary to achieve a good process control and scale-up.

In spite of the importance and the widespread use of high shear wet granulation, it is not totally clear how a change in the formulation or process parameters can affect the granule growth behaviour.

Some researchers recently tried to separate and analyse the different granulation stages for best explaining the agglomeration process [Iveson et al., 2001; Mort, 2005]. Some granulation maps have therefore been proposed with a view to describing the nucleation, growth and breakage phenomena. For instance, Iveson and Litster (1998) proposed a granule growth regime map for liquid-bound granules. In accordance with this method, the granule growth behaviour was described by two dimensionless groups: a Stokes deformation number, which accounts the granule deformation during collision, and the maximum pore saturation.

On the other hand, the initial nucleation phase and the liquid distribution were described using a nucleation regime map [Litster et al., 2001]. Accordingly, a new dimensionless number was developed: the dimensionless spray flux number characterises some of the most important process parameters in the nucleation stage, such as the powder flux, the liquid flow rate and liquid drop size.

In practice, the dimensionless spray flux is the measure of the liquid density on the powder surface. The lower is the dimensionless spray flux number, the closer are the nucleation conditions to the droplet controlled regime and the better is the liquid distribution [Litster et al., 2001; Hapgood et al., 2003]. One of the main assumptions of this method is that the flux of drops on the powder surface is mainly controlled by the process conditions (i.e. impeller speed, liquid flow rate, spray nozzle characteristics). Moreover, particles have often been

considered as inert material held together by a simple Newtonian liquid added in the liquid phase. The solid-liquid interactions have rarely been contemplated.

However, the reality is frequently more complicated. Pharmaceuticals as well as fine chemicals or food particles are often composed of crystalline and amorphous materials. In particular, amorphous materials absorb the liquid binder, changing their mechanical properties and becoming sticky [Cavinato et al., 2010a,b; Palzer, 2010]. This phenomenon noticeably affects the granule growth mechanism and needs a thorough analysis, as pointed out by Palzer (2009). Thus, for systems composed of crystalline and amorphous materials, it is no longer enough to simply consider the processing conditions, neglecting the material properties change during the process.

With a view to describing the effects of the amorphous material on the granule growth behaviour, Cavinato et al. (2010)a,b proposed a new procedure for the estimation of the liquid amount needed to yield the granule growth onset as a function of the formulation composition. In accordance with this method, the liquid addition causes the decrease of the glass transition temperature of the amorphous material. A critical liquid amount is then required to increase the molecular mobility in the amorphous matrix, promoting the molecular migration into the liquid on the particle surface when the glass transition temperature equals the powder temperature. The increase in the liquid viscosity on the particle surface determines the increase in stickiness [Palzer, 2009; Fitzpatrick, 2007].

In this context, the present work seeks to fill the gap in understanding how a mixture of commonly-used pharmaceutical powders, composed of crystalline and amorphous materials, behaves under different nucleation and liquid distribution regimes (i.e. different processing conditions).

The glass transition concept was thus coupled with the well-known nucleation regime map in order to develop a more systematic and quantitative procedure for the estimation of the growth onset and the description of the growth kinetics in the presence of an amorphous binder and a hygroscopic filler.

A FBRM probe was furthermore used in order to monitor the particle size evolution during the process and validate the estimated values.

4.3 Materials and methods

4.3.1 Equipment and materials

The granulation experiments were performed in a small scale, bottom-driven granulator (Diosna P1-6, 6 l) with a stainless steel vessel, a chopper and a three bladed impeller.

Variations of a mixture of some commonly-used pharmaceutical powders were considered: dicalcium dihydrate phosphate (DICAL) (Innophos, Chicago IL, U.S.A.), microcrystalline

cellulose (MCC) (FMC, Philadelphia PA, U.S.A.) were used as fillers and polyvinylpirrolidone (PVP) (Kollidon® K30, BASF, Livonia MI, U.S.A.) as dry binder within the initial formulation.
Deionized water at 20°C was introduced into the powder bed as wetting agent through a flat spray pattern nozzle (Spraying Systems Co., U.S.A.). Two different types of spray nozzle were used (see Table 4.1).

Table 4.1 Liquid addition system: characteristics of the spray nozzles

Spray nozzle type	Flow rate (ml water/min)	Spray angle (°)	Droplet diameter d_{30} (μm)
Type 1	22	40	40
Type 2	29	60	55

The granulator fill was 30% of the total vessel volume. A premixing stage at 400 rpm and for 5 min was performed before the wetting phase.

4.3.2 Experimental plans

Firstly, four granulation experiments were performed in order to determine the effect of the liquid distribution on the granule growth kinetics. Each experiment was run in triplicate for testing the reproducibility of the FBRM profiles. In the attempt to change the liquid distribution regime during the granulation, the impeller speed and the spray nozzle type were changed, as shown in Table 4.2.
The composition of the powder mixture was held constant and was (on weight basis): dicalcium dihydrate phosphate (96%) as crystalline filler and PVP (4%) as amorphous dry binder. The total amount of added liquid was 15% of the batch size.

Table 4.2 First experimental set: changes of the impeller speed and spray nozzle type in order to achieve different liquid dispersion regimes

Experiment	Impeller speed (rpm)	Spray nozze type
1	250	Type 1
2	350	Type 1
3	250	Type 2
4	350	Type 2

The second experimental plan involved changes in the formulation composition in order to determine the dependence of the granule growth kinetics on the main filler hygroscopicity.
Different concentrations of MCC were tested. The primary particle size distributions of the two main fillers were similar. Formulation compositions are listed in Table 4.3. The

granulation trials were performed under the same operative conditions, as experiment number 2 in Table 4.2.

Table 4.3 Second experimental set: variations of the formulation composition in order to change the main filler hygroscopicity

Experiment	Component	Composition (on weight basis)	Structure type	Mixture bulk density (g/cm^3)	Liquid binder amount (% on the batch size)
exp.2 (Table 2)	DICAL PVP	96 % 4 %	Mainly cristalline Amorphous	0.686	15 %
exp.2 w/o dry binder	DICAL	100 %	Mainly cristalline	0.686	15 %
exp.2 + 20% MCC	DICAL MCC PVP	76 % 20 % 4 %	Mainly cristalline Mainly cristalline Amorphous	0.637	20 %
exp.2 + 40% MCC	DICAL MCC PVP	56 % 40 % 4 %	Mainly cristalline Mainly cristalline Amorphous	0.540	30 %

The impeller speed was held constant during the wetting and the massing phase (mixing phase with liquid feeding system switched off). The duration of the massing phase was 5 min for all the experiments in Tables 4.2 and 4.3.

4.3.3 Particle size and shape analysis (off-line measurements)

Image analysis was carried out in order to monitor the particle size distribution (PSD) and the granule shape during the agglomeration process.
Several samples were taken during each granulation trial at constant intervals (4-5 samples during the wetting phase, 2 samples during the massing phase). The weight of each sample was about 2-3 g. Images of each sample were taken using a digital camera interfaced with an image analysis program (ImageTool©, Copyright 2008, Evans Technology, Inc.).
Granule shape was estimated analysing the whole projected area and considering small protrusions have a negligible effect on the value of the area. Accordingly, the Roundness index Φ was used in order to describe the shape [Nazar et al., 1996; Allen, 1997]:

$$\Phi = \frac{4\pi A}{P^2}, \qquad \text{Eq.(4.1)}$$

where A is the granule projected area and P is the granule perimeter. Roundness values are included between 0 and 1: the larger the value, the rounder the object. The Roundness index provides a first significant estimation of the granule morphology.

Granules particle size distribution was also characterized by sieve analysis. The sieving method consisted on 5 mm of vibration amplitude for a 10 min analysis time. Sieves apertures

were: 45, 63, 90, 125, 180, 250, 355, 500, 710, 1000 μm. Granules were gently dried beforehand in static conditions (oven: 24 h at 20°C, 1 atm and then 2 h at 50°C, 1 atm).

4.3.4 Drop penetration time measurements

A 1 μl syringe was placed above a loosely packed powder bed. The loosely packed powder bed was formed by carefully dosing the powder into a petri dish and scraping the level in order to produce a smooth powder surface. Magnified movies of binder drops falling from the needle and lying down on the loosely packed powder bed were taken using a fast digital camera at 1000 frames per second. The magnified movies were then analysed using the image analysis program. The drop penetration time was taken as the number of frames between when the drop hits the surface and when the last liquid drained away [Hapgood et al. 2002].
The drop falling height was optimized in according to Hapgood and Khanmohammadi (2009) in order to allow the drop detaching and avoid the drop distortion and breakage.

4.3.5 Powder surface velocity measurements

The powder surface velocity was measured using the fast digital camera at 1000 frames per second. Magnified movies of the powder bed at the spray area during the dry mixing and during the first wetting phase were taken. The camera was placed perpendicularly to the moving powder surface as shown in Fig.4.1.

Fig.4.1. Picture of the experimental apparatus for the measurement of the powder surface velocity

The magnified movies were then elaborated using MATLAB and the image analysis program. The powder surface velocity was measured in several points of the spray zone so that the final value was the average of several measurements.

4.3.6 Water sorption isotherm determination

The water sorption isotherm for each formulation component was determined using a gravimetric analysis system (IGAsorp, Hiden Isochema, Warrington, UK).
The powder samples were kept at different relative humidity grades under nitrogen flow at 20°C; the weight change of each binder sample during the time course analysis was measured by a hygrometer. The exposure time of each sample to the different humidity grade corresponded to the time at which the sample weight did not change anymore or otherwise to a maximum time of 10 h.

4.3.7 FBRM probe setting

A Focused Beam Reflectance Measurement probe (FBRM® C35, Mettler Toledo, Columbia MD, USA) was used in order to carry out real time PSD measurements. The probe was equipped with a scraper for clearing the optical window during the process without stopping the granulator. The wiping time was 3 s.
The probe was set in accordance with the scheme in Fig.4.2.

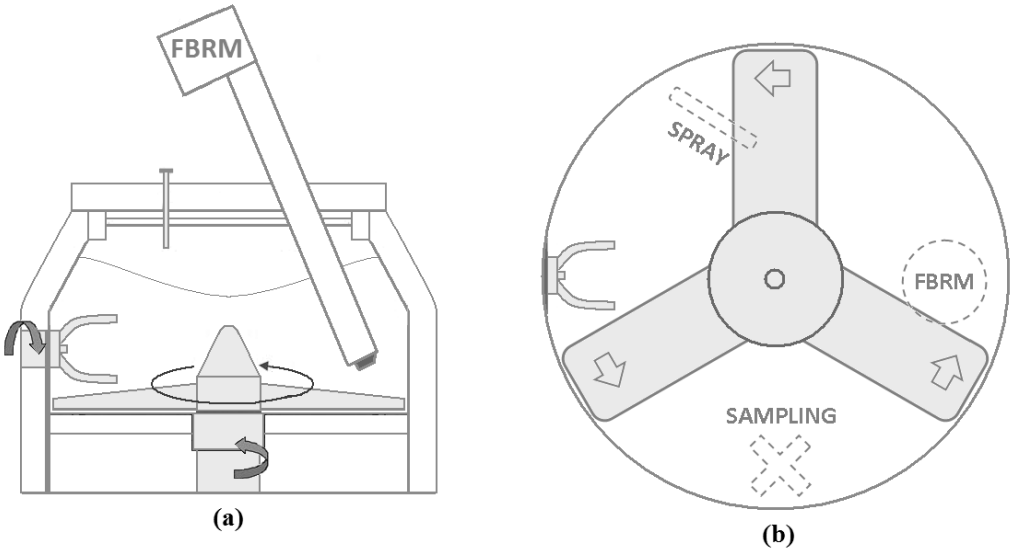

Fig.4.2. Schematic of the high shear mixer: location of the FBRM probe, the spray nozzle and the sampling point for the off-line measurements. (a) Side view and (b) top view of the granulator

As can be seen in Fig.4.2, the footprint of the flat spray pattern nozzle defines the spray area. The position and orientation of the spray nozzle was fixed in order to perpendicularly intersect and wet the moving powder bed. The scheme describes the pathway of the powder as well: the wet granules firstly hit the chopper and then they meet the FBRM probe.
The size measured by the FBRM is the granule chord length, which is the straight line between any two points on the edge of a granule. The probe measures up to tens of thousands of chords per second, resulting in a statistically significant chord-length distribution.

The FBRM results are furthermore represented by the chord length weighted mean, which is the $d_{2,1}$:

$$d_{2,1} = \frac{\sum_i x_i^2 y_i}{\sum_i x_i y_i}, \qquad \text{Eq.(4.2)}$$

where x is the chord length and y is the particles count.

The powder patterns can be affected by the presence of the probe and obviously the smaller is the granulator, the stronger is the influence of the probe on the powder flow. It has been visually verified that the presence of the FBRM probe in the system illustrated in Fig.4.2 does not strongly affect the flow pattern or noticeably slow down the powder flow during the granulation process.

4.4 Results and discussion

Firstly, the reproducibility and reliability of the FBRM results were verified repeating three times each granulation experiment and comparing the resulting profiles.

As described in the Materials and Methods section, the formulation for the first experimental set was composed of dicalcium dehydrate phospahate as filler and PVP as dry binder.

The experiment 1 in Table 4.2 can be considered as an example. Fig.4.3 shows the comparison between the FBRM profiles obtained repeating the trial three times. The starting point for the liquid addition in Fig.4.3 is 0 min. The wet massing is the mixing phase with liquid feeding system switched off.

The change in the granule size was also evaluated by analysing the binary images of the wet granules collected during the process.

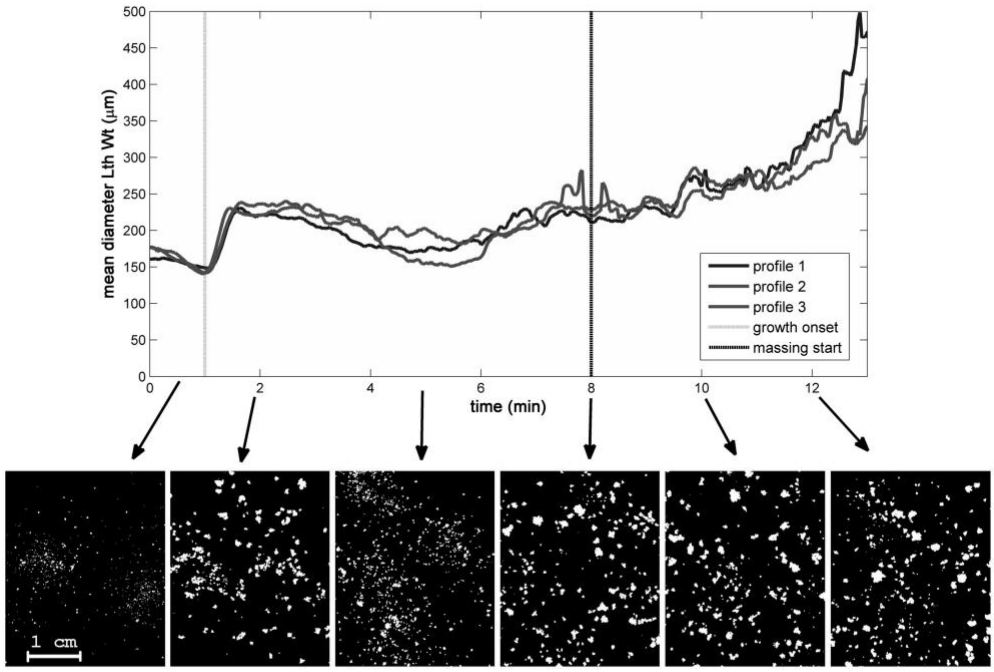

Fig.4.3. Repeatability and reliability of the FBRM results: comparison between three repetitions of the experiment 1 in Table 2 and results of the image analysis performed on the wet granules

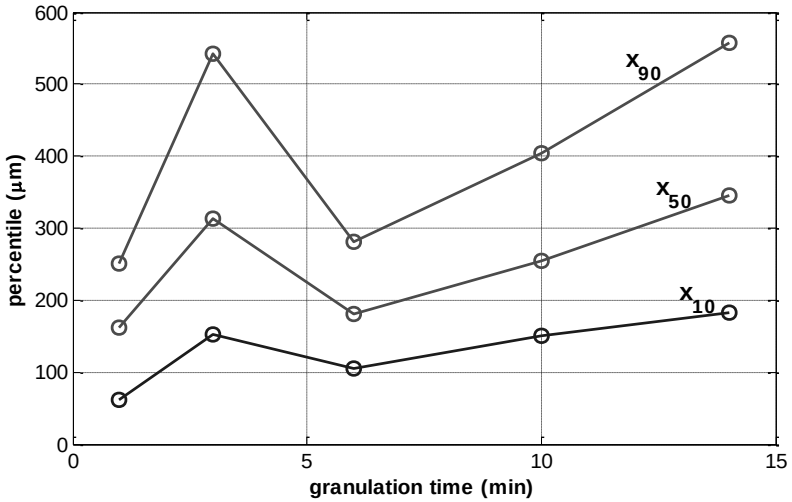

Fig.4.4. Results of sieve analysis for the experiment 1 in Table 4.2.

As can be noted in Fig.4.3, the repeatability of the FBRM profiles is satisfactory. Moreover the comparison with the binary images of the wet granules attests the reliability of the profiles, since the granule size trend is well reproduced by the FBRM curves.

Outcomes of the FBRM probe and sieve analysis were also compared with the PSDs obtained through sieve analysis. Experiment 1 in Table 4.2 was run 5 times: it was stopped after about 0.5, 3, 6, 10 and 14 min. Granules obtained from the 5 trials were sampled for PSD determination through sieve analysis. Fig.4.4 shows sieve analysis results. The variation of 10^{th}, 50^{th} and 90^{th} percentiles follows the same trend noted in Fig.4.3: it can be noted an increase in the granule size after 0.5-1 min, then a decrease after 2-3 min and finally a progressive increase.

It is therefore interesting to note from the FBRM profiles, the binary images and sieve analysis that the mean granule size suddenly increases after 1 min of wetting. This particular point can be identified as the onset of significant granule growth.

As demonstrated by some authors [Cavinato et al. (2010)a,b; Palzer 2009], the sudden increase in agglomerate size in presence of amorphous powders can be explained in the light of the glass transition concept. A method for the estimation of the liquid volume required to start most of the granule growth was therefore proposed [Cavinato et al., 2010a,b].

According to this method, the addition of liquid causes the decrease in the dry binder glass transition temperature (T_g), since the dry binder is the only amorphous substance in the formulation.

When the dry binder T_g equals the powder temperature (T_p), the molecular mobility of the amorphous material increases. The consequent migration of the amorphous material on the particle surface determines the increase in stickiness and promotes the granule growth onset. Fig.4.5 shows the decrease of the $T_{g,PVP}$ as a function of the water content [Cavinato et al. (2010)a,b; Hancock and Zografi (1994); Gordon and Taylor (1952)].

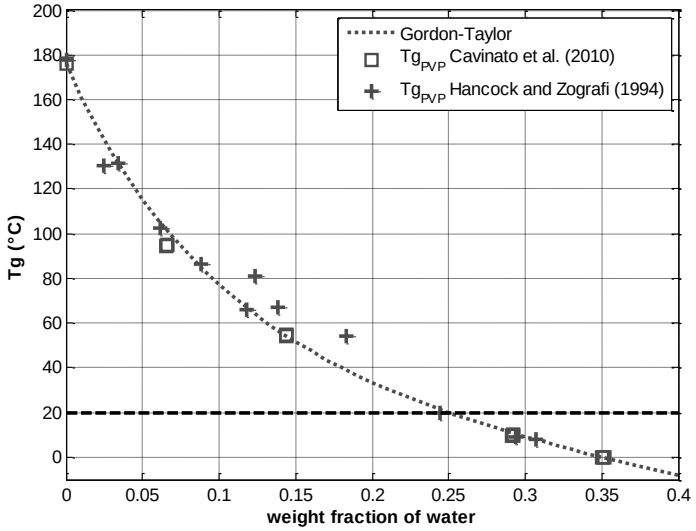

Fig.4.5. Effect of the water content on the PVP glass transition temperature: experimental data [Cavinato et al. (2010)a,b, Hancock and Zografi (1994)] fitted to the Gordon-Taylor model [Gordon and Taylor (1952)]

Considering the powder temperature constant during the process and approximately equal to ambient temperature, it is possible to estimate the liquid amount required for the glass transition as the intersection between the T_g profile and the ambient temperature (i.e. about 25% of the dry PVP weight).
According to these preliminary considerations, two experimental sets were performed, changing the impeller speed, the spray nozzle characteristics (first set) and the main filler hygroscopicity (second set).

4.4.1 Role of the process conditions on the growth kinetics

The process parameters have been changed in order to obtain different values of the dimensionless spray flux number and operational conditions closed to the droplet controlled regime [Litster et al., 2001]. The aim of this experimentation was to evaluate the effect of the liquid distribution regime on the growth onset value and the growth kinetics type.
Profiles in Fig.4.6 represent the variation of the chord length weighted mean, fine particles and large agglomerates count as a function of liquid amount (% on the batch size) and during the massing phase. Broken lines indicate the beginning of the massing phase. The massing phase duration was 5 min.

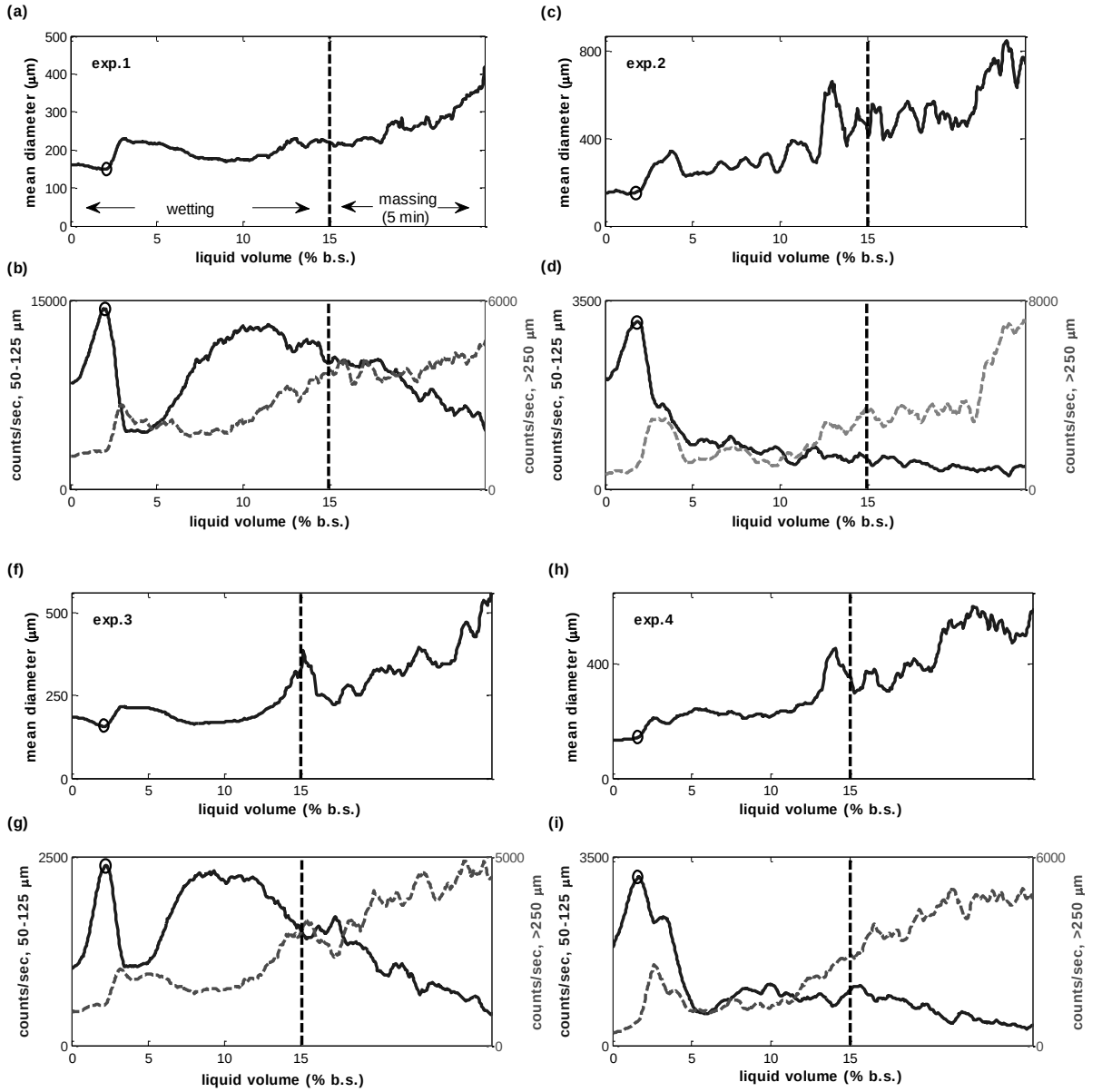

Fig.4.6. Results of the first experimental plan: effect of the processing parameters on the granule growth. The profiles represent the evolution of the chord length weighted mean, the number of particles whose diameter ranges from 50 to 125 µm and the number of particles whose diameter exceeds 250 µm for the experiment number (a, b) 1, (c, d) 2, (e, f) 3 and (g, h) 4 (see Table 2).

As can be seen in Fig.4.6, the granule size trend is represented by the chord length weighted mean, the number of particles whose diameter ranges from 50 to 125 µm and the number of agglomerates whose diameter exceeds 250 µm.

In particular, the number of particles whose diameter ranges from 50 to 125 µm seems to be a good index for describing the growth kinetics. As can be appreciated in the graphs, the evolution of the number of fines clearly discriminates between the different process conditions.

A decrease in fines count is shown at the beginning of each experiment: this fact might be due to the formation of nuclei and therefore the enlargement of very small particles (< 50 μm).
The onset of significant granule growth is then clearly identified by a sudden increase in the chord length weighted mean or a sudden decrease in the number of fine particles, as pointed out by circular markers in Fig.4.6.
The experiment 2 and experiment 4 were performed using the highest impeller speed value (see Table 4.2). They both show a similar decrease trend in the number of fines. The decrease in the number of fine particles is gradual and starts at the growth onset point. On the other hand, experiment 1 and 3 lead to different results: a sudden decrease in the number of fines occurs after the growth onset but subsequently a strong increase can be noted. Then a gradual decrease in the number of fine particles occurs again during the final wetting stage and massing.
The comparison between the final granule size measured using the FBRM probe and that obtained with image analysis can be appreciated in Fig.4.7. Mean size of PSDs obtained through image analysis represents $d_{2,1}$ in Eq.(4.2), where x_i is the Feret diameter y_i and the particles count.

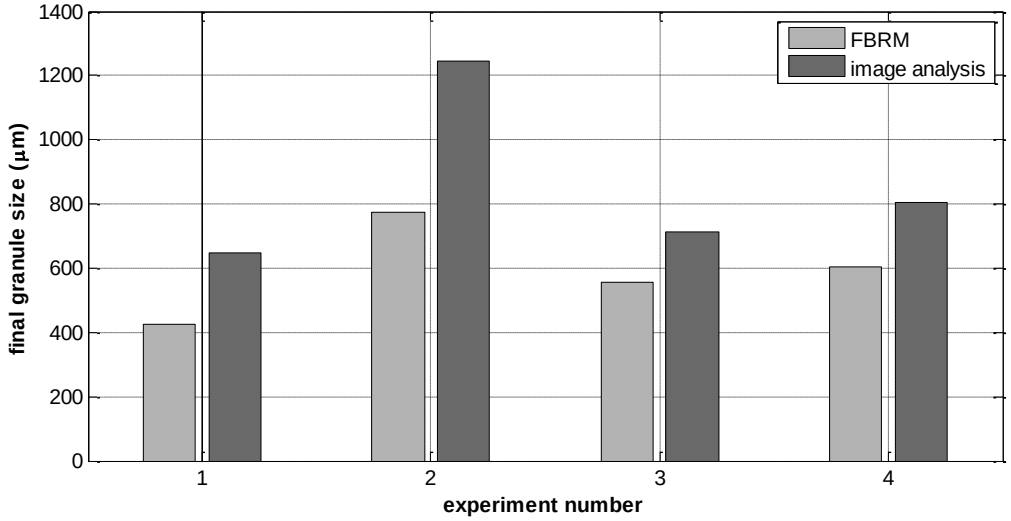

Fig.4.7. Final granule size: comparison between results obtained using FBRM probe and those obtained using image analysis. In this last case, the mean size represents $d_{2,1}$ (Eq.(2)) of Feret diameter distribution, evaluated by image analysis.

As can be appreciated in Fig.4.7, experiment 2 presents the highest final granule size, followed by experiment number 4, 3 and 1.
In order to best describe the discrepancies in growth behaviours (see for instance Figs. 4.6a-b and Figs. 4.6h-i), image analysis was carried out on the samples collected during the granulation experiments. The Roundness index was then calculated and used for describing the granule morphology during the process and how the granule structure was affected by the different process conditions. The experiment 1 and experiment 4 are considered as a

significant example in Fig.4.8, which shows the Roundness index values for samples of more than one thousand granules each, collected at constant time intervals (i.e. different liquid contents) during the process.

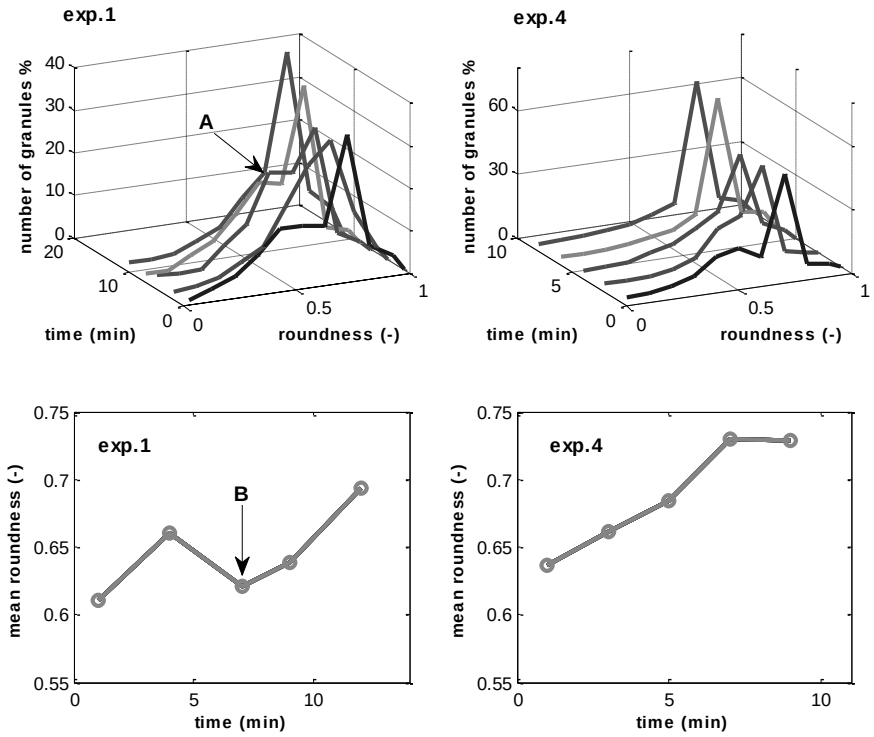

Fig.4.8. Roundness index distributions during the granulation experiments (experiment 1 and 4 in Table 2) and variation of the mean roundness value. The lowest impeller speed (i.e. experiment 1) leads to a less gradual variation of the Roundness index: a minimum in the mean Roundness can be identified, as pointed out by the arrow B

Fig.4.8 clearly shows a non-monotonic increase of Roundness value when the impeller speed is lower (i.e. experiment 1). In particular, a minimum in the mean Roundness value can be noted, as pointed out by the arrow B. The cause of the minimum in mean Roundness can be easily discerned in the bi-modal Roundness distribution (see the arrow A in Fig.4.8).

Contrarily, the mean Roundness value steadily increases during the wetting phase and stabilizes around 0.72 during the massing phase when the impeller speed is higher (i.e. experiment 4), reaching higher Roundness values in shorter time. It is also interesting to note that in this last case the Roundness distribution becomes narrower and narrower during the process.

A possible explanation for this phenomenon might be a breakage process occurring after the growth onset point at the lowest impeller speed. As a consequence of these breakage phenomena, final granule size is lower at the end of experiment 1 and 3 as shown in Fig.4.7.

In this case, contrary to probable expectations, the highest impeller speed does not seem to promote a stronger breakage phenomenon.

In order to give a better explanation for these different behaviours, the dimensionless spray flux concept was then considered.

The dimensionless spray flux number is defined as [Litster et al., 2001]:

$$\Psi_a = \frac{3\dot{V}}{2\dot{A}d_d}, \qquad \text{Eq.(4.3)}$$

where $\dot{V}$ is the liquid flow rate, $\dot{A}$ is the powder surface flux which is traversing the spray zone and d_d is the droplet diameter. Thus, the dimensionless spray flux number represents the ratio of the wetted area covered by the nozzle to the spray area in the nucleation zone.

The powder surface flux is defined by:

$$\dot{A} = vW, \qquad \text{Eq.(4.4)}$$

where v is the powder velocity past the spray and W is the width of the powder being wet. As described previously, the powder velocity was measured using the fast camera and the image analysis software. It has been assumed in this work that the powder velocity does not strongly vary during the granulation process with the liquid binder addition.

In order to describe the drop penetration kinetics, Hapgood et al. (2003) considered the dimensionless drop penetration time:

$$\tau_p = \frac{t_p}{t_c}, \qquad \text{Eq.(4.5)}$$

where t_p is the penetration time of the spray drops and t_c is the circulation time, which is the time interval between a packet of powder leaving and re-entering the spray zone.

The penetration time t_p was taken as the time a liquid drop needs in order to be absorbed by a static powder bed, as described previously. It is opportune to note that the vigorous mixing inside the granulator leads to a dynamic system, thus the effective penetration time is supposed to be lower.

The circulation time t_c was estimated to be the ratio between the bowl circumference and the powder surface velocity. As already mentioned by Hapgood et al. (2003), the circulation time is a function of the powder flow patterns and the mass fill. Whereas the powder flow patterns within the granulator outline a toroidal trajectory [Nilpawar et al., 2006], the path covered by the powder is supposed to be larger than the bowl circumference and thus the real circulation time is supposed to be higher than the estimated value.

The evaluation of the dimensionless drop penetration time was therefore carried out in order to obtain a precautionary estimation of the real nucleation conditions (i.e. higher τ_p values).

In practice, the lower is the dimensionless spray flux and dimensionless drop penetration time, the better is supposed to be the liquid binder distribution. At low dimensionless spray flux (approximately $\Psi_a < 0.1$) the system operates in the drop-controlled regime, where one drop forms one nucleus and the nuclei size distribution is narrower [Litster et al., 2001].

According to the dimensionless spray flux concept, the granulation conditions were pointed out in the nucleation regime map [Hapgood et al., 2003]. The liquid volumes required to yield

the growth onset were then estimated (see Fig.4.5) and compared as a function of the different nucleation regimes. The comparison between the liquid volumes is shown in Fig.4.9.
In addition, dimensionless spray flux values, penetration times and liquid amounts required to yield the initial growth onset are reported in Table 4.4.

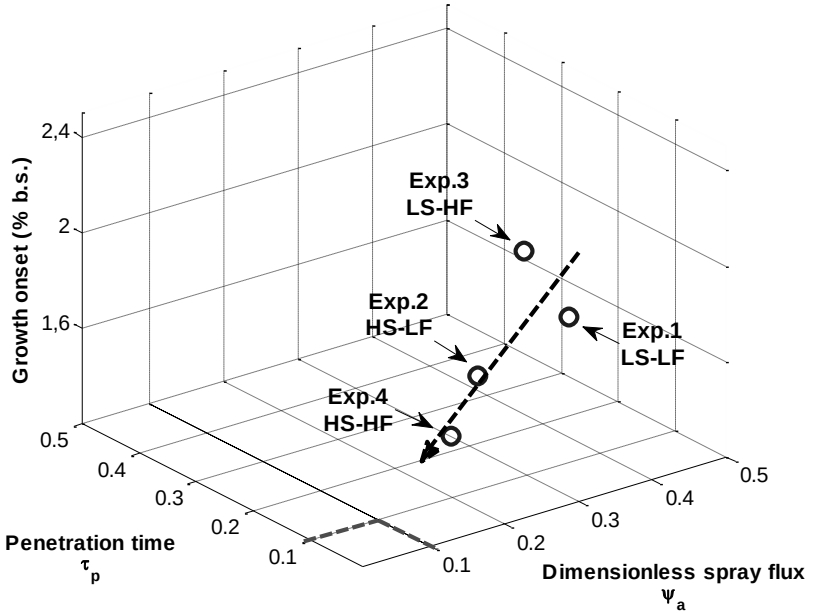

Fig.4.9. Liquid volume required to start the granule growth process as a function of the nucleation regime (H: high, L: low, S: impeller speed, F: liquid flow rate)

Table 4.4 Values of the dimensionless spray flux, penetration times and percentage of liquid corresponding to the sudden increase in granule mean size (FBRM measurements)

Experiment	Dimensionless spray flux (-)	Penetration time (-)	Growth onset (% on batch size)
1	0.293	0.0175	1.97 ± 0.05
2	0.179	0.0286	1.82 ± 0.04
3	0.234	0.0175	2.30 ± 0.05
4	0.143	0.0286	1.60 ± 0.06

As can be seen in Fig.4.9, the nucleation regime map is identified by the horizontal xy-plane. The experiments 4 and 2 present lower dimensionless spray flux values: a higher impeller speed results to be critical for achieving a good liquid distribution. On the other hand, the dimensionless penetration time does not strongly vary with the process conditions (see Table 4).
The z-axis in Fig.4.9 shows the liquid amount experimentally required for the growth onset (% on batch size). The origin of the z-axis represents the estimated liquid amount for the growth onset given by the intersection between $T_{g,PVP}$ and the ambient temperature (see Fig.4.5), as from the method presented by Cavinato et al. (2010)a,b.

It is interesting to note that the liquid volume required for the growth onset (see z-axis in Fig.4.9) decreases with decreasing the dimensionless spray flux – i.e. approaching to the droplet controlled regime threshold and the predicted liquid amount.
Summarizing, the first examination shows that the liquid distribution strongly affects the granule growth onset and the growth kinetics. Poor liquid distribution (i.e. lower dimensionless spray flux values) leaded to a delay in the growth onset and non-monotonic growth trend. Particularly, the presence of non-uniform wet zones seems to promote more prominent breakage phenomena, thus resulting in lower roundness value and lower final granule size.

4.4.2 Role of the formulation properties on the growth kinetics

The effect of the formulation properties on the granule growth onset and kinetics was studied in detail by changing the formulation composition, as described in Table 4.3. The influence of the dry binder as well as the amount of the hygroscopic filler was analysed (Table 4.3).
The components of a powder mixture can be classified according to their supramolecular structure and their interaction with polar liquids [Palzer, 2010]: thus materials can present several amorphous/crystalline degrees and different hygro-capacities and hygro-sensitivities. The hygro-capacity (i.e. hygroscopicity) can be deduced from the water sorption isotherms in Fig.4.10.
According to this theory, the main components of the processed formulations are:

- dicalcium dehydrate phosphate as main filler, which is crystalline, water insoluble and non-hygroscopic;
- microcrystalline cellulose as second filler, which is mainly crystalline, water insoluble and hygroscopic;
- polivinilpyrrolidone as dry binder, which is amorphous, water soluble and very hygroscopic.

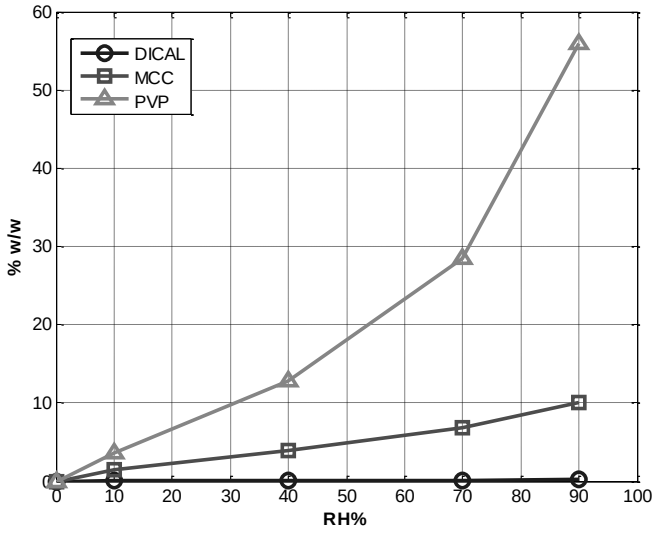

Fig.4.10. Water sorption isotherms (20°C) for dicalcium dihydrate phosphate (DICAL, circles), microcrystalline cellulose (MCC, squares) and polyvinylpirrolidone (PVP, triangles)

The results of the second experimentation are illustrated in Fig.4.11.

Fig.4.11a and Fig.4.11b show the FBRM profiles in absence of the dry binder: as already pointed out by Cavinato et al. (2010)a,b , the dry binder contributes to accelerate and boost the agglomeration process, even if its amount within the initial dry formulation is small (e.g. 1-5% w/w). The variation of the chord length weighted mean is irregular mainly because of the formation of temporary lumps and weak agglomerates. Anyhow, the growth process occurs but it is slower than in presence of the dry binder, as demonstrated by the slight decrease in the number of fine particles. Moreover the sudden increase of the mean diameter (see growth onset in Fig.6) was not noted.

Figs.4.11(c-f) considers the presence of hygroscopic filler within the initial formulation. They show that the growth onset is delayed with increasing the hygroscopic filler content (i.e. MCC amount) thus indicating a higher lack of liquid binder for starting most of the growth process. As can be seen in the Figs.4.11(c-f), the identification of the growth onset results to be more complicated in presence of MCC. In fact, the increase of the chord length weighted mean starts at the beginning of the wetting phase. This phenomenon might be due to the prominent MCC swelling properties [Nikolakakis et al., 2006]. Moreover, the mean diameter profiles reach a plateau during the final wetting and the massing phase.

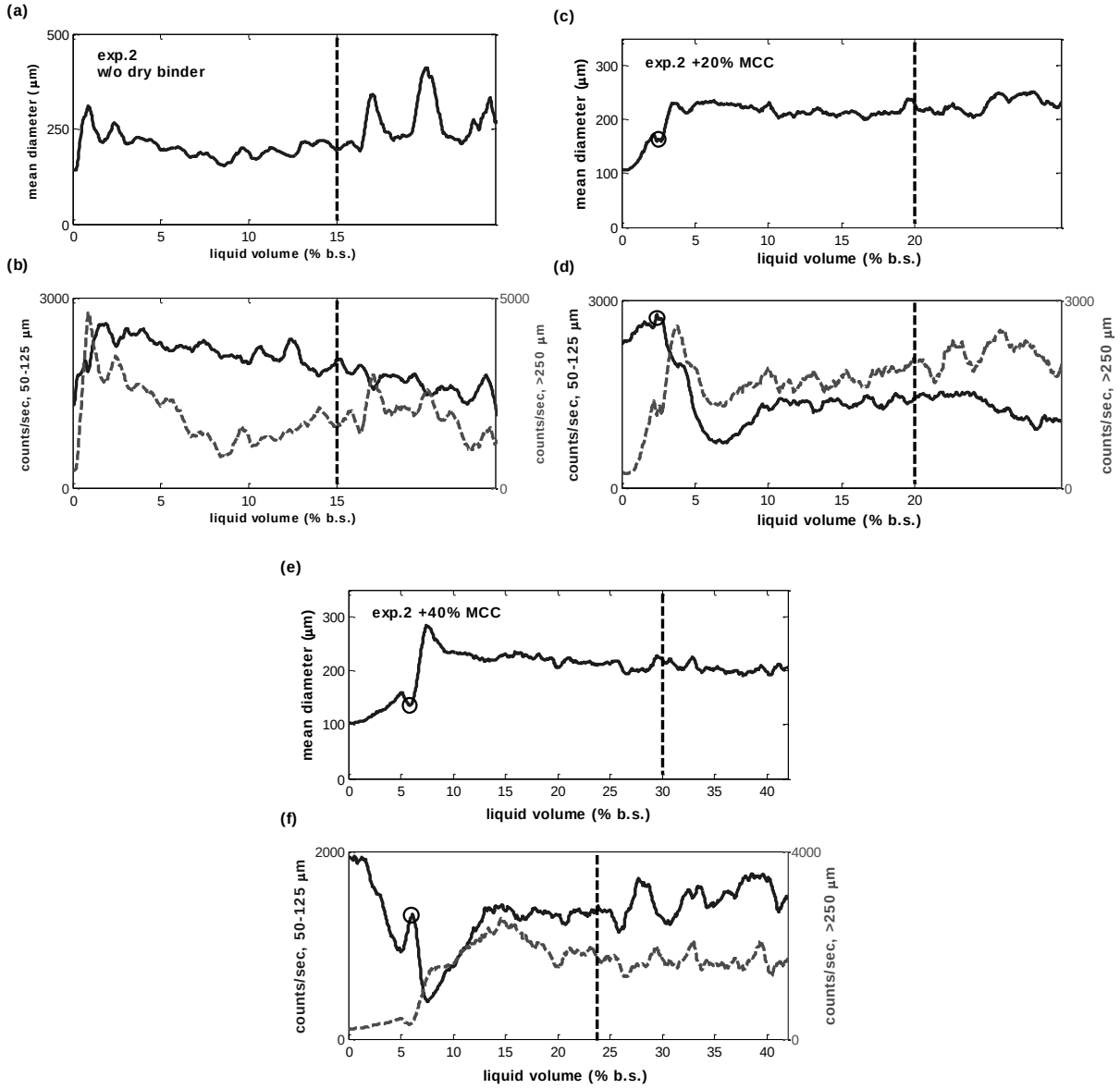

Fig.4.11. Second experimental plan: effects of the formulation composition on the granule growth. Profiles represent the variation of the chord length weighted mean, the number of fine particles (50-125 µm) and larger particles (> 250 µm). Experiment 2 in Table 2 was chosen as a reference for the experiments (a,b) without the dry binder, (c,d) with 20% w/w of MCC and (e,f) with 40% w/w of MCC (see Table 3).

In order to estimate the liquid amount required to yield the growth onset in presence of additional hygroscopic filler, a new simplified procedure has been developed. The graphical construction is shown by Fig.4.12a.

Considering a good liquid distribution (i.e. close to the droplet controlled regime), the water amount (% w/w) absorbed by PVP can be deduced in Fig.4.12a as:

$$w_{\mathrm{H2O,PVP}} = w_{\mathrm{H2O,PVP}}(RH\%^{*}), \qquad \text{Eq.(4.6)}$$

in accordance with the condition $T_{g,PVP} = T_{powder}$ (Figure 4).

The water amount absorbed by the MCC results to be:

$$w_{\mathrm{H2O,MCC}} = w_{\mathrm{H2O,MCC}}(RH\%^{*}). \qquad \text{Eq.(4.7)}$$

The total water amount required for the growth onset can be therefore approximated to:

$$m_{H2O} = m_{H2O,MCC} w_{H2O,MCC} + m_{H2O,PVP} w_{H2O,PVP}, \quad \text{Eq.(4.8)}$$

where *m* is the MCC or PVP mass amount.

The Fig.4.12b shows the comparison between the experimental values and the theoretical values in accordance with Eq.(4.8).

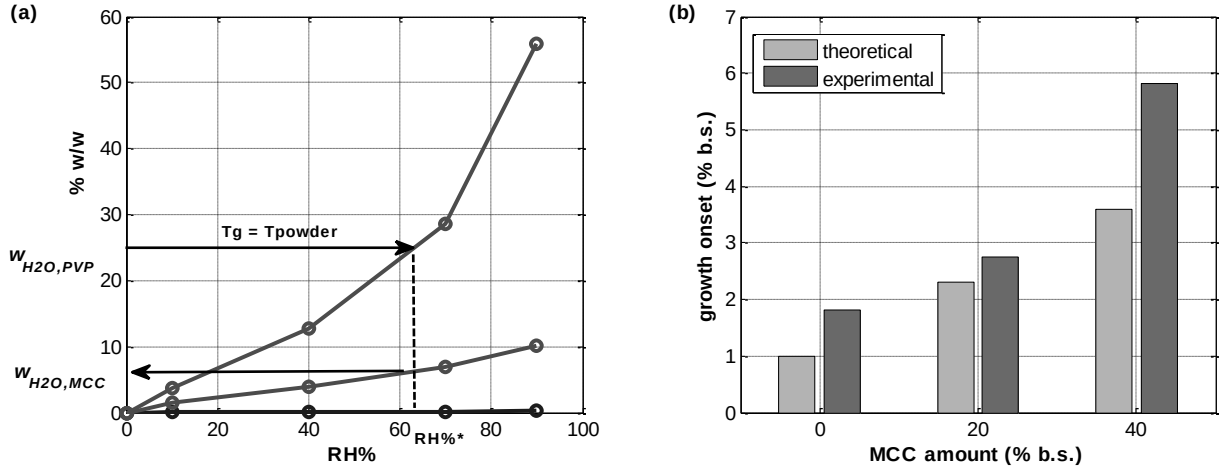

Fig.4.10. Estimation of the liquid volume required for the growth onset in presence of hygroscopic fillers (MCC): (a) graphical construction on the water sorption isotherms, (b) comparison between theoretical values and experimental values, experiments in Table 3

As can be seen in Fig.4.12b, the theoretical values predicted with Eq.(4.5) are in agreement with the experimental values. A certain delay in the actual growth onset can be noted, which was probably due to the non-optimal liquid distribution.

Summarizing, the second examination shows the effect of the filler hygroscopicity on the granule growth process: results show that the growth onset is delayed in presence of the hygroscopic filler. Two crystalline fillers were chosen: they are not soluble in water, so that the solubilization phenomena were not considered for the explanation of the agglomeration mechanism.

4.5 Conclusions

Concluding, the effects of some important process and formulation variables on the granule growth onset and kinetics were systematically analysed. A mixture of commonly-used pharmaceutical powders, composed of crystalline and amorphous materials, were processed through high shear wet granulation.

A FBRM probe was used in order to monitor the particle size distribution (PSD) on-line. Image analysis was furthermore carried out in order to validate the FBRM results and measure the granule shape evolution.

The nucleation regime map [Litster et al., Powder Technology 114 (2001) 29–32] was combined with a method for the prediction of the granule growth onset based on the glass transition concept [Cavinato et al., International Journal of Pharmaceutics 387 (2010) 48–55] in order to evaluate the effect of the liquid distribution on the granule growth process. A simplified procedure for the prediction of the growth onset in presence of hygroscopic fillers was furthermore developed.

Main conclusions can be summarized as follows:

- impeller speed and spray nozzle characteristics were changed in order to achieve different nucleation regimes and liquid distributions (i.e. dimensionless spray flux values). Results show that the lower is the dimensionless spray flux and the better the liquid distribution, the lower is the liquid amount required to yield the growth onset, considered as the sudden increase in the chord length weighted mean. Approaching the droplet controlled regime (approximately $\Psi_a < 0.1$), the liquid amount required for the growth onset approaches the estimated value, which represents the water amount needed for the dry binder glass transition;
- liquid distribution strongly affects the growth kinetics, considered as the granule growth trend. Poor liquid distribution leaded to less regular growth and promoted more prominent breakage phenomena, as pointed out by the FBRM profiles and the granule shape analysis;
- the presence of dry binder (i.e. amorphous material) within the initial formulation strongly influences the growth mechanism. This substance absorbs water, changing its mechanical properties and becoming sticky. FBRM profiles show that the dry binder contributes to accelerate and boost the growth process;
- the hygroscopicity of the main filler was changed adding microcrystalline cellulose (MCC) into the initial formulation. The fillers present similar primary PSDs; both of them are water insoluble, so that the solubilization phenomena can be disregarded. As resulted from the experimentation, the growth onset results to be delayed with increasing the hygroscopic filler amount. Moreover, the growth process seems to be slowed down in presence of MCC;
- a new simplified procedure for the prediction of the growth onset in presence of hygroscopic fillers was furthermore proposed. Considering a good liquid distribution, the total liquid amount absorbed by the formulation is assumed to be the sum of the contributions of each component, in accordance with its hygro-capacitive behaviour. Results show that the experimental values match the estimated values reasonably well.

4.6 References

T. Allen, Particle Size Measurement, Volume 1: Surface Area And Pore Size Determination, Chapman and Hall, 1997.

M. Cavinato, M. Bresciani, M. Machin, G. Bellazzi, P. Canu, A. Santomaso, Formulation design for optimal high-shear wet granulation using on-line torque measurements, International Journal of Pharmaceutics 387 (2010)a 48–55.

M. Cavinato, M. Bresciani, M. Machin, G. Bellazzi, P. Canu, A. Santomaso, The development of a novel formulation map for the optimization of high shear wet granulation, Chemical Engineering Journal (2010)b in press.

M. Cavinato, E. Franceschinis, S. Cavallari, N. Realdon, A. Santomaso, Granule structure obtained using biphasic binder in high shear wet granulation, World Congress on Particle Technology, 26 – 29 April (2010)c, Nuremberg (Germany).

B.J. Ennis, Theory of Granulation: An Engineering Perspective, Handbook of Pharmaceutical Granulation Technology, 2nd ed., Taylor and Francis Group, 2006.

J.J Fitzpatrick, Particle properties and the design of solid food particle processing operations, Food and Bioproducts Processing 85 (2007) 308–314.

M. Gordon, J.S. Taylor, Ideal co-polymers and the second order transitions of synthetic rubbers. 1. Non-crystalline co-polymers, Journal of Applied Chem- istry 2 (1952) 493–500.

K.P. Hapgood, J.D. Litster, S.R. Biggs, T. Howes, Drop Penetration into Porous Powder Beds, Journal of Colloid and Interface Science 253- 2 (2002) 353-366.

B.C. Hancock, G. Zografi, The relationship between the glass transition temperature and the water content of amorphous pharmaceutical solids, Pharmaceutical Research 11 (1994) 471–477.

K.P. Hapgood; J.D. Litster; R. Smith, Nucleation regime map for liquid bound granules, AIChE Journal 49-2 (2003) 350-361.

K.P. Hapgood, B. Khanmohammadi, Granulation of hydrophobic powders, Powder Technology, Volume 189 (2009) 253-262.

S.M. Iveson, J.D. Litster, Growth regime map for liquid-bound granules, AIChE Journal 44 (1998) 1510–1518.

S.M. Iveson, J.D. Litster, K.P. Hapgood, B.J. Ennis, Nucleation, growth and breakage phenomena in agitated wet granulation processes: a review, Powder Technology 117 (2001) 3–39.

J.D. Litster, K.P. Hapgood, J.N. Michaels, A. Sims, M. Roberts, S.K. Kameneni, T. Hsu, Liquid distribution in wet granulation: dimensionless spray flux, Powder Technology 114 (2001) 29–32.

J.D. Litster, B. Ennis, The science and engineering of granulation process, Kluwer academic publishers, Dordrecht, The Netherlands, 2004.

P.R. Mort, Scale-up of binder agglomeration processes, Powder Technology 150 (2005) 86–103.

A.M. Nazar, F.A. Silca, J.J. Amman, Image processing for particle characterisation, Materials Characterization 36 (1996) 165-173.

I. Nikolakakis, K. Tsarvouli S. Malamataris, Water retention and drainage in different brands of microcrystalline cellulose: Effect of measuring conditions, European Journal of Pharmaceutics and Biopharmaceutics 63 (2006) 278-287.

A.M. Nilpawar, G.K. Reynolds, A.D. Salman, M.J. Hounslow, Surface velocity measurement in a high shear mixer, Chemical Engineering Science 61 (2006) 4172 - 4178.

S. Palzer, Influence of material properties on the agglomeration of water- soluble amorphous particles, Powder Technology 189 (2009) 318–326.

S. Palzer, Agglomeration of pharmaceutical, detergent, chemical and food powders - Similarities and differences of materials and processes , Powder Technology (2010) in press.

Chapter 5

Relationship between particle shape and some process variables in high shear wet granulation using binders of different viscosity

5.1 Summary

The effects on granule shape of binders of different viscosities have been compared in the high shear wet granulation process. Water and different emulsions where used as liquid binders. The observed differences in shape have been explained in terms of the granule growth regime map and show that it is easier to control the shape of granules obtained using emulsions as binder. Moreover, evidences have been collected showing that high shear wet granulation is a viable solution for solid self-emulsifying drug delivery systems.

5.2 Introduction

There is evidence in the literature that lipid-based systems are successful in enhancing the bioavailability of Class II Active Pharmaceutical Ingredients (APIs), which are poorly water-soluble but highly permeable drug molecules [Prabhu et al., 2005]. One of the most popular approaches of lipid formulations is the self-emulsifying drug delivery system (SEDDS). SEDDSs are mixtures of oils and surfactants, sometimes containing co-solvents, which are able to spontaneously emulsify and produce fine oil-in-water emulsion when introduced into aqueous phase under gentle agitation.
Upon peroral administration, these systems form fine oil-in-water emulsions (or microemulsion) in the gastro-intestinal tract with mild agitation provided by gastric motility [Patil and Paradkar, 2007; Humberstone and Charman, 1997].

However, SEDDSs are mostly prepared as liquid dosage forms such as emulsions. They can be contained within soft capsules and present some disadvantages especially in the

Published in:
M. Cavinato, E. Franceschinis, S. Cavallari, N. Realdon, A. Santomaso. Chemical Engineering Journal 164 (2010) 292-298.

manufacturing process with consequent high production costs. Moreover, incompatibility problems with the capsule shell such as leaking of components are usual. Accordingly, the new drug delivery technology solid SEDDS started to interest researchers because it combines the advantages of SEDDS with those of solid dosage forms [Tang et al., 2008]. Various methods were used to incorporate lipids into solid matrices, which were summarized in a recently published review [Cannon, 2006] and high shear wet granulation (HSWG) is a promising solution. Some researchers [Newton et al., 2001; Franceschinis et al., 2005] demonstrated that it is possible to incorporate a self-emulsifying system into cellulose microcrystalline by extrusion-spheronization and high shear wet granulation. Moreover, they found that to make this possible it is necessary to incorporate water into the SEDDS in order to form an oil-in-water emulsion and to ensure that the process would function.

However, the use of emulsions in wet granulation results in binders of increased viscosity which give granules with physical characteristics different from those obtained with simple water. In particular the attention is here focused on the shape of the granules. Controlling granule shape may be desirable for many reasons; among these are for example the flow properties. A spherical shape possesses a minimum surface area to volume ratio resulting in reduced cohesive forces and mechanical interlocking thereby resulting in improved flowability of the bulk powder [Ennis, 2006]. Obtaining more spherical shape is a desired prerequisite also when a subsequent coating or drug layering of the granules is necessary.

The advantage of HSWG is that mixing, massing and granulation are performed in a few minutes in the same equipment. However HSWG does not always warrant more spherical granules. The process variables need to be controlled with care as the granulation progresses so rapidly and usable granules can be transformed very quickly into unusable ones.
A certain number of works dealing with granule shape were performed in the past on pharmaceutical powders granulated using water or aqueous polymer solutions as granulating liquid.
For example some authors have used a granulation map in order to discriminate between different growth/breakage mechanisms as a function of formulation and process variables [Iveson and Litster, 1998; Iveson et al., 2001; Bouwman et al., 2006; Tu et al., 2009]. As a result of a specific growth/breakage mechanism, final granule shape has been correlated with a particular area in the growth regime map [Bouwman et al., 2006; Tu et al., 2009]. A similar approach will be here adopted for solid SEDDS. Differences in the granule shape will be explained in the light of the Stokes deformation number approach and the comparison with classical water-bound granules will be presented as well. The results of granule characterization will be also compared with those obtained by other researchers [Newton et al., 2001; Abdalla et al., 2008].

5.3 Experimental set-up

The granules were obtained using a 2 l one-step mixer granulator Rotolab® (Zanchetta SpA, Italy). Granulation procedure was standardized on the basis of preliminary trials. 250 g of a fixed powder mixture composed by 70% of microcrystalline cellulose (Acef, Italy), 27% of monohydrate lactose (Meggle, Germany) and 3% of polyvinyl pirrolidone K-90 (Acef, Italy) was dry-mixed using an impeller speed of 150 rpm for 10 min. Successively binder solution was added on dry powders through a tube with a 0.5 mm internal diameter, using a constant rate of 10 ml/min.

Two different liquid binders were considered: water and emulsions. Emulsions were chosen in order to study the effect of an increasing viscosity on pellet performances and to evaluate the possibility to produce self-emulsifying pellets containing the model drug. Formulation of emulsions was selected using a pseudo-ternary phase diagram constructed using the water titration technique. Emulsion 1 (E1) contained: Lauroglycol 90 (Gattefossè, France), Transcutol (Gattefossè, France), Cremophore EL (BASF, Germany) and water. A second emulsion was considered: Emulsion 2 (E 2) had the same composition of the first one and contained also 5% of Simvastatine (Polichimica, Italy) as model drug.
Viscosity for the three liquid binders were determined by the viscosimeter Rotovisco RV 20 (Haake, Karlsuhe, Germany) and resulted: 0.001, 0.009, 0.017 Pa·s for water, E1 and E2, respectively. The amount of binder solution used to prepare pellets was fixed at 80% (w/w) of total weight of powders. To reduce the number of experiments needed to obtain the highest amount of information on granule characteristics, the screening was planned using an experimental design technique, in particular a factorial plan was used were two variables were studied at 2 levels and one variable was studied at 3 levels as shown in Table 5.1. The factorial plan is reported in Table 5.2.

Table 5.1 Process and formulation variables studied and their codified values

Variable	Levels
X1- Impeller Speed (rpm)	800 1200
X2- Massing Time (min)	3 5
X3- Binder or viscosity	Water Empty emulsion (E1) Emulsion with API (E2)

During massing time impeller speed was increased according to Table 5.2. Massing time was 3 or 5 min. At the end of granulation process the granules were dried in oven at 40°C until

constant weight was achieved. Dry granules were sieved in order to remove lumps larger than 3 mm and stored in well closed bags before characterizations.

For size distribution analysis 100 g of granulation product was poured over a set of sieves (300, 500, 600, 800, 1000, 2000 and 3000 μm). A vibrating apparatus (Retsch AS200, Germany) was used at medium vibration level for 10 min. The fractions were collected and then weighted. Resulting PSDs will be here represented by the normalized-sectional frequency distribution (mass-based) [Allen, 1997; Litster and Ennis, 2004] in order to perform a more reliable and reproducible comparison between the PSDs.

Table 5.2 Experimental plan

Experiment number	Impeller Speed (rpm)	Massing Time (min)	Liquid binder
1	800	3	water
2	1200	3	water
3	800	5	water
4	1200	5	water
5	800	3	E1
6	1200	3	E1
7	800	5	E1
8	1200	5	E1
9	800	3	E2
10	1200	3	E2
11	800	5	E2
12	1200	5	E2

Shape analysis of granulates were performed using a camcorder equipped by CCD 2/3 inch (mod CV-300, Jai) and interfaced with Image Tool PC program (ImageTool©, Copyright 2008, Evans Technology, Inc.).

Porosity and density of final granules were measured using respectively a mercury porosimeter (Pascal 140, Thermo Scientific, Italy) and a helium pycnometer (Pycnomatic ATC, Thermo Scientific, Italy).

The measurements of compression strength were performed using a computer controlled uniaxial mechanical testing instrument (TA-XT2i Texture analyzer, Stable Micro Systems, UK) equipped with very sensitive force and motion transducers mounted to the upper probe of the instrument and a fixed lower fulcrum that forms the base of instrument. A monolayer of granules (600-800 μm size range) was placed on the instrument plate and then pressed for 80% of the monolayer height. The resultant stress-deformation plot links the total measured force depending on the press displacement. The last and highest compression force value was recorded as the sample compression strength and plotted. Each experiment was repeated more than 50 times in order to obtain a reliable compression strength value.

Binder/powder wettability was also taken into account by measuring liquid surface tension and liquid-solid contact angle with the drop pendant and the sessile drop methods

respectively: magnified movies of binder drops dropping from the tube and lying down on dry formulation were taken using a fast digital camera (FastCam PCI 1000, Photron, UK) at 250 frames per second.

5.4 Results

Experimental data concern four main aspects of the problem:
- liquid binder properties and powder wettability;
- final granule shape;
- particle size distribution of the final product;
- granule compression strength.

Liquid drop size and liquid-solid contact angle were measured using image analysis.
A sample of the initial dry formulation was poured into a Petri dish and the surface gently levelled.
Magnified movies of droplets detaching the dosimeter tube and lying on the dry formulation within the Petri dish were taken. The droplet detachment can be described by the following force balance, which represents the force required to contracts the droplet surface against the gravitational force:

$$\gamma_{LV}\pi d\cos\theta = \rho g\left(\frac{\pi D^3}{6}\right), \qquad \text{Eq.(5.1)}$$

where γ_{LV} is the surface tension, θ the angle between the droplet and the tube, ρ the liquid density, g the gravitational constant, d the tube diameter and D the droplet diameter.
Assuming θ = 0 just before the droplet detachment [Mauri, 2005], the ratio between the droplet and the tube diameters can be expressed as:

$$\frac{D}{d} = \left(\frac{6\gamma_{LV}}{d^2\rho g}\right)^{1/3} = \left(\frac{6}{\mathrm{Bo}}\right)^{1/3} = k\mathrm{Bo}^{-1/3}, \qquad \text{Eq.(5.2)}$$

where k results to be 1.82 and Bo is the Bond number:

$$\mathrm{Bo} = \frac{d^2\rho g}{\gamma_{LV}}. \qquad \text{Eq.(5.3)}$$

which is a dimensionless group describing the relative magnitude of forces due to gravity and surface tension. The presence of residual liquid on the tube after droplet detaching suggests an experimental correction of the k value in Eq.(5.1), so that it results to be around 1.6 [Mauri, 2005]. Accordingly, liquid surface tension was calculated using the equation:

$$\gamma_{LV} = 0.244\frac{d^3\rho g}{D} \qquad \text{Eq.(5.4)}$$

where d and D_d are droplet and tube diameters, ρ is liquid density.

Table 5.3 summarizes liquid properties and drop characteristics (tube with a 0.5 mm diameter).

Table 5.3 Liquid properties resulting from experimental measurements and image analysis

Liquid binder	Density (kg/m^3)	Viscosity (Pa·s)	Liquid surface tension (mN/m)	Contact angle liquid-solid (°)
Water	1000	0.001	73.537	67.647
E1	888	0.009	38.783	105.820
E2	995	0.017	38.237	108.117

Table 5.3 shows that liquid E1 and E2 present a contact angle larger than 90°: for this reason it is possible to consider them as hydrophobic liquids [Lazghab et al., 2005].

Even though the experimental plan contains a relatively small number of variables (the three variables of Table 5.1), it can be complex to synthetically describe them. We start by considering their effects on the shape of the granules expressed in terms of roundness and elongation. Roundness is computed as:

$$R = \frac{4\pi A}{P^2} \qquad \text{Eq.(5.5)}$$

where A is the granule area and P is the granule perimeter. Roundness resulting values are included between 0 and 1. The larger the value, the rounder the object.

Elongation, or aspect ratio, is defined as the ratio between the length of the major axis *L* and the length of the minor axis *W*:

$$E = \frac{L}{W} \qquad \text{Eq.(5.6)}$$

Elongation takes values larger than 1: the closer the value to 1, the rounder the object. All measurements in this work were carried out on granules belonging to the 600-800 μm size fraction.

Average roundness values with corresponding error bars are represented in Fig.5.1. Data are presented in the following order: each set of data (diamonds, square and triangles) correspond to a different binder and is plotted presenting first the experiments with shorter massing time (3 min) at 800 and 1200 rpm respectively and then the same for experiments with longer massing time (5 min) as indicated in Fig.5.1. This order has been followed also for all the other Figures in the paper.

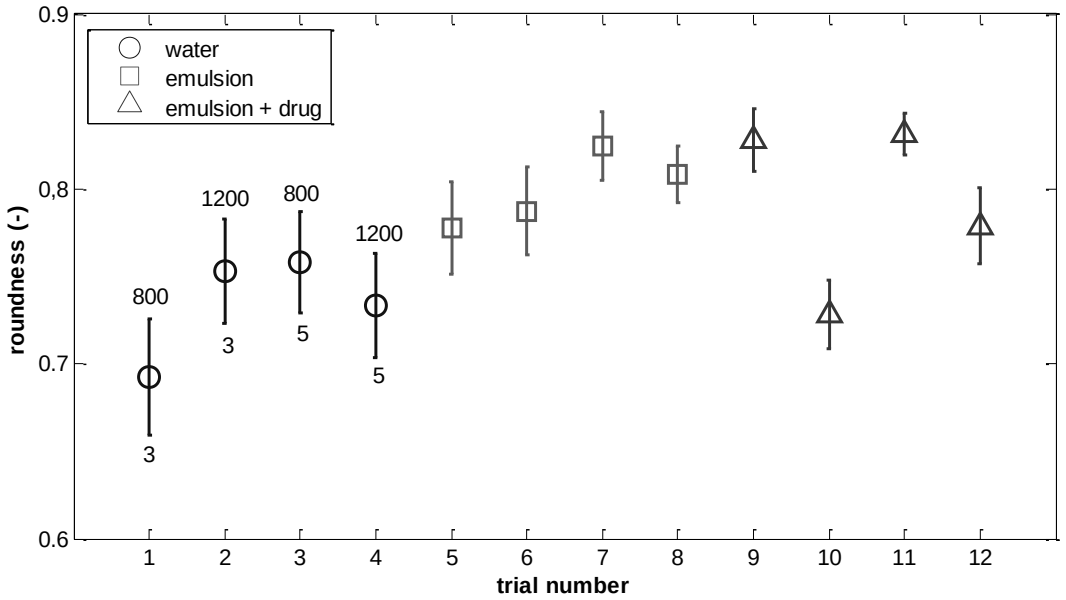

Fig.5.1. Data obtained from image analysis of the granules (600-800μm size range): roundness index as a function of the liquid binder type and the process conditions. Massing times (3 and 5) and impeller speeds (800 and 1200) are reported in just one case for sake of clarity. The sequence is the same in all the other cases.

As can be seen in Fig.5.1, water-based granules present, on average, lower roundness values. It is clearly noticeable that at lower impeller speed (800 rpm), roundness increases with viscosity both for short and long massing time. At higher impeller speed the trend is different instead: the roundness value reaches a maximum for the intermediate binder viscosity. As can be deduced from the error bars extent, the standard deviation values decrease with increasing the binder viscosity. Granules obtained with E2 as granulating liquid show the lowest standard deviation values: this might be a sign of strengthening properties due to the high viscosity and more homogeneous shear stress conditions in the bulk.

Summarizing, the use of E1 or E2 seems to lead to the formation of rounder granules, especially if the massing phase is performed with the lowest impeller speed.

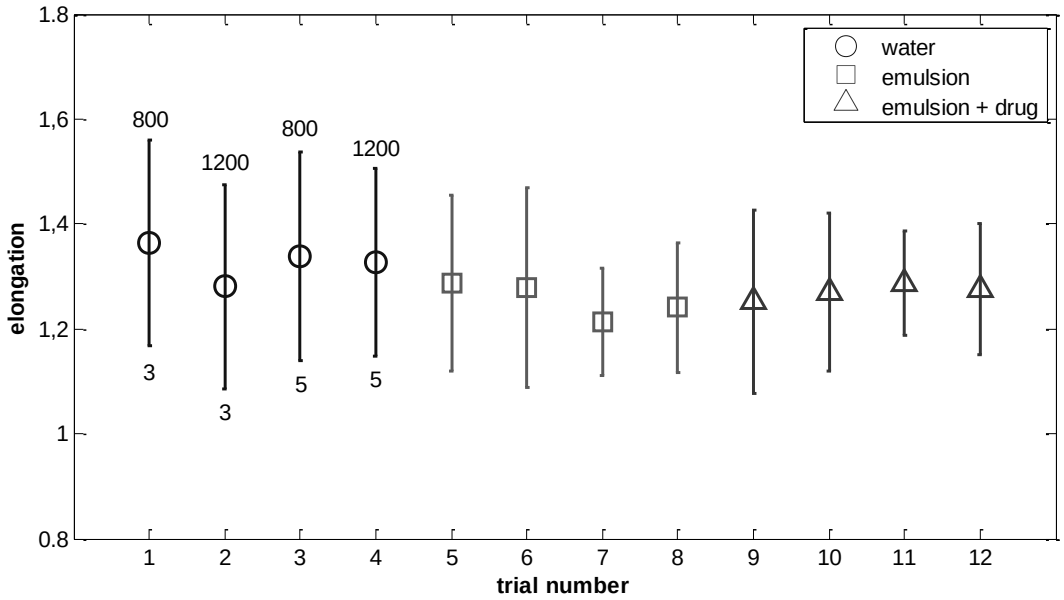

Fig.5.2. Elongation values obtained from the image analysis, considering different liquid binders and process conditions

On the other hand, Fig.5.2 shows the average elongation values with corresponding error bars. Mean elongation values roughly decrease with binder viscosity, thus indicating a lower deformability of the granules. On the whole however the effects of the chosen variables are less definite on elongation than on roughness which therefore should be chosen as the reference shape factor. The standard deviation of elongation values slightly decreases with increasing the binder viscosity. The variability of elongation values is furthermore noticeably higher than for roundness values.

Some researchers performed shape and surface roughness analysis of granules obtained using SEDDSs as liquid binders: Newton et al. (2001) and Abdalla et al. (2008) turned to extrusion/spheronization in order to produce pellets containing SEDDSs. Even if the analysis of aspect ratio and eccentricity did not show considerable differences between water-based granules and those produced using SEDDSs, both of these authors reported surface roughness values noticeably lower when SEDDS was used. Thus, the use of an emulsion as binder seems to give smoother granule surface. As explained in the same papers [Newton et al., 2001; Abdalla et al., 2008], the presence of the oil phase within the cellulose crystalline structure might lead to a more “fluid-like” and hence smoother surface.

The final PSDs obtained using the three different liquid binders are shown in Fig.5.3. The PSDs obtained using E1 and E2 as liquid binders tend to be narrower than the PSD of the water-based granules: the narrowest PSDs were obtained after 3 min, using the lowest impeller speed - see Fig.5.3(a). Moreover, the PSDs obtained using water and E1 do not greatly depend on the process conditions. Contrarily both the impeller speed during the wet

massing and the massing time affect the PSDs of the E2-based granules. The higher is the impeller speed and the massing time, the broader is the PSD of the E2-based granules and the higher is the mean size value.

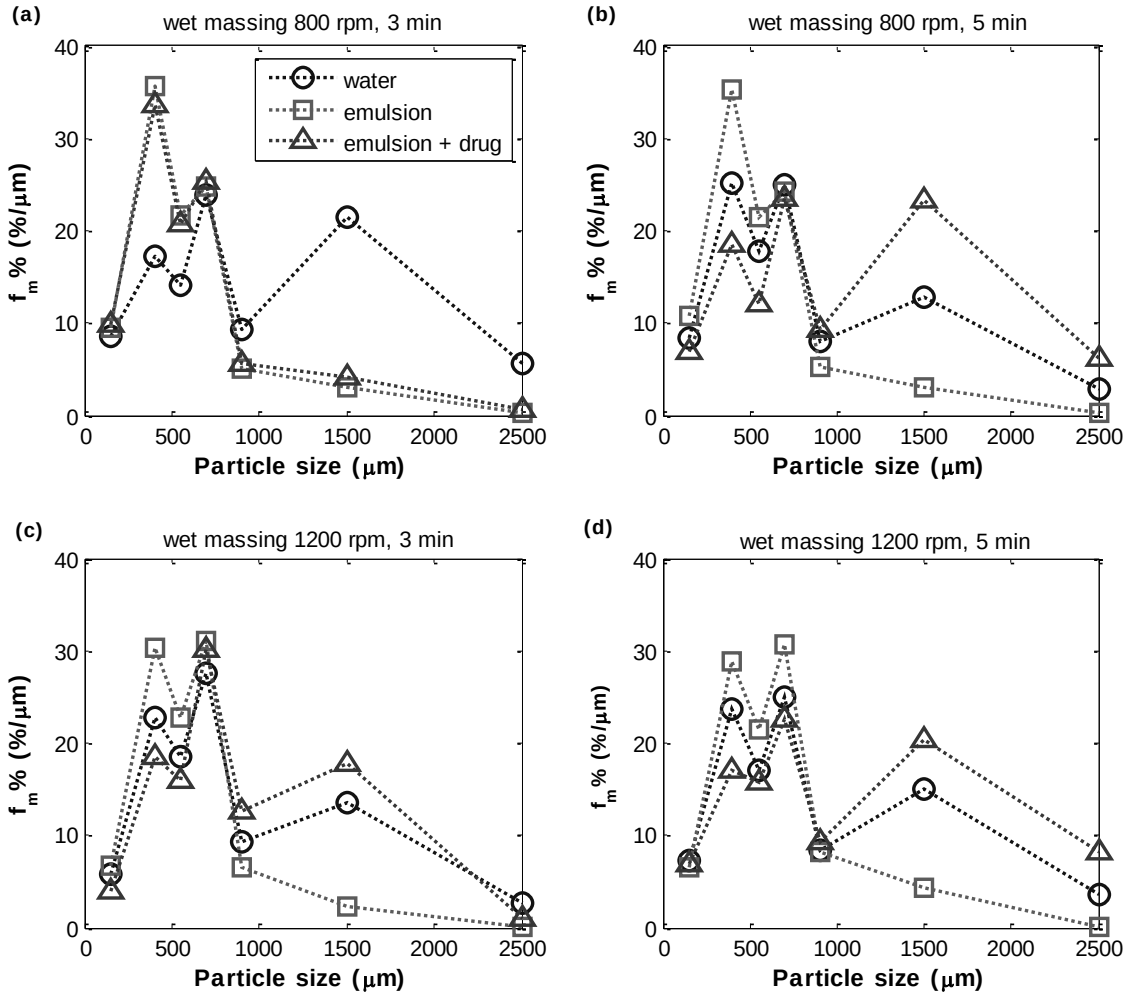

Fig.5.3. Particle size distribution of the final product, comparison between different liquid binders and process conditions during the wet massing phase: (a) 800 rpm for 3 min, (b) 800 rpm for 5min, (c) 1200 rpm for 3 min and (d) 1200 rpm for 5 min

Both particle shape and size are connected to the structure of the granule so that the compression strength of the dry granules was measured in addition. The compression test has been frequently applied to granules, tablets or wet samples in order to achieve some information about the sample structure strength [Iveson et al., 2001; Reynolds et al., 2005]. In this work, the final dry granule was compressed with a view to describing the compression strength as a function of the process parameters-liquid binder type combination.

Fig.5.4 shows the strength values for the granules and the corresponding standard deviations. As the Fig.5.4 clearly denotes, the longer is the massing the higher is the granule compression strength of the water-based granules. On the contrary, the breakage behaviour of granules

obtained using E1 or E2 as liquid binders does not tightly depend on the operative conditions during the massing phase.

This behaviour might be explained in terms of the existence of persistent liquid bridges between primary particles after the drying process because of the oily phase in the emulsion and the consequent reduced final number of solid bridges due to lactose crystallization after water removal. The presence of lubricated contacts makes the final granule strength only slightly dependent on the operating conditions.

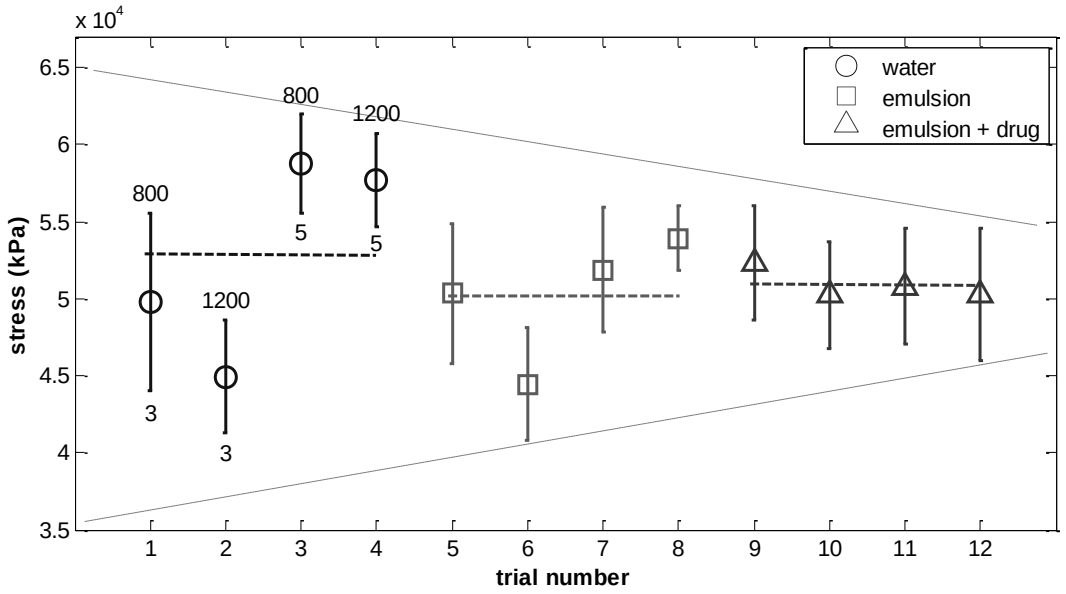

Fig.5.4. Compression strength test on the granules (600-700μm size range)

The average compression strength for each liquid binder is represented by a plain-dotted line. As can be appreciated in Fig.5.4, the difference between the average strength values is not very remarkable: only a very slight decrease in the mean compression strength can be noted for the granules obtained using E1. These results can be compared with those obtained by Abdalla et al. (2008) and Newton et al. (2001). These authors found that the friability of granules increases with increasing the oil phase percentage in the liquid binder. They explained this phenomenon by considering the weaker interactions within the pellets in presence of the oily phase, which was not absorbed by the cellulose solid matrix. Compression strength values in Fig.4 are of the same order of magnitude as those presented in other literature works [Bika et al., 2005; Girya et al., 2009],

5.5 Discussion

Some authors correlated final granule properties (e.g. shape and size) with process and formulation variables, using granulation maps to describe particular growth/breakage mechanisms [Bouwman et al.,2006; Tu et al., 2009]. This approach considers the existence of

two broad granule growth regimes [Litster and Ennis, 2004; Hoornaert et al., 1998]: steady growth and induction growth.

Steady growth regime is typical of granulation system with weak, deformable granules with coarse, narrowly-sized particles and low surface tension and/or low viscosity binder liquids. In this case, two moving granules absorb impact kinetic energy during collision through plastic deformation of their structure. Liquid might be squeezed onto the granule surface forming a bond which can be strong enough to link the granules and form a new larger granule [Litster and Ennis, 2004].

On the other hand, induction growth regime occurs in granulation systems with strong, non-deformable, slowly-consolidating granules composed of fine particles and/or viscous binders. An induction time is usually necessary to allow granules to consolidate sufficiently, then the liquid might be squeezed to their surface. Thus, granules coalescence occurs without the application of large amounts of deformation and rapid granule growth is often observed [Litster and Ennis, 2004].

If the system is too weak or the mixing energy too high, a non-granular "crumb" material will be formed [Tardos et al., 1997].

A granule growth regime map was developed in order to define these different growth behaviours (see Fig.5.5) as a function of two important dimensionless numbers: the Stokes deformation number and maximum granule pore saturation [Iveson et al., 2001].

Granule deformation during impact can be characterized by Stokes deformation number, which is the ratio between impact energy and granule dynamic strength [Iveson et al., 2001; Tardos et al., 1997; van der Dries and Vromans, 2002]:

$$St_{def} = \frac{\rho_g v_c^2}{2\sigma_p} \qquad \text{Eq.(5.7)}$$

where ρ_g is the granule density, v_c is the representative collision velocity for the granulator.

Granule dynamic strength can be identified as following [van der Dries and Vromans, 2002]:

$$\sigma_p = \frac{9}{8}\frac{(1-\varepsilon)^2}{\varepsilon^2}\frac{9\mu\pi v_p}{16 d_{3,2}} \qquad \text{Eq.(5.8)}$$

where ε is the granule porosity, $d_{3,2}$ is the Sauter mean diameter of the granules' constituent particles, μ is the granulating liquid viscosity and v_p is the relative velocity of moving particles after impact.

Maximum granule pore saturation can be used as a measurement of liquid content [Iveson et al., 2001; Liu et al., 2009]:

$$S_{\max} = \frac{w\rho_s(1-\varepsilon_{\min})}{\rho_l \varepsilon_{\min}} \qquad \text{Eq.(5.9)}$$

where w is the ratio between liquid and solid masses, ρ_s and ρ_l are solid particles and liquid density respectively, $\varepsilon_{\min}$ is minimum porosity for the particular set of operating conditions.

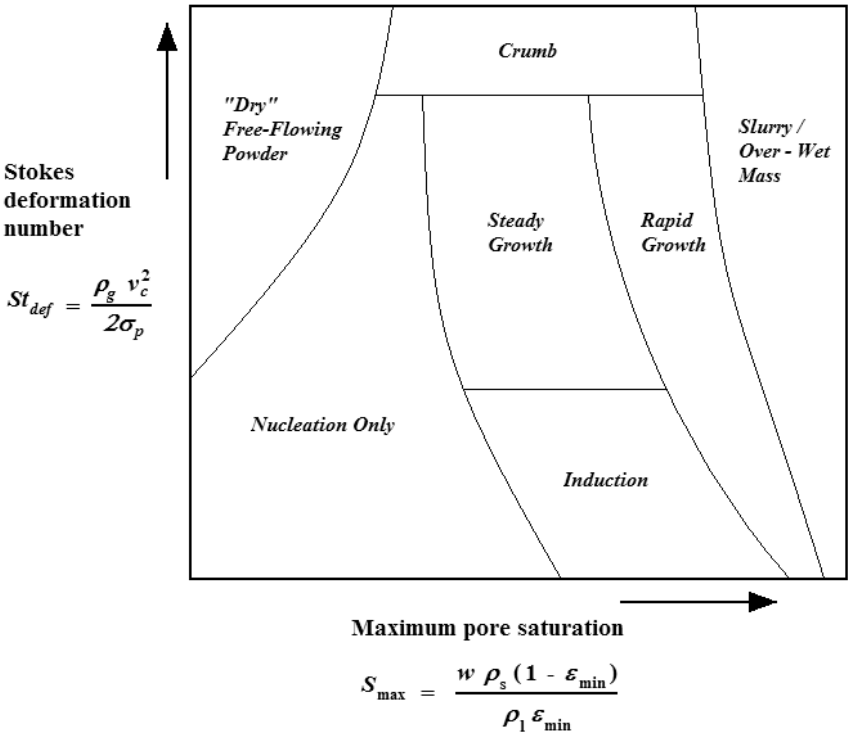

Fig.5.5. Granule growth regime map [Iveson et al., 2001]

The boundary between breakage behaviour and no breakage behaviour (i.e. steady growth - crumb regime boundary) was experimentally established by Tardos et al. (1997) and resulted to be St_{def} ~ 0.2. Iveson et al. (2001) found that this boundary occurred at St_{def} ~ 0.04. The boundary between steady and induction growth occurred at St_{def} between 0.001 and 0.003.

The Stokes deformation number was therefore estimated for each granulation experiment in Table 5.2. The procedure aims at locating the granulation system conditions in the growth regime map, in order to identify the state related to granulation with water, or rather, E1 and E2.

The ratio between liquid mass and powder mass can take the place of maximum granule pore saturation for sake of simplicity in the comparison between the three different systems [Iveson et al., 2001]. The velocity v_c and v_p are assumed to be 15% of the impeller tip velocity during the wetting phase [Liu et al., 2009].

ε and ρ_g are assumed to be respectively the average granule porosity and density of the final granules (see Table 5.4). Mercury porosimeter and helium pycnometer were used for characterizing the granules belonging to the 600-800 μm size fraction. Several samples of about 1 g each were analyzed. As can be noted from the values in Table 5.4, E1 and E2-based granules show lower porosity and density values.

Table 5.4 Average granule porosity, granule density and mean pore diameter for the granules obtained using the three different liquid binders

Liquid binder	Granule porosity %	Granule density (Kg/m^3)
Water	60.7 ± 1.3	1470.6 ± 0.5
E1	53.9 ± 0.9	1365.6 ± 0.2
E2	53.5 ± 1.0	1361.3 ± 0.3

The conditions related to the three different granulation systems are represented in the growth map of Fig.5.6. Stokes deformation numbers were estimated using Eq.(5.7) and Eq.(5.8).
The comparison in Fig.5.6 can be considered a first qualitative estimation since some approximations are involved in the derivation of Stokes deformation number, but a considerable difference can be noted between conditions related to water-granulation and E1 or E2-granulation.
As described by Bouwman et al. (2006), different material exchange mechanisms are exhibited increasing the Stokes deformation number: distribution, deformation (respectively steady growth and induction area in Fig.5.5, lower Stokes deformation number) and disintegration mechanism (crumb areas in Fig.5.5, higher Stokes deformation number).

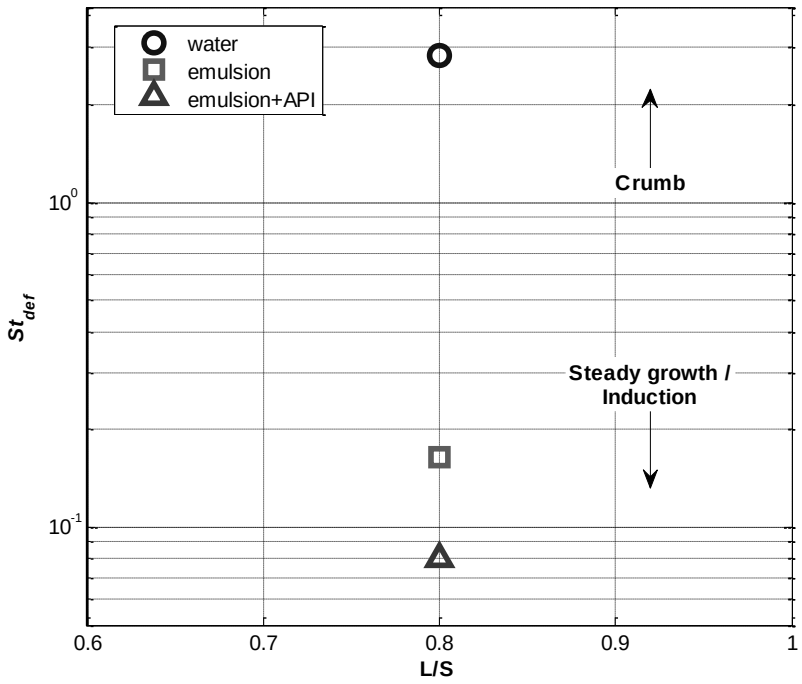

Fig.5.6. Growth regime map with points related to the three different systems: granulation using water, emulsion and emulsion containing the drug (SEDDS) as liquid binders

Water-granulation conditions seem to belong to the disintegration mechanism area: granules tend to be less spherical, as can be deduced from Fig.5.1 and Fig.5.2. This mechanism occurs

when granules quickly grow and break in fragments. The causes are mainly the low viscosity of water and the granules brittleness.
E1 and E2 granulation conditions are very close to each other in the growth map. High viscosity binder promotes a distribution/deformation mechanism: granules grow more slowly and the fragmentation propensity is lower due to a higher shear resistance. Results show more spherical granules which are slightly dependent on the operating conditions during the massing phase (see Fig.5.1 and Fig.5.2).
Similar results were obtained by Bouwman et al. (2006): in this work a formulation mainly composed of cellulose or lactose was processed using high-shear granulation with water or viscous binders. The viscous binder strongly lowered the Stokes deformation number, thus leading to rounder granules with smoother surface. On the other hand, granules obtained using water as liquid binder resulted to be less spherical and presented rougher surface.
As can be noted in Fig.6, St_{def} for water-granulation results to be higher than breakage / non-breakage boundary [Iveson et al., (2001), Tardos et al., (1997)]. Similar or higher St_{def} values were obtained for similar systems using water as liquid binder [Bouwman et al., 2006]. Notwithstanding this discrepancy, agglomeration clearly occurred during all the experiments. This fact might be due to the presence of a small amount of viscous polymer (PVP) within the initial formulation. Accordingly, the actual viscosity in Eq.(5.8) might be higher, thus lowering the Stokes deformation number.
Another explanation of this discrepancy might consider possible errors in (over)estimating impact velocity in Eq.(5.7). As suggested by Litster and Ennis [Litster and Ennis, 2004], it is difficult to estimate the characteristic speed to use to characterize a high shear mixer granulator and any error is greatly magnified, since St_{def} is proportional to impact velocity squared.

5.6 Conclusions

A study on the shape of granules obtained with three different liquid binders was performed. The analysis showed that increasing the viscosity by using oil in water emulsions resulted in granules that were more spherical than those obtained with addition of simple water. The growth regime map was used to explain this observation. Water based granules resulted to have higher Stokes deformation number and therefore resulted to be more deformable and brittle during their growth. Because of the intense breakage irregular granules were obtained. The opposite was obtained for emulsion bound granules. An analysis of the strength of dry granules revealed that those obtained with the emulsions were not weaker than those obtained with water, as it could be expected from the presence of a second oily phase. On the contrary the strength of emulsion based granules appeared to be independent of the operating variables such as massing time and impeller speed. This was particularly true for the case with

emulsion plus API and represents a potential advantage for the production process. The collected observations show that using HSWG to obtain solid SEDDS is a viable solution which merit further consideration since many points still need to be disclosed. The role of the binder surface tension for example was not considered here but just as an anticipation of future research directions let notice that the trends of binder surface tension in Table 5.3 and of the Stokes deformation number in Fig.5.6 are the same indicating a possible important role of this variable on the granule growth mechanism.

5.7 References

A. Abdalla, S. Klein, K. Mäder, A new self-emulsifying drug delivery system (SEDDS) for poorly soluble drugs: Characterization, dissolution, in vitro digestion and incorporation into solid pellets, European Journal of Pharmaceutical Sciences 35 (2008) 457–464.

T. Allen, Particle Size Measurement, Volume 1: Surface Area And Pore Size Determination, Chapman and Hall, 1997.

D. Bika, G.I. Tardos, S. Panmai, L. Farber, J. Michaels, Strength and morphology of solid bridges in dry granules of pharmaceutical powders, Powder Technology 150 (2005) 104–116.

A.M. Bouwman, M.R. Visser, G.M.H. Meesters, H.W. Frijlink, The use of Stokes deformation number as a predictive tool for material exchange behaviour of granules in the ‘equilibrium phase’ in high shear granulation, International Journal of Pharmaceutics 318 (2006) 78-85.

J.B. Cannon, Lipid-based oral solid dosage forms for poorly soluble drugs, Bulletin Technique Gattefossè 99 (2006) 51-61.

B.J. Ennis, Theory of Granulation: an Engineering Perspective, in: D.M. Parikh (2nd Ed.), Handbook of Pharmaceutical Granulation Technology. Taylor and Francis Group, 2006.

E. Franceschinis, D. Voinovich, M. Grassi, B. Perissutti, J. Filipovic-Grcic, A. Martinac, F. Meriani-Merlo, Self-emulsifying pellets prepared by wet granulation in high-shear mixer: influence of formulation variables and preliminary study on the in vitro absorption, International Journal of Pharmaceutics 291 (2005) 87-97.

K. Girya, M. Viana, M. Genty, P. Wüthrich, D. Chulia, Switch from single pot to multiphase high shear wet granulation process, influence of the volume of granulation liquid in a pilot scale study, Chemical Engineering and Processing 48 (2009) 1293–1301.

F. Hoornaert, P.A.L. Wauters, G.M.H. Meesters,. S.E. Pratsinis, B. Scarlett, Agglomeration behaviour of powders in a lödige mixer granulator, Powder Technology 96 (1998) 116–128.

A.J. Humberstone, W.N. Charman, Lipid-based vehicles for the oral delivery of poorly water soluble drugs, Advanced Drug Delivery Reviews 25 (1997) 103-128.

S.M. Iveson, J.D. Litster, Growth regime map for liquid-bound granules, AIChE Journal 44 (1998) 1510–1518.

S.M. Iveson, J.D. Litster, K.P. Hapgood, B.J. Ennis, Nucleation, growth and breakage phenomena in agitated wet granulation processes: a review, Powder Technology 117 (2001) 3–39.

S.M. Iveson, P.A.L. Wauters, S. Forrest, J.D. Litster, G.M.H. Meesters, B. Scarlett, Growth regime map for liquid-bound granules: further development and experimental validation. Powder Technology 117 (2001) 83–97.

M. Lazghab, K. Saleh, I. Pezron, P. Guigon, L. Komunjer, Wettability assessment of finely divided solids, Powder Technology 157 (2005) 79-91.

L.X. Liu, R. Smith, J.D. Litster, Wet granule breakage in a breakage only high-shear mixer: Effect of formulation properties on breakage behaviour, Powder Technology 189 (2009) 158-164.

J.D. Litster, B. Ennis, The science and engineering of granulation processes, Kluwer Academic Publisher, 2004.

R. Mauri, Elementi di fenomeni di trasporto, Edizioni Plus - Pisa University Press, 2005.

M. Newton, J. Petersson, F. Podczeck, A. Clarke, S. Booth, The Influence of Formulation Variables on the Properties of Pellets Containing a Self-Emulsifying Mixture, Journal of Pharmaceutical Sciences 90 (2001) 987-995.

P.V. Patil, A. Paradkar, Formulation of self-emulsifying system for oral delivery of simvastatin: In vitro and in vivo evaluation, Acta Pharmaceutica 57 (2007) 111-122.

S. Prabhu, M. Ortega, C. Ma, Novel lipid-based formulations enhancing the in vitro dissolution and permeability characteristics of a poorly water-soluble model drug piroxicam, International Journal of Pharmaceutics 301 (2005) 209-216.

G.K. Reynolds, J.S. Fu,Y.S. Cheong, M.J. Hounslow, A.D. Salman, Breakage in granulation: a review, Chemical Engineering Science 60 (2005) 3969 – 3992.

B. Tang, G. Cheng, J-C. Gu, C.-H. Xu, Development of solid self-emulsifying drug delivery systems: preparation techniques and dosage forms, Drug Discovery Today 13/14 (2008) 606-612.

G.I. Tardos, M. Irfan Khan, P.R. Mort, Critical parameters and limiting conditions in binder granulation of fine powder, Powder Technology 94 (1997) 245–258.

W.D. Tu, A. Ingram, J. Seville, S.S. Hsiau, Exploring the regime map for high-shear mixer granulation, Chemical Engineering Journal 145 (2009) 505-513.

K. van den Dries, H. Vromans, Relationship between inhomogeneity phenomena and granule growth mechanisms in a high-shear mixer, International Journal of Pharmaceutics 247 (2002) 167-177.

Chapter 6

Predicting scale-up effects on flow pattern in high shear mixing of cohesive powders

6.1 Summary

Granular material processing often requires mixing steps in order to blend cohesive powders, distribute viscous liquids into powder beds or create agglomerates from wet powder mass. For this reason, using bladed, high-speed mixers is frequently considered a good solution by many types of industry. However, despite the great importance of such mixers in powder processing, the granular flow behaviour inside the mixer bowl is generally not totally clear.

The aim of the present work is to propose a new and more detailed method for describing the complex powder rheology inside a high shear mixer based on impeller torque and current consumption analysis. Particularly, a new dimensionless torque number is proposed for the torque profile analysis. This model clearly isolates the contribution of mass fill and impeller height, identifying the transition from the "bumping" regime to the "roping" regime [Powder Technology 124 (2002) 272-280].

Extensive experimentation was then performed using a lab-scale mixer (2 l vessel volume) and a pilot-scale mixer (65 l vessel volume). A mixture of some pharmaceutical excipients (e.g. lactose, cellulose) was processed.

Impeller torque and impeller current consumption were monitored during mixing at bench-scale and pilot-scale respectively.

A high speed CCD camera was furthermore used in combination with particle image velocimetry (PIV) to obtain more information about the surface velocity variation and flow pattern changes in the pilot-scale mixer. Results showed that mass fill is one of the most critical variables, as predicted by the torque model applied at lab-scale, strongly affecting powder surface velocity at pilot-scale.

To be submitted in:
M. Cavinato, R. Artoni, M. Bresciani, P. Canu, A. Santomaso. AIChE Journal.

6.2 Introduction

High shear mixers are widely used in the granular material processing. They can be used for simple mixing or for complex operations which involve both granular solids and liquids. For example in a wet granulation process, a high shear mixer can promote good liquid dispersion and proper consolidation of the product, in order to obtain aggregates and compacts with useful structural forms and better flow properties (Litster and Ennis, 2004).

Despite the great importance of this type of mixers in many industrial activities, granular flow behaviour inside the vessel is currently not totally understood: it is not completely clear how changes in operative variables or in mixer geometry affect the powder flow patterns. Among all the operative variables, mass fill results to be one of the most critical parameters both for the design of the mixer (Paul and Obeng, 2003) and the prediction of the effects of the mixing on the final products (Mangwandi et al., 2010).

Many techniques have been used in order to carry out a good description of the powder flow within the mixer. Amperage as well as motor power consumption, impeller torque and motor slip have frequently been monitored as indirect effects of the mixing process on the mixer. Particularly, power consumption and impeller torque were used to identify how the flow patterns in a mixer depend on the geometric configuration (impeller shape as well as the bowl shape) and the impeller speed (e.g. Paul et al., 2003; Darelius et al., 2007).

For example Knight et al. (2004) developed a model for predicting impeller torque in a high shear mixer. They represented the effect of the mass of powder M and the bowl radius R using a dimensionless torque group T/MgR as a function of the impeller Froude number and considered different changes of the operative conditions: they changed the impeller geometry, the impeller shape, the mass fill, the bowl diameter, the impeller height and the powder size distribution. They obtained a good correlation between the proposed model and the experimental data.

As pointed out by Mort (2009), experimentation on small batch scale with instrumented equipment is commonly performed as a starting point for scale-up to larger batch or continuous processing. However, the maintenance of equivalent flow and stress fields on scale-up is often a big issue. In fact, although geometrical similitude has frequently been identified as an essential prerequisite for scale up of powder mixers (Litster et al., 2002) the design of industrial mixer granulator actually varies from manufacturer to manufacturer and presents, for instance, different bowl size/shape and impeller blades with several variations in bevel angle and shape.

The high-shear mixers considered in the present research are in practice not geometrically similar. The shape of the small-scale bowl is a little bit more smoothed in the bottom border (i.e. close to the impeller tip), thus small-scale blades are slightly more curved. On the other hand, blade bevel angle is similar for both small-scale mixer and pilot-scale mixer.

The aim of the present work is to close the gap in understanding the scale-up effects on the flow patterns in geometrically non-similar mixers. Particularly, this work focuses on the effects of mass fill at different scales.
A more detailed model for the torque prediction was furthermore proposed and validated on the results of the experimentation on small batch scale. This model considers a new dimensionless torque number and clearly isolates the contribution of the mass fill and the impeller height. Extensive experimentation was performed at pilot scale as well. As resulted from particle image velocimetry (PIV) measurements at pilot-scale, mass fill is one of the most critical variables and strongly affects the powder surface velocity.

6.3 Materials and methods

Experiments were performed using a bench-scale and a pilot-scale mixer.
The small-scale mixer (MiPro, 1900 ml vessel volume, ProCepT®, Zelzate, Belgium) was top driven and the pilot-scale mixer (Aeromatic Fielder PMA 65 L, Eastleigh, Hampshire, UK) was bottom driven. Both of the mixers had stainless steel vessels and three bladed impellers. Impeller bevel angle was 30° for both of them.
Impeller torque was measured and recorded during the experiments with the small scale mixer. The pilot-scale mixer was equipped with a system for measuring the impeller current values.
A mixture of some pharmaceutical excipients was used: lactose monohydrate 150 mesh, 73.5% w/w (Lactochem® Regular Powder 150 M, Friesland Foods, Zwolte, The Netherlands), microcrystalline cellulose (MCC), 20% w/w (Pharmacel® 101, DMV International, Veghel, The Netherlands), hydroxypropylmethylcellulose (HPMC), 5% w/w (Pharmacoat® 603/Methocel® E5, Shin-Etsu Chemicals, Niigata, Japan) and croscarmellose sodium, 1.5% w/w (Ac-Di-Sol®, FMC Biopolymer, Philadelphia, USA).
The mass fill was varied between 20% and 40% for both the mixers. The impeller height in the small-scale mixer was also modified including one or more ring-like spacers between the bowl and the mixer support, since the friction of the impeller with vessel wall exerted through a thin layer of strongly sheared powder was expected to give an important contribution to overall torque value.

Powder flow patterns in the pilot-scale mixer were characterized by measuring the powder surface velocity. A high speed camera (FastCam PCI 1000, Photron) at 1000 fps and particle image velocimetry (PIV) software were used. Since surface velocity measurements could not be acquired for the dry mixture due to dusting, a very small amount of water (less than 2% w/w of the batch size) was added. The high speed CCD camera was placed perpendicularly to

the moving powder surface as shown in Fig.1a. The coordinate system chosen for the analysis is also shown in Fig.6.1b.

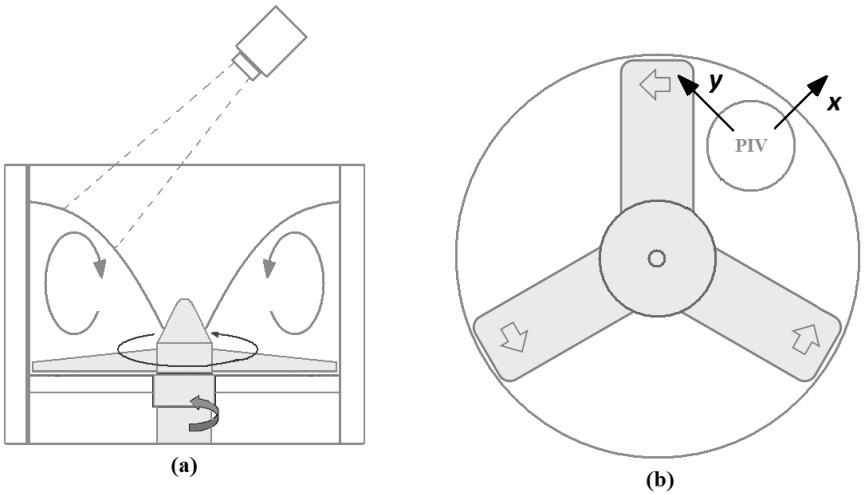

Fig.6.1. Schematic of the pilot scale mixer: (a) location of the high speed CCD camera and (b) coordinate system for the surface velocity measurements Y-direction (tangential velocity) is parallel to the impeller tip speed. X-direction (radial velocity) is pointing towards the centre of the bowl and perpendicular to the impeller tip speed.

6.4 Results and discussion

6.4.1 Lab-scale experiments

Mixing of dry powders was performed using high shear mixers at bench scale (1.9 l). Mixing was performed changing the fill ratio (from 20% to 40% v/v on the vessel volume) and the impeller height. Impeller torque values were monitored and recorded.

Knight et al. (2001) measured the impeller torque values during the mixing of sand of different size fractions in high shear mixers, changing the impeller blade design, rotational speed, fill and bowl size. They represented experimental data by a dimensionless torque number T (Knight et al, 2001):

$$T = \frac{t}{gRM_{tot}}, \tag{6.1}$$

where t is the actual torque value (Nm), R is the bowl radius (m), M_{tot} is the bowl mass capacity (kg) and g is the gravitational constant (9.81 m s^{-2}).

For best representing the results obtained using the small-scale mixer, a new dimensionless torque number is here considered:

$$T = \frac{t}{gRM_{tot}X^{\beta}}, \tag{6.2}$$

which is also function of the fill ratio X and the new parameter β. The role of parameter β is to describe the effects of centrifugal force on the powder mass which is actually in contact with the impeller. The parameter β therefore accounts the effect of a "static" contribution (i.e.

independent on the impeller speed) and a "dynamic" contribution (i.e. function of the impeller speed):

$$\beta = \alpha_1 + \alpha_2 \sqrt{Fr_I}\ , \tag{6.3}$$

where α_1 and α_2 are two constants and Fr_I is the Froude number related to the impeller speed:

$$Fr_I = \frac{\omega_I^2 R}{g}, \tag{6.4}$$

and thus ω_I is the angular speed (rad/s) of the impeller.

The static S_1 and the dynamic S_2 part in Eq. (6.2) can be clearly separated as follows:

$$T = tC \frac{1}{X^{\alpha_1} X^{\alpha_2 \sqrt{Fr_I}}} = tC \frac{1}{S_1 S_2}, \tag{6.5}$$

where C is a constant which depends on the bowl geometry and mass capacity.

Experimental data obtained by Knight et al. (2001) can be fitted by the model in Eq. (6.2) in order to obtain a single master curve, as shown in Fig.6.2a and Fig.6.2b.

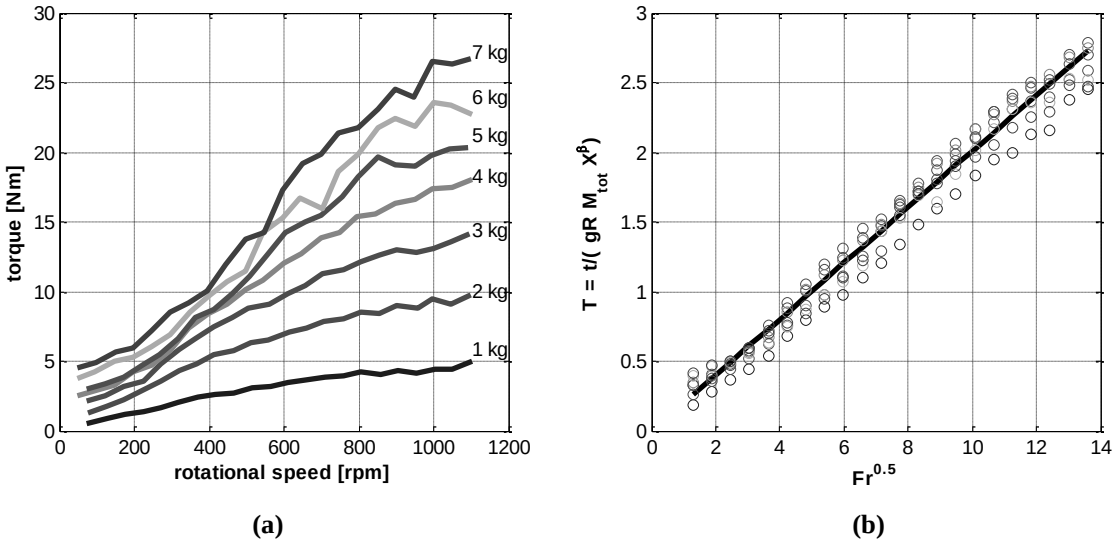

Fig.6.2. Torque profiles (a) obtained by Knight et al. (2001) for different mass fills, using a high shear mixer with a bowl diameter of 0.30 m, and (b) dependence of the new dimensionless torque number on the square root of Fr_I, impeller torque data presented by Knight et al. (2001)

The results show that the impeller torque data are properly described by a common curve when they are plotted in the form of the new dimensionless torque number against the square root of the impeller Froude number. Moreover, it is interesting to see that model in Eq.(6.2) seems to better describe experimental data presented by Knight et al.(2001) than the model proposed by the same authors and described by Eq.(6.1).

Torque profiles obtained using the small-scale mixer at different impeller heights (the clearance values between the impeller and the bottom of the bowl were 0.5, 2 and 4 mm) and mass fills (20, 30 and 40%) are shown in Fig.6.3. Each measurement was repeated at least

three times and torque profiles resulted to be almost overlying for a given mass fill and impeller height. For this reason, error bars are not reported in Fig.3 since they are negligible.

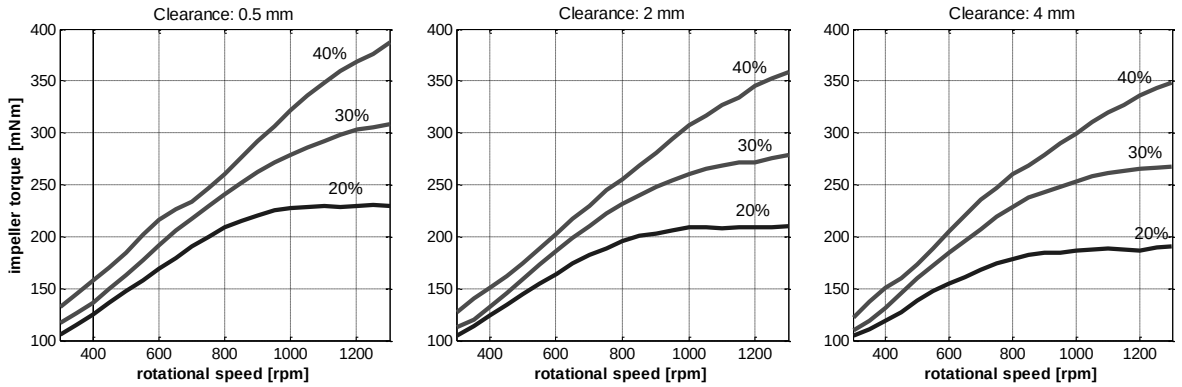

Fig.6.3. Torque profiles obtained using the small-scale mixer at different mass fills and clearance values

As can be seen in Fig.6.3, the fill ratio strongly affects the impeller torque value at different impeller speeds during the mixing of dry powders. In particular it can be noted that torque profiles can be roughly divided into two parts. Firstly, impeller torque linearly increases with increasing the impeller speed. Secondly, impeller torque tends to be almost constant at higher impeller speed values, especially at low mass fill: decrease of slope in the second part of torque profile results to be more accentuated with decreasing the fill ratio. When the mass fill is 20%, the break point in the torque profile corresponding to the change in slope can be clearly distinguished. The change in slope occurs at 800-900 rpm for the smallest fill ratio and shifts to higher impeller speed with increasing the fill ratio.

These results slightly differ from the findings of Knight et al. (2001). They also noted that the dependence of torque on impeller speed displayed s-shaped character (i.e. decrease in torque profile slope for impeller speed higher than a critical value) but the degree of s-shaped character lightly increased with increasing the mass fill. This discrepancy might be caused by the different impeller blade design: Knight et al. (2001) used an impeller bevel angle of 90° for the comparison between different mass fill instead of 30° bevel angle used in the present work. This difference might lead to different flow patterns, thus determining different impeller torque profiles.

The break point in torque profiles in Fig.6.3 can be explained by considering the results presented by Litster et al. (2002). They measured the variation of powder surface velocity during mixing of a similar granular mixture at different rotational speeds. The mixture was composed of lactose monohydrate. According to their results, two mixing regimes can be identified. At low impeller speeds, "bumping" regime was observed: powder surface remained horizontal and the bed was raised as the impeller passed underneath. At higher

impeller speeds, “roping regime” was noted. The powder flow regime was determined from the well-known toroidal flow pattern and the powder bed resulted to be more fluidized.
The transition between the two different regimes was clearly described by the surface velocity measurements. The velocity values increased linearly with the impeller speed during the bumping regime. During the roping regime, surface velocities are no longer proportional to the rotational speed of the blades and tend to stabilize around a constant value. Similar results were recently presented by Remy et al. (2010)a.

It is thus suggested that slope variation in torque profiles in Fig.6.3 (i.e. break point) can represent the transition between the bumping regime and the roping regime. As a matter of fact, impeller torque represents the resistance of the powder to the mixing. Powder results to be more fluidized during the roping regime and vertical turnover is very effective, thus resistance exerted from the powder on the impeller blades is expected to be less influenced from the increase of rotational speed in this case. Moreover, it is suggested that powder fluidization can be harder to achieve when fill ratio is higher and more energy (i.e. higher rotational speed) might be required in order to force up the powder and obtain the transition between the two flow regimes. This phenomenon might explain the increase in rotational speed required to determine the break point in torque profiles when mass fill is higher, as reported in Fig.6.3. Similar considerations about the effects of mass fill on the achievement of roping flow have been proposed by Litster et al. (2002) in their published work.

On the other hand, Fig.6.3 shows that changes in the impeller height determine a smaller variation of torque profiles compared to the effects of mass fill variation. Particularly, it can be noted that torque values tend to decrease with increasing the impeller height. It is suggested that increasing the impeller height might decrease the compression of the powder layer between the impeller and the bottom of the bowl, thus decreasing the attrition. However, the shape of the profiles seems to be independent on the impeller clearance.
Model in Eq.(6.2) was then used to fit torque profiles in Fig.6.3. Accordingly three master curves were obtained: each of them represents a certain impeller height and summarizes the effect of the mass fill on the impeller torque value (Fig.6.4).

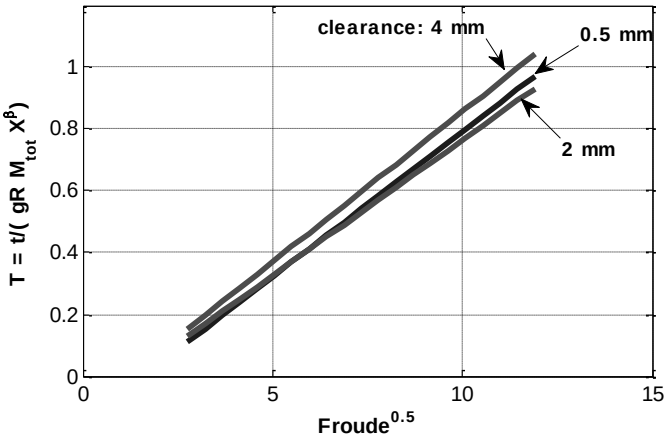

Fig.6.4. Dependence of the new dimensionless torque number on the square root of impeller Froude number: each of the curves represents an impeller clearance value

The three master curves in Fig.6.4 are close to each other but a certain difference in slope and intercept can be noted. A more considerable difference in slope can be observed between curve representing 4 mm and 2 mm height. Particularly, the slope of the master curve increases with increasing the impeller height from 2 mm to 4 mm. These results are in agreement with those presented by Knight et al. (2001).

The effect of the variation of mass fill and impeller clearance on the static term S_1 can be seen in Table 6.1. Moreover, S_2 is plotted and related to the square root of the impeller Froude number: Fig.6.5 shows the S_2 values and the comparison between different impeller heights and bowl mass fills.

Table 6.1 Values of the parameter S1 in Eq.4 as a function of the mass fill and the impeller clearance, during mixing of dry powders at bench scale

Mass fill	S_1 (0.5 mm clearance)	S_1 (2 mm clearance)	S_1 (4 mm clearance)
20%	0.79	0.85	1.01
30%	0.83	0.89	1.01
40%	0.87	0.91	1.01

As can be appreciated in Tab.6.1, the static term S_1 distinctly depends on the impeller clearance for a given mass fill. Particularly, S_1 increases with increasing the impeller clearance.

It can be therefore noted that the higher is the impeller clearance (i.e. impeller height) the weaker is the dependence of S_1 on the mass fill. As can be seen in Tab.6.1, S_1 values corresponding to the highest impeller clearance (4 mm) does not show any dependence on the mass fill.

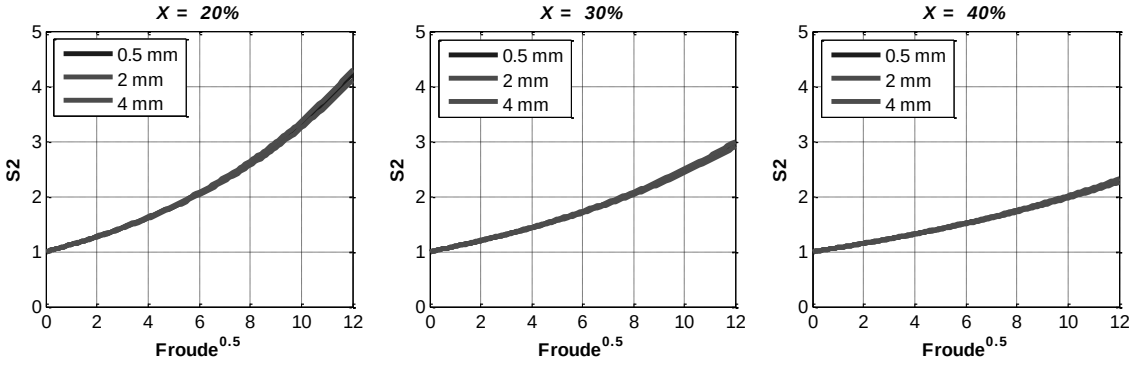

Fig.6.5. Dependence of the parameter S_2 in Eq.4 on the square root of the impeller Froude number: effect of the mass fill X and the impeller clearance during mixing of dry powders at bench scale

On the other hand the dynamic term S_2 mainly depends on the mass fill (see Fig.6.5). It is interesting to note that the slope of S_2 profiles tend to be higher when mass fill is lower. A higher slope in S_2 profile can be correlated with a sharper change in slope of torque profiles at lower impeller speed values (see Fig.6.3): in fact the change in slope in torque profiles was more pronounced when mass fill was lower. As can be seen in Fig.6.5, any dependence of S_2 on the impeller clearance can be neglected, since S_2 profiles at different impeller clearances are almost superimposed for a given mass fill.

Summarizing, the static term S_1 predominantly depends on the impeller height and weakly depends on the mass fill, whereas the dynamic term S_2 is mainly affected by the mass fill.

6.4.2 Pilot-scale experiments

Mixing of the same mixture of dry powders was performed using a pilot scale mixer (65 l) as well. The results of this first analysis on impeller torque profiles at bench scale suggested the essential importance of mass fill in determining the granular flow behaviour within the mixer bowl (see Fig.6.3). For this reason, the second analysis was mainly focused on the effects of mass fill variation on the flow patterns during powder mixing using the pilot-scale mixer.

As a first assumption, minimum and maximum rotational speeds of the pilot-scale mixer were chosen in order to keep the same range of impeller tip speed as in the small-scale mixing. Thus, the range of impeller tip speed was about 2-10 m/s.

The impeller tip speed v was calculated using the Eq.(6.6):

$$v = \frac{\pi D N}{60}, \tag{6.6}$$

where N is the rotational speed (rpm) and D is the impeller blade diameter (m) (Paul et al., 2003). Accordingly, rotational speeds for the pilot-scale mixer result to be lower compared to the small-scale mixer for a given range of impeller tip speed. Fig.6.6 shows the variation of the impeller tip speed with increasing rotational speed for both the mixers.

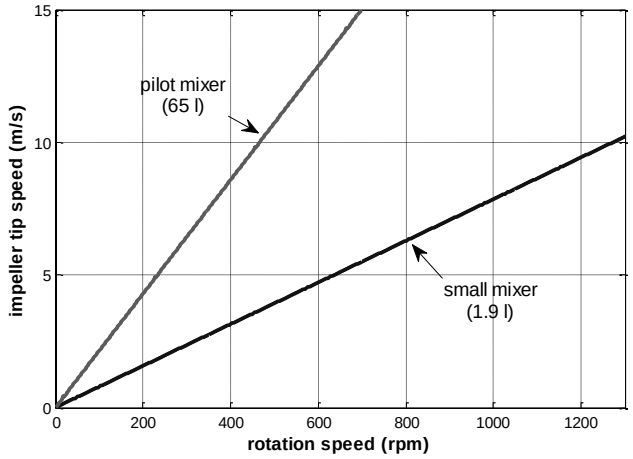

Fig.6.6. Variation of the impeller tip speed as a function of the impeller rotational speed for the bench scale mixer and pilot scale mixer

Impeller current values were then measured at different rotational speeds (150-400 rpm) and for three different mass fills (20, 30 and 40%). Resulting profiles are reported in Fig.6.8.

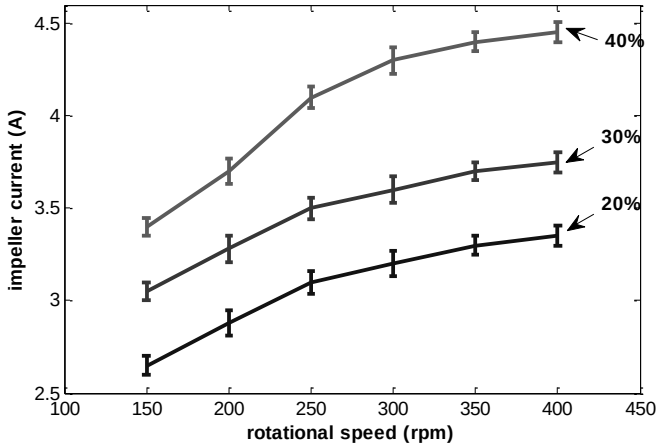

Fig.6.8. Impeller current measurements during the mixing of dry powders with the pilot-scale mixer at different rotational speeds (150-400 rpm) and mass fill (20, 30 and 40%)

Even though impeller current is known to be less accurate than impeller torque for monitoring bladed mixing (Cliff, 1990; Levin, 2006), impeller current profiles in Fig.6.8 are here considered as an indication of the load on the main impeller and qualitatively compared with torque profiles in Fig.6.3. As can be easily noted from the comparison, slope of impeller current profiles tends to decrease with increasing the rotational speed as well. The change in slope is not as sharp as in torque profile, but still the impeller current profiles can be ideally divided into two parts characterized by different slopes. Surface velocity measurement was therefore performed in order to get more accurate information about the powder flow behaviour and to determine how the transition between bumping and roping regime is affected by the mass fill variation during mixing at pilot scale.

A high speed camera and particle image velocimetry (PIV) software were used. Fluctuation of surface velocity in x and y-directions during the measurement time and for a given rotational speed and mass fill can be effectively described by attractor plots (Fig. 6.9).

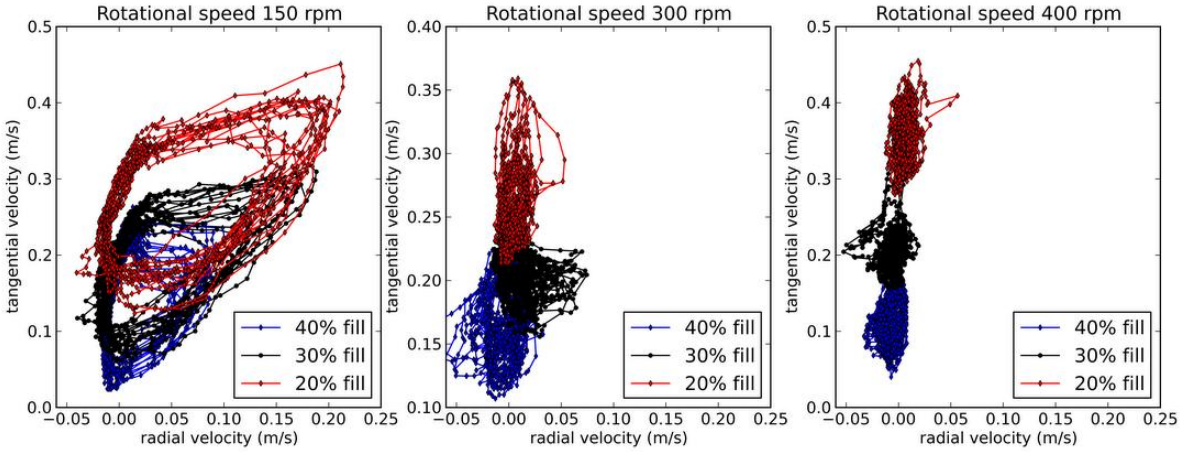

(a) **(b)** **(c)**

Fig.6.9. Attractor plot representing the variation of powder surface velocity for the pilot-scale mixer at different mass fills (20, 30 and 40%) and (a) at 150 rpm, (b) 300 rpm and (c) 400 rpm.

As can be noted from the annular shape of attractors in Fig.6.9a, powder movement tended to be periodic: bed was raised as the impeller passed underneath and, as a consequence of the raising, powder was forced along the radial direction from the centre of the bowl to the vessel wall. This phenomenon determined peaks of the x-velocity component at regular intervals (i.e. corresponding to the rotational frequency) and it can be considered as a typical feature of the bumping regime. It can be furthermore noted that powder flow towards x-direction resulted to be more important when mass fill was lower. This fact can be due to the higher ratio of mixing energy to powder mass, which caused a higher raising force.

On the other hand, the attractor plots which describe mixing at high rotational speed (Fig.6.10) show three smaller, concentrated areas with some isolated peaks of the x-velocity component. Moreover, it is interesting to note how the variation of x-velocity component is much more restricted than the variation of the same component at low rotational speed, thus determining a much higher ratio of y-component on x-component. In practice, powder surface motion at high rotational speed resulted to be mainly mono-directional. Powder flow was therefore likely to follow the well-known toroidal pattern; hence the roping regime was well developed. It can be furthermore noted in Fig.10 that y-velocity component strongly increases with increasing impeller rotational speed.

The mean surface velocity $\bar{v}$ (m/s) can be calculated using the Eq.(6.7):

$$\bar{v} = \text{mean}\left(\sqrt{\bar{v}_x^2 + \bar{v}_y^2}\right), \tag{6.7}$$

where $\bar{v}_x$ is the radial velocity and $\bar{v}_y$ is the tangential velocity.

Standard deviation of surface velocity values can be furthermore considered:

$$\delta = \text{mean}\left(\sqrt{\left(\bar{v}_x - \text{mean}\left(\bar{v}_x\right)\right)^2 + \left(\bar{v}_y - \text{mean}\left(\bar{v}_y\right)\right)^2} \right) \Big/ 2 \,. \tag{6.8}$$

The variation of mean surface velocity as a function of rotational speed is shown in Fig.6.11a. Standard deviation of surface velocity values is also shown in Fig.6.11b.

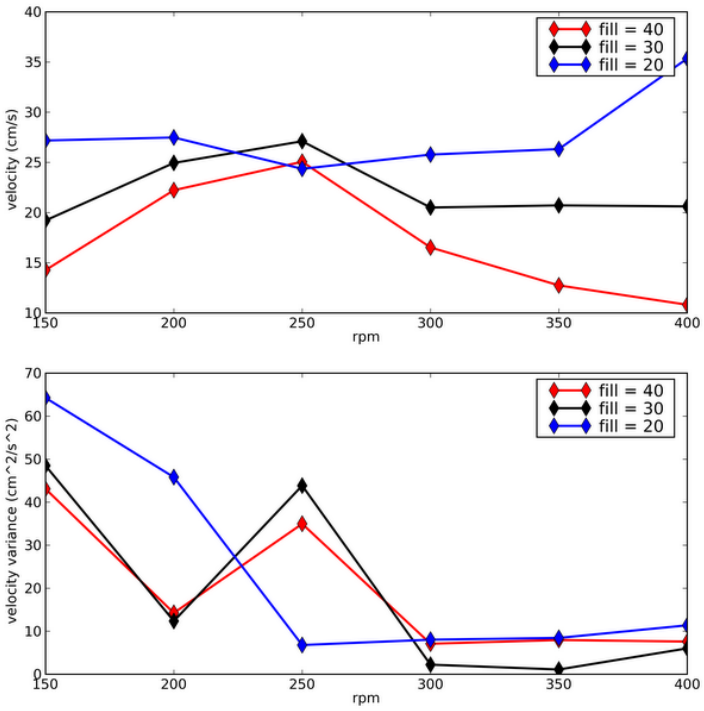

Fig.6.11. Variation of surface velocity as a function of impeller rotational speed during the mixing at pilot-scale: (a) variation of mean values and (b) standard deviation

As can be seen in Fig.6.11, mean surface velocity and standard deviation values are clearly affected by the mass fill and the impeller rotational speed. Particularly, mean surface velocity profiles at 30 and 40% mass fill show a maximum value around 250 rpm, then surface velocity monotonically decreases (40% mass fill) or decreases and stabilizes around a constant value (30% mass fill). On the other hand, mean surface velocity at 20% mass fill results to be almost constant until 350 rpm and then increases when impeller rotational speed is set at 400 rpm. As a general comment, it can be observed that mean surface velocity tends to be higher when mass fill is low (20%).

Standard deviation profiles in Fig.6.11b also show different trends depending on the mass fill. Trends at 30 and 40% mass fill are similar: standard deviation decreases with increasing impeller rotational speed, then increases at 250 rpm and finally stabilizes around a minimum value after 300 rpm. Standard deviation profile at 20% mass fill shows a sudden decrease after 200 rpm and stabilizes around a minimum value after 250 rpm.

Summarizing, it is suggested that transition between bumping and roping regime can be described by a sudden decrease of the standard deviation, which reaches a minimum value after a critical impeller rotational speed. After this transition point, powder flow is expected to be more mono-directional and follow the toroidal pattern, as described by Fig.6.10 and related comments. The decrease of mean velocity after the transition point at higher mass fills (especially at 40% mass fill, see Fig.6.11a) can be explained by considering the formation of two ideal mixing layers: a bottom layer which wraps the impeller surrounding area, and a top layer which is less affected by the blade convective mixing. With increasing the mass fill, the transport of powder from the bottom to the surface might be reduced, thus leading to a less effective mixing. These comments are in agreement with the results recently obtained by Remy et al. (2010)b and Koller et al. (2010). In the former research (Remy et al., 2010b), simulation studies based on discrete element method (DEM) of the mixing process of monodisperse, cohesionless spheres in a bladed mixer were presented. They found that for low mass fill a three dimensional recirculation zone develops and promotes a good vertical and radial mixing. At high mass fills, the convective zone is compressed to the bottom and the transport of material to the bed surface is limited. Koller et al. (2010) experimentally proved Remy et al. (2010)b results by analyzing convective and diffusive properties of a binary pharmaceutical powder blend. Using NIR spectroscopy for monitoring the powder-blend composition, they demonstrated that for high fill levels diffusive mixing is prevailing and strongly reduces blending kinetics.

Concluding, rotational speed and mass fill resulted to affect the transition between bumping and roping regime and scheme in Fig.6.12 roughly describes such influences.

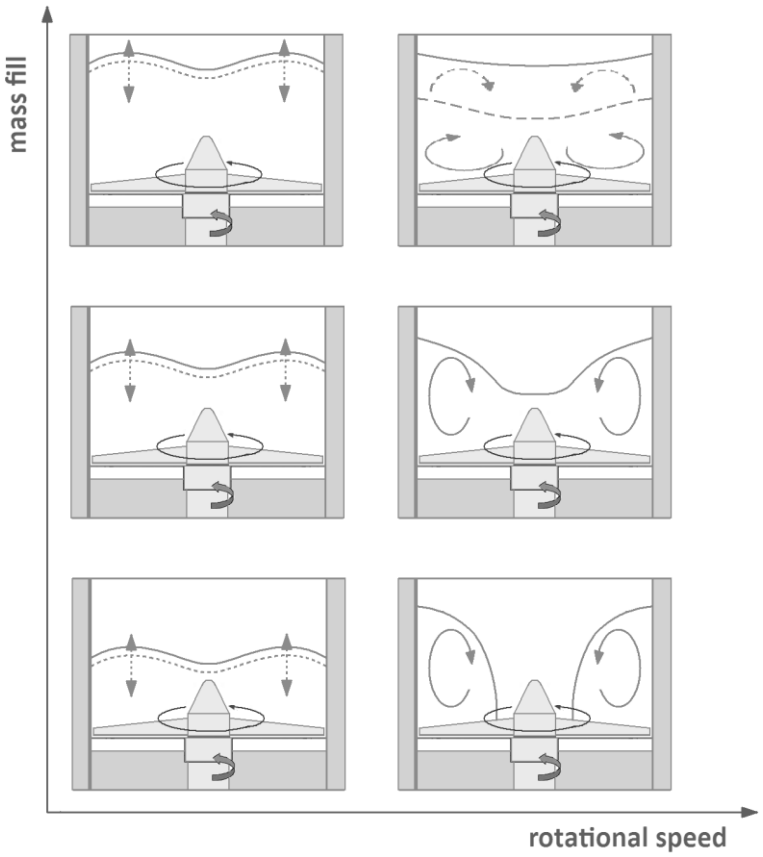

Fig.6.12. Scheme representing the effects of mass fill and rotational speed on the transition between bumping and roping regime

Results of the present research clearly show the strong influence of mass fill on the powder flow patterns at pilot scale as well. Even though low mass fill and high impeller speed seem to promote the achievement of the best mixing conditions (i.e. roping flow, see scheme in Fig.6.12), other variables should be taken into account during the design of high shear mixers. As an example, the ratio between mechanical energy and powder mass increases by increasing impeller speed and decreasing mass fill. This fact might affect the properties of the granular material during the process (Mangwandi et al., 2010).

6.5 Conclusions

The present research aims at closing the gap in understanding the scale-up effects on the powder flow patterns during the high shear mixing of cohesive powders. Particularly, this work focuses on the effects of mass fill at different scales. Extensive experimentation was performed using a small scale mixer as a starting point for scale-up to a larger, non-geometrically similar mixer.

Some of the most widespread techniques for monitoring high shear mixers were considered: impeller torque and impeller current were used to monitor respectively the small scale and the

pilot scale mixer. Particle image velocimetry (PIV) measurements were also used at pilot scale to examine the variation of powder surface velocity.

Using experimental data collected at small scale, a new model for the prediction of impeller torque profiles was proposed. This model was used to plot experimental torque values in the form of a new dimensionless torque number against the square root of the impeller Froude number. Accordingly, two key terms were identified: a static term, which mainly depends on the impeller height and weakly depends on the mass fill, and a dynamic term, which depends on the mass fill. Among the variables analyzed by the model, mass fill resulted to most affect the powder flow patterns and the transition between poor mixing (i.e. bumping regime) and more effective mixing conditions (i.e. roping regime).

According to the results of small scale trials, experimentation at pilot scale was mainly focused at understanding the role of mass fill on the powder flow patterns. Trends of impeller current profiles at pilot scale resulted to be similar to those of impeller torque profiles at small scale, identifying the transition between bumping and roping mixing regimes. PIV was furthermore used for best understanding the dependence of mixing regime transition on mass fill and impeller speed. As resulted from the PIV analysis, considerable higher values of tangential velocity (velocity component parallel to the impeller tip speed) compared to radial velocity values (velocity component perpendicular to the impeller tip speed) clearly identify roping regime and toroidal powder motion. At the highest mass fill and impeller speed, the transport of powder from the bottom to the surface resulted to be strongly reduced and a upper poorly-mixed zone was formed. As a consequence of this phenomenon, powder surface velocity visibly decreased.

6.6 References

M.J. Cliff. Granulation end-point and automated process control of mixer-granulators: Part 2. Pharmaceutical Technology 5 (1990) 38-44.

A. Dareliusa, E. Lennartssona, A. Rasmusona, I.N. Björnb, S. Folestadb. Measurement of the velocity field and frictional properties of wet masses in a high shear mixer. Chemical Engineering Science 62 (2007) 2366-2374.

P.C. Knight, J.P.K. Seville, A.B. Wellm, T. Instone. Prediction of impeller torque in high shear powder mixers. Chemical Engineering Science 56 (2001) 4457-4471.

D.M. Koller, A. Posch, G. Hörl, C. Voura, S. Randl, N. Urbanetz, S.D. Fraser, W. Tritthart, F. Reiter, M. Schlingmann, J.G Khinast. Continuous quantitative monitoring of powder mixing dynamics by near-infrared spectroscopy. Powder Technology (2010), doi: 10.1016 / j.powtec.2010.08.070

M. Levin. Wet Granulation: End point Determination and Scale-Up. In: Encyclopedia of Pharmaceutical Technology, Francis and Taylor, 2006.

J.D. Litster, K.P. Hapgood, J.N. Michaels, A. Sims, M. Roberts, S.K. Kameneni. Scale-up of mixer granulators for effective liquid distribution. Powder Technology 124 (2002) 272-280.

J.D. Litster, B. Ennis. The science and engineering of granulation processes. Kluwer Powder Technology Series, 2004.

C. Mangwandi, M.J. Adams, M.J. Hounslow, A.D. Salman. Effect of batch size on mechanical properties of granules in high shear granulation. Powder Technology (2010), doi:10.1016/j.powtec.2010.05.025.

P.R. Mort. Scale-up and control of binder agglomeration processes – Flow and stress fields. Powder Technology 189 (2009) 313-317.

E.L. Paul, V.A. Obeng, S.M. Kresta. Handbook of Industrial Mixing: Science and Practice. Wiley-Interscience, 2003.

B. Remy, T.M. Canty, J.G. Khinast, B.J. Glasser. Experiments and simulations of cohesionless particles with varying roughness in a bladed mixer. Chemical Engineering Science 65 (2010) 4557-4571.

B. Remy, B.J. Glasser, J.G. Khinast. The effect of mixer properties and fill level on granular flow in a bladed mixer. AIChE Journal 56 (2010) 336-353.

Chapter 7

Conclusions and future perspectives

The work presented in this thesis mainly focuses on the agglomeration of pharmaceutical powders in high shear mixers.

Research activities concerned the effects of formulation and process variables on the granule growth behaviour.
In particular:

- a new formulation map was developed. According to this new procedure, granule growth onset can be predicted as a function of the initial powder mixture composition and using the glass transition concept;
- initial powder mixture components can be ideally classified in two main categories: crystalline and amorphous powders. Glass transition of amorphous material occurs during wet granulation. This phenomenon promotes the formation of inter-particle bonds and determines the start of substantial granule growth.
- critical points in the formulation map (i.e. growth onset conditions for a given formulation) can be predicted performing independent measurements: measurements of glass transition temperature of the amorphous material, measurements of water sorption isotherms for each mixture component;
- further investigation should be performed in order to identify the role of water sorption kinetics during the agglomeration process: competition in water sorption can strongly affect the growth onset prediction assessed with the new formulation map (equilibrium measurements).
- granule growth behaviour in presence of three common active ingredients was analyzed: the effects of drug characteristics (primary particle size distribution, hygroscopicity and solubility) as well as some important process variables (impeller speed and liquid flow rate) on the granule growth behaviour were evaluated;
- smaller mean particle size, lower impeller speed and higher flow rate leaded to slower granule growth and stronger content uniformity problems;

- bigger mean particle size, higher impeller speed and lower flow rate leaded to faster granule growth. In this case growth mechanism was likely to be a breakage/layering mechanism.
- effects of operative variables, such as impeller speed and liquid flow rate, on the granule growth onset was evaluated. A probe was furthermore used in order to monitor the particle size evolution during the process (online measurements);
- the dimensionless spray flux concept was used in order to describe the liquid distribution at different process conditions: poor liquid distribution (i.e. low impeller speed and high flow rate) leaded to slower granule growth;
- an emulsion containing a lipophilic drug (self-emulsifying drug delivery system) was used as liquid binder in high shear wet granulation and compared with conventional techniques (water-granulation);
- results showed that granules obtained using the new liquid binder appeared to be more spherical and less dependent on the operating variables, such as massing time and impeller speed;
- Stokes deformation number approach was used in order to explain the differences between the granulation mechanisms.
- scale up from bench scale (2 l) to pilot scale (65 l) was performed: effects of changes in mass fill and impeller speed on the mixing regime were analyzed by monitoring the impeller torque (bench scale), impeller current (pilot scale) and powder surface velocity (pilot scale);
- a new dimensionless torque number was developed: this number clearly isolate the contribution of mass fill, impeller speed and impeller height at bench scale;
- results of experimentation at pilot scale demonstrated that mass fill strongly affect the powder flow patterns;
- more effective mixing can be achieved when mass fill is low and impeller speed is high (i.e. roping regime);
- poorly mixed zones were formed at high mass fill and impeller speed values, thus leading to a less effective mixing;
- further analysis is required in order to apply the new dimensionless torque number at pilot scale and evaluate the effect of higher energy density (i.e. ratio between mixing energy and powder mass) on the final product if granulation is performed.

List of Publications and Presentations

International Journals

Published:

- M. Cavinato, M. Bresciani, M. Machin, G. Bellazzi, P. Canu and A. Santomaso, "Formulation design for optimal high-shear wet granulation using on-line torque measurements" - International Journal of Pharmaceutics 387 (2010) 48-55.
- M. Cavinato, E. Franceschinis, S. Cavallari, N. Realdon and A. Santomaso, "Relationship between particle shape and some process variables in high shear wet granulation using binders of different viscosity" - Chemical Engineering Journal 164 (2010) 292-298.
- M. Cavinato, M. Bresciani, M. Machin, G. Bellazzi, P. Canu and A. Santomaso, "The development of a novel formulation map for the optimization of high shear wet granulation" - Chemical Engineering Journal 164 (2010) 350-358.

To be submitted:

- M. Cavinato, E. Andreato, M. Bresciani, I. Pignatone, G. Bellazzi, E. Franceschinis, N. Realdon, P. Canu, A. C. Santomaso, "Combining formulation and process aspects for optimizing the high-shear wet granulation of common drugs" – International Journal of Pharmaceutics.
- M. Cavinato, R. Artoni, M. Bresciani, P. Canu, A. C. Santomaso, "Predicting scale-up effects on flow pattern in high shear mixing of cohesive powders"- AIChE Journal.
- M. Cavinato, D. Kayrak-Talay and J.D. Litster"Predicting the growth kinetics based on the formulation properties in high shear wet granulation"- Powder Technology.

International Conferences

AIChE Annual Meeting, Salt Lake City (U.S.A.), November 2010:

- Podium presentation – M. Cavinato, M. Bresciani, I. Pignatone, G. Bellazzi, R. Artoni, P. Canu, A. C. Santomaso, "Scale-up Effects On the Growth Kinetics in High-Shear Wet Granulation: a Case Study".
- Podium presentation – M. Cavinato, E. Andreato, M. Bresciani, I. Pignatone, G. Bellazzi, E. Franceschinis, N. Realdon, P. Canu, A. C. Santomaso, "Combining

Formulation and Process Aspects for Optimizing the High-Shear Wet Granulation of Common Drugs".

World Congress on Particle Technology, Nuremberg (Germany), April 2010 :

- Podium presentation - M. Cavinato, E. Franceschinis, S. Cavallari, N. Realdon and A. Santomaso, "Granule structure obtained using diphasic binder in high shear granulation".
- Poster - M. Cavinato, D. Kayrak-Talay and J.D. Litster, "Predicting the growth kinetics based on the formulation properties in high shear wet granulation".
- Poster - M. Cavinato, M. Bresciani, M. Machin, G. Bellazzi, P. Canu and A. Santomaso, "Formulation design for optimal high-shear wet granulation using on-line torque measurements".
- Poster - M. Cavinato, M. Bresciani, M. Machin, P. Canu and A. Santomaso, "Development of a predictive model for impeller torque in high shear mixing of cohesive powders".
- Poster - L. Susana, M. Cavinato, E. Franceschinis, M. Rosso, N. Realdon, P. Canu, A. Santomaso, "On the characterization of powder wettability by drop penetration observation".
- Poster – E. Franceschinis, C. Bortoletto, M. Cavinato, A. Santomaso, N. Realdon, "Design of self-emulsifying pellets to improve bioavailability of liphophyilic pharmaceutical actives"

Formulation Symposium, GlaxoSmithKline Ware (U.K.), March 2010 :

- Podium presentation - M. Cavinato, M. Bresciani, M. Machin, G. Bellazzi, P. Canu and A. Santomaso, "Prediction of HSWG onset on the basis of single components physical properties and torque measurements".

AIChE Annual Meeting, Nashville (U.S.A.), November 2009 :

- Poster - M. Cavinato, E. Franceschinis, S. Cavallari, N. Realdon and A. Santomaso, "High shear wet granulation using self-emulsifying system: granule shape and size as a function of some important process variables".

International Symposium on Agglomeration, Sheffield (U.K.), June 2009 :

- Podium presentation - M. Cavinato, M. Bresciani, M. Machin, G. Bellazzi, P. Canu and A. Santomaso, "Formulation design for optimal high-shear wet granulation using on-line torque measurements"

- Poster - M. Cavinato, E. Franceschinis, S. Cavallari, N. Realdon and A. Santomaso, “Relationship between particle shape and some process variables in high shear wet granulation using binders of different viscosity”.

Italian Conferences

Symposium A.F.I. (Association Pharmaceutical Industry), Rimini (Italy), June 2009 :

- Poster - E. Franceschinis, A. Santomaso, M. Cavinato and N. Realdon, “Utilizzo di emulsioni quali leganti in granulazione ad umido: valutazioni tecnologiche”.

Congress GR.I.C.U. (Chem. Eng., Italian Research Group),Crotone (Italy), September 2008

- Poster - M. Cavinato, M. Bresciani, M. Machin, F. Cappitelli, P. Canu and A. Santomaso, “Granulazione farmaceutica umida high-shear: controllo di processo e monitoraggio del momento torcente”

Chemical Development Executive Meeting, GlaxoSmithKline Verona (Italy), September 2007 :

- Poster - M. Cavinato, M. Machin, S. Carucci and N. Brun, “High Shear Wet Granulation monitoring and control using Impeller Torque”